

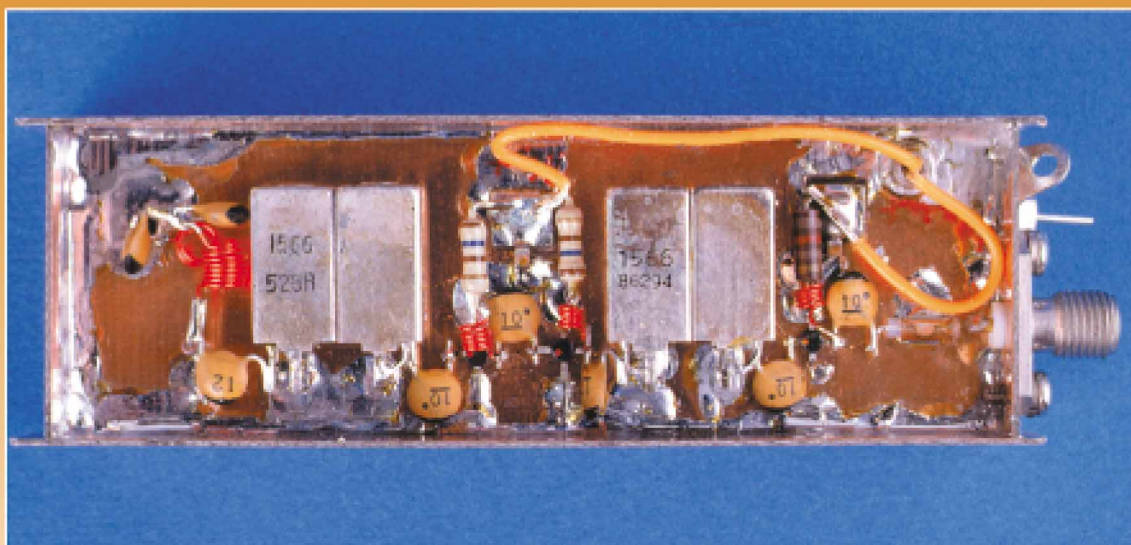
\$5



QEX

INCLUDING:
COMMUNICATIONS
QUARTERLY

Forum for Communications Experimenters September/October 2001



W1VT Uses Cell-Phone Parts in an 852-MHz LO

ARRL *The national association
for AMATEUR RADIO*
225 Main Street
Newington, CT USA 06111-1494

ACQUIRE THE ESSENTIALS

FOR SUCCESSFUL RF AND MICROWAVE DESIGN



Q from A to Z

Randy Rhea

Understanding the concept of Q is essential for the design and specification of oscillator resonators, filters and matching networks. Combining audio, video and text, this tutorial presents a comprehensive explanation of Q and includes sample problems and solutions, along with a bibliography of source materials. Running time for the course is approximately 50 minutes.

KEY CONCEPTS

- Unloaded Q or Component Q
- Loaded Q
- Q and Matching Concepts

2001, CD-ROM, ISBN 1-884932-22-3

\$79 plus shipping order NP-41



Filter Design by Transmission Zeros

Randy Rhea

This practice-oriented course helps you understand the design of L-CD filters based on the specifications of the transmission zeros. Mastering this powerful technique will allow you to design customized filters with reduced component count and more easily realized element values. Session includes sections on classic design methods and practical issues associated with building filters. Running time for the course is approximately 60 minutes.


KEY CONCEPTS

- Classic Filter Design
- Transmission Zero Introduction
- The Extraction Process
- Network Transforms
- Practical Issues

2001, CD-ROM, ISBN 1-884932-23-1

\$99 plus shipping order NP-42

For more information, or to place your order online,
point your web browser to www.noblepub.com


NOBLE
PUBLISHING

FOR INFORMATION OR TO ORDER CONTACT:

Noble Publishing Corporation
630 Pinnacle Court, Norcross, GA 30071, USA
Tel: 770-449-6774 Fax: 770-448-2839 www.noblepub.com

EUROPEAN CUSTOMERS PLEASE ORDER THROUGH:

American Technical Publishers
27-29 Knowl Piece, Wilbury Way, Hitchin, Herts. SG4 0SX England
Tel: +44 (0) 1462 437933 Fax: +44 (0) 1462 433678 www.ameritech.co.uk

QEX

INCLUDING: COMMUNICATIONS
QUARTERLY

QEX (ISSN: 0886-8093) is published bimonthly in January, March, May, July, September, and November by the American Radio Relay League, 225 Main Street, Newington CT 06111-1494. Yearly subscription rate to ARRL members is \$22; nonmembers \$34. Other rates are listed below. Periodicals postage paid at Hartford, CT and at additional mailing offices.

POSTMASTER: Send address changes to: QEX, 225 Main St, Newington, CT 06111-1494 Issue No 208

Mark J. Wilson, K1RO
Publisher

Doug Smith, KF6DX
Editor

Robert Schetgen, KU7G
Managing Editor

Lori Weinberg
Assistant Editor

Peter Bertini, K1ZJH
Zack Lau, W1VT
Contributing Editors

Production Department

Steve Ford, WB8IMY
Publications Manager

Michelle Bloom, WB1ENT
Production Supervisor

Sue Fagan
Graphic Design Supervisor

David Pingree, N1NAS
Technical Illustrator

Joe Shea
Production Assistant

Advertising Information Contact:

John Bee, N1GNV, *Advertising Manager*
860-594-0207 direct
860-594-0200 ARRL
860-594-0259 fax

Circulation Department

Debra Jahnke, *Manager*
Kathy Capodicasa, N1GZO, *Deputy Manager*
Cathy Stepina, *QEX Circulation*

Offices

225 Main St, Newington, CT 06111-1494 USA
Telephone: 860-594-0200
Telex: 650215-5052 MCI
Fax: 860-594-0259 (24 hour direct line)
e-mail: qex@arrl.org

Subscription rate for 6 issues:

In the US: ARRL Member \$24,
nonmember \$36;

US by First Class Mail:
ARRL member \$37, nonmember \$49;

Elsewhere by Surface Mail (4-8 week delivery):
ARRL member \$31, nonmember \$43;

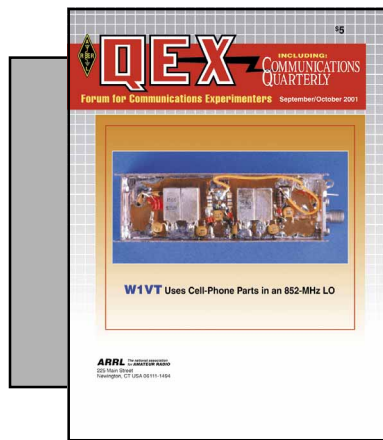
Canada by Airmail: ARRL member \$40,
nonmember \$52;

Elsewhere by Airmail: ARRL member \$59,
nonmember \$71.

Members are asked to include their membership control number or a label from their QST wrapper when applying.

In order to ensure prompt delivery, we ask that you periodically check the address information on your mailing label. If you find any inaccuracies, please contact the Circulation Department immediately. Thank you for your assistance.

Copyright ©2001 by the American Radio Relay League Inc. For permission to quote or reprint material from QEX or any ARRL publication, send a written request including the issue date (or book title), article, page numbers and a description of where you intend to use the reprinted material. Send the request to the office of the Publications Manager (permission@arrl.org)



About the Cover

The 8× multiplier from the 852-MHz LO. See “RF” for details.



Features

3 A Spreadsheet for Remote Antenna Impedance Measurement

By Ron Barker, G4JNH, VK2INH

12 A Flat Impedance Bandwidth for any Antenna

By Grant Bingeman, KM5KG

18 160-Meter Propagation: Unpredictable Aspects

By Robert R. Brown, NM7M

26 The Art of Making and Measuring LF Coils

By Paolo Antoniazzi, IW2ACD and Marco Arecco, IK2WAQ

33 The Q of Single-Layer, Air-Core Coils: A Mathematical Analysis

By George Murphy, VE3ERP

38 Build this Simple, High-Resolution DC Voltmeter

By Ron Tipton, ex-K5UJC

45 Deconvolution in Communication Systems

By Doug Smith, KF6DX

Columns

52 Tech Notes

64 Letters to the Editor

61 RF By Zack Lau, W1VT

64 Next Issue in QEX

Sept/Oct 2001 QEX Advertising Index

American Radio Relay League: 64,

Cov III, Cov IV

Atomic Time, Inc.: 11

Denny & Associates: 44

Roy Lewallen, W7EL: 25

Mike's Electronics: 63

Nemal Electronics International, Inc.: 60

Noble Publishing: Cov II

Tucson Amateur Packet Radio Corp: 17

TX RX Systems Inc.: 51

Universal Radio, Inc.: 25, 60

West Mountain Radio: 37



The American Radio Relay League, Inc. is a noncommercial association of radio amateurs, organized for the promotion of interests in Amateur Radio communication and experimentation, for the establishment of networks to provide communications in the event of disasters or other emergencies, for the advancement of radio art and of the public welfare, for the representation of the radio amateur in legislative matters, and for the maintenance of fraternalism and a high standard of conduct.

ARRL is an incorporated association without capital stock chartered under the laws of the state of Connecticut, and is an exempt organization under Section 501(c)(3) of the Internal Revenue Code of 1986. Its affairs are governed by a Board of Directors, whose voting members are elected every two years by the general membership. The officers are elected or appointed by the Directors. The League is noncommercial, and no one who could gain financially from the shaping of its affairs is eligible for membership on its Board.

"Of, by, and for the radio amateur," ARRL numbers within its ranks the vast majority of active amateurs in the nation and has a proud history of achievement as the standard-bearer in amateur affairs.

A bona fide interest in Amateur Radio is the only essential qualification of membership; an Amateur Radio license is not a prerequisite, although full voting membership is granted only to licensed amateurs in the US.

Membership inquiries and general correspondence should be addressed to the administrative headquarters at 225 Main Street, Newington, CT 06111 USA.

Telephone: 860-594-0200
Telex: 650215-5052 MCI
MCIMAIL (electronic mail system) ID: 215-5052
FAX: 860-594-0259 (24-hour direct line)

Officers

President: JIM D. HAYNIE, W5JBP
3226 Newcastle Dr, Dallas, TX 75220-1640

Executive Vice President: DAVID SUMNER, K1ZZ

The purpose of *QEX* is to:

- 1) provide a medium for the exchange of ideas and information among Amateur Radio experimenters,
- 2) document advanced technical work in the Amateur Radio field, and
- 3) support efforts to advance the state of the Amateur Radio art.

All correspondence concerning *QEX* should be addressed to the American Radio Relay League, 225 Main Street, Newington, CT 06111 USA. Envelopes containing manuscripts and letters for publication in *QEX* should be marked Editor, *QEX*.

Both theoretical and practical technical articles are welcomed. Manuscripts should be submitted on IBM or Mac format 3.5-inch diskette in word-processor format, if possible. We can redraw any figures as long as their content is clear. Photos should be glossy, color or black-and-white prints of at least the size they are to appear in *QEX*. Further information for authors can be found on the Web at www.arrl.org/qex/ or by e-mail to qex@arrl.org.

Any opinions expressed in *QEX* are those of the authors, not necessarily those of the Editor or the League. While we strive to ensure all material is technically correct, authors are expected to defend their own assertions. Products mentioned are included for your information only; no endorsement is implied. Readers are cautioned to verify the availability of products before sending money to vendors.

Empirically Speaking

During discussions with readers, authors and others, I've seen that I should explain a bit more about our editorial process. Much of this information is in our Author's Guide (www.arrl.org/qex), but it's time for me to dispel a few persistent misconceptions.

We are happy to respond to proposals sent via e-mail, but we must review a complete manuscript before deciding on acceptance. A positive reaction from us to your query is not a guarantee that the finished manuscript will be acceptable. We like to get your articles in both printed and diskette form at headquarters in Newington. On receipt, Maty Weinberg sends you an acknowledgment by regular mail.

Your article then enters a review phase in which I often employ outside help. External review sometimes takes several weeks. I'm free to ask ARRL Technical Advisors or anyone else I trust to help me decide, but the final decision rests with me. Criteria used to evaluate articles are in the Author's Guide; the relative importance of each of those may depend on some of the others. For example: We may have to weigh the amount of work we must do on an article against its novelty or import. As explained in the Author's Guide, articles submitted in the standard form have a better chance of acceptance. In fact, many magazines automatically return articles just because they aren't formatted correctly.

One common mistake is putting graphics in the main body of the text: Put them in separate files on diskette. Captions belong in a list at the end of the manuscript. Electronic images should be submitted with the highest-possible resolution. We need at least 300 pixels/inch at the final image size in the magazine. (That is about 675 pixels wide for a one-column image, 1350 for two, 2025 for three.)

Another frequent error is the excessive use of word-processor tools. Avoid formatting codes such as tab set, block protect and so forth. Pick one font and stick with it inside the main text. Notes or references should be indicated by a superscript numeral at the first occurrence and by plain English at subsequent occurrences (eg, "see Note 4").

After an article is accepted, I edit it and, if necessary, put it into standard form. I don't like to make major changes or alter your style, but I will recast a sentence occasionally or fix wasteful locutions like "in order to." The most common thing I do is to add commas; I often break up long sentences with other punctuation. If I think your meaning is unclear or if something I do may alter it, I'll contact you. Two to three months before the cover date of an issue, Bob Schetgen gets the edited copy and he parses it again. He always finds things I missed and he may have questions that didn't occur to me. Then he prepares the article for production.

The last thing you see before publication is a final layout of your article, usually in a PDF file sent via e-mail. We strive to give you several days to look it over. At that stage, we generally don't have time to make major revisions, since we are within a week or two of our deadline. Bob and the production crew must make everything fit; still, it's your name under the title and we want the thing to be right.

In This Issue

Ron Barker, G4JNH, takes us on a journey down a feed line from the transmitter to the antenna and back. He shows a way to measure antenna impedance without climbing the tower. Grant Bingeman, KM5KG, explains how to get a bit more usable bandwidth out of your antenna by inserting an SWR-bandwidth broadening network. Robert Brown, NM7M, contributes another installment about the vagaries of MF propagation.

Paolo Antoniazzi, IW2ACD, and Marco Arecco, IK2WAQ, present their studies of LF coils. George Murphy, VE3ERP, summarizes formulas for coils in general. Ron Tipton gives us a high-resolution voltmeter you can build. My article about "deconvolution" describes a DSP technique to correct some forms of distortion. In Tech Notes, Pete Bertini, K1ZJH, presents Sam Ulbing, N4UAU's piece about a class-D audio amplifier.

In RF, Zack Lau, W1VT, uses cell-phone components to facilitate an 852-MHz local oscillator.—73, Doug Smith, KF6DX □□

A Spreadsheet for Remote Antenna Impedance Measurement

If you're interested in measuring the feed-point impedance of your antenna from the comfort of the shack, without knowing the length of the feedline, this spreadsheet in MS Excel is for you.

By Ron Barker, G4JNH, VK2INH

When experimenting with antennas, there are situations when it can be extremely useful to know the feed-point impedance. Perhaps the most obvious way to get that information would be to climb the tower with a self-contained portable impedance bridge; but, even apart from the safety aspect, there are disadvantages in this approach. The proximity of the person making the measurement so close to the antenna and the fact that the feeder has to be disconnected could lead to changes in the impedance value. A more popular method is to use a feedline of the shortest possible length

to reach the ground whilst being an exact number of electrical half wavelengths long. This method is restricted to one spot frequency for any particular length of feedline and furthermore, it provides no compensation for the effect of feedline loss.

A much better method is to utilize the Smith chart, since the feedline can be of random length, which means that measurements can be taken at any frequency from the comfort of the shack. Furthermore, the effects of line loss can be taken into account. It is a two-stage operation: Stage one determines the Smith-chart length of the line, which is then used in stage two to determine the impedance of the antenna. Smith-chart line length is defined as the electrical length of the line in wavelengths by which it exceeds the highest whole

number of half wavelengths. Its value is within the range 0.000 to 0.500. For example, the Smith-chart length of a line of 2.702 wavelengths would be 0.202 and that of a line of 3.343 wavelengths would be 0.343. Alternatively, it can be defined as the length in wavelengths by which it differs from the nearest whole number of half wavelengths when its value is within the range -0.250 to $+0.250$. By this definition, the examples given above would be 0.202 and -0.157 . It can also be quoted in degrees or radians where one wavelength is equal to 360° or 2π radians.

To determine its Smith-chart length, the line is disconnected from the antenna and terminated with a resistive load, preferably having a value of either $1/3$ to $1/2$, or 2 to 3 times the characteristic impedance of the line. $R \pm jX$

171 Leicester Rd
Ashby de la Zouch
Leicestershire, LE65 1TR, UK
ron.g4jnh@talk21.com

readings are taken at the transmitter end of the line and these together with the value of the terminating resistor are entered onto the Smith chart. Lines are then projected from the prime center through these points to the circumference of the chart. The Smith-chart line length corresponds to the distance around the chart between the two intersections starting in a clockwise direction from the resistive-load position. Line loss has no effect on the result of this operation. Preferred limits for the value of the load resistor are stipulated so that the value is not too close to the characteristic impedance of the line. When the load value is close to Z_0 , accuracy is impaired because very small changes in $R \pm jX$ correspond to significant changes in Smith-chart line length. On the other hand, if the value chosen is too far removed from Z_0 , the $R \pm jX$ readings may be outside of the range of the impedance bridge. The best load value is one as far as possible from line Z_0 , whilst giving readings within the range of the impedance bridge. For use with 50- Ω line, I use either a 20- Ω or 120- Ω resistor with good results.

Having determined the Smith-chart length of the feeder, the antenna is re-connected and $R \pm jX$ readings are taken again at the transmitter end of the line. The new results are entered on the chart and a line is projected from the prime center through that point to the circumference. The impedance of the antenna is obtained by going back around the circumference in an anti-clockwise direction by an amount equal to the Smith-chart line length. A line is projected from this point to the prime center and the impedance of the antenna then corresponds to the point on this line which is the same distance from the prime center as the measured $R \pm jX$ point. (Distance from center corresponds to SWR—*Ed.*)

The effects of line loss can be included via the sidebar on the chart, which provides a correction factor for the distance from the prime center to the antenna impedance point, depending on the known line loss. The finer points of Smith chart use are beyond the scope of this article. Interested readers can learn them from Chapter 28 of any recent *ARRL Antenna Book*.¹ We shall return to the subject of correcting for line loss later.

The method of impedance measurement just outlined works very well, but it is tedious and time-consuming. I know from my own experience how easy

it is to make mistakes in counting the small divisions on the chart. For many years, computer programs have performed Smith-chart impedance transformations when the Smith-chart line length is known. I found none, however, that would reveal the Smith-chart line length from known impedance values at both ends of the line, except in the special situations of either open or shorted terminations. For reasons that we shall examine later, the open and short options are not acceptable. Therefore, I began to devise a mathematical method that would accept the range of line terminations as just described, work with a paper Smith chart and that could be easily incorporated into a computer program. The result is a very easy to use spreadsheet, the derivation of which is described below.

The Method

Stage 1: Determination of Smith-Chart Line Length

As we saw in the introduction, remote antenna-impedance measurement is a two-stage process. The same approach is taken when the procedure is carried out by computer, so the first challenge is to devise a mathematical procedure for calculating Smith-chart line length that can be incorporated into a computer program.

When the remote end of a transmission line is either shorted or left open, there are very simple mathematical relationships between the reactance at the input end and the Smith-chart line length:

$$\tan \theta = \frac{X_{IN}}{Z_0} \quad (\text{Eq 1})$$

for a shorted termination and:

$$\tan \theta = \frac{Z_0}{X_{IN}} \quad (\text{Eq 2})$$

for an open termination, where θ is the Smith-chart line length in degrees or radians.

There is, however, a major problem with this simple approach: The equations do not consider line loss, and the error resulting from a loss of only 1 dB (typical in an amateur station) would render the result doubtful, particularly if the Smith-chart line length were in the range 0.2 to 0.3. Furthermore, it is difficult to measure high values of reactance, although I don't see this as being insurmountable. I decided to seek a method compatible with my own bridge (which is typical of impedance bridges available to amateurs) and that would correct for line loss.

Two rather formidable equations

relate the parameters involved in Smith-chart impedance transformations. These equations appear in many older editions of the *ARRL Handbook*, but they have been replaced by a single equation since 1995. The "new" equation looks less formidable at first sight, but it involves complex numbers and hyperbolic functions that put me off its use for this application. The equations I chose were taken from *The 1989 ARRL Handbook*.² They are:

$$R_{IN} = \frac{R_a(1 + \tan^2 \theta)}{\left(1 - \frac{X_a}{Z_0} \tan \theta\right)^2 + \left(\frac{R_a}{Z_0} \tan \theta\right)^2} \quad (\text{Eq 3})$$

and

$$X_{IN} = \frac{X_a(1 - \tan^2 \theta) + \left(Z_0 - \frac{R_a^2 - X_a^2}{Z_0}\right) \tan \theta}{\left(1 - \frac{X_a}{Z_0} \tan \theta\right)^2 + \left(\frac{R_a}{Z_0} \tan \theta\right)^2} \quad (\text{Eq 4})$$

where

- R_{IN} = input resistance
- X_{IN} = input reactance
- R_a = antenna or load resistance
- X_a = antenna or load reactance
- Z_0 = feeder characteristic impedance
- θ = Smith-chart line length in degrees or radians

These equations take no account of line loss and we need to decide how to address that before applying them to the determination of Smith-chart line length. When a paper chart is used line loss is automatically accommodated; here it must be separately considered.

Let us assume that we have an unknown length of 50- Ω line terminated at the antenna end with a 20- Ω resistor. The SWR at that end of the line would be 50 divided by 20 giving 2.5:1, but at the transmitter end of the line, it would be less than that because of line loss. Let us assume a value of 2.0:1, which would be the case if the line loss were slightly more than 1 dB. If we were to use values of resistance and reactance at the input and antenna ends that related to different values of SWR, which would always be the case in a real situation due to line loss, the result for $\tan \theta$ would be incorrect. However, if we use the measured resistance and reactance at the transmitter end of the line to calculate SWR, we can then calculate very easily what the notional value of a purely resistive load at the antenna end of the line would have had to be to produce the measured resistance and reactance had there been no line loss.

¹Notes appear on page 11.

Therefore, in the situation above, the notional value of R_a would be:

$$\text{notional } R_a = \frac{Z_0}{SWR} = \frac{Z_0}{2} = 25 \Omega \quad (\text{Eq 5})$$

There is no need to work out the notional value of R_a because, as we shall see later, it can be entered into the equation we shall use to calculate $\tan\theta$ as Z_0/SWR . Furthermore, it is not necessary to know the actual value of the terminating resistor, but only whether it is higher or lower than Z_0 . For the time being, we shall work on the basis that it is lower than Z_0 .

So, as we saw in the introduction, the first stage of determining the Smith-chart line length is to terminate the feeder with a resistive load of suitable value and measure $R \pm jX$ at the transmitter end. The results are used to calculate reflection coefficient and SWR at the transmitter end of the line using the familiar equations as follows:

$$\rho = \frac{\sqrt{(Z_0 - R_{IN})^2 + X_{IN}^2}}{\sqrt{(Z_0 + R_{IN})^2 + X_{IN}^2}} \quad (\text{Eq 6})$$

and

$$SWR = \frac{1 + \rho}{1 - \rho} \quad (\text{Eq 7})$$

We can now turn our attention to the determination of Smith-chart line length. For this, we shall only need to use Eq 3. Because the load is purely resistive, that simplifies to the following:

$$R_{IN} = \frac{R_a(1 + \tan^2 \theta)}{1 + \frac{R_a}{Z_0} \tan \theta} \quad (\text{Eq 8})$$

However, as we saw earlier, R_a can be entered as Z_0/SWR , which gives:

$$R_{IN} = \frac{Z_0(1 + \tan^2 \theta)}{1 + \frac{SWR}{\tan^2 \theta}} \quad (\text{Eq 9})$$

To the derive Smith-chart line length, we need to isolate $\tan\theta$ on one side of the equation. First, multiply both the numerator and denominator of the right-hand side by SWR^2 , which gives:

$$R_{IN} = \frac{SWR(Z_0)(1 + \tan^2 \theta)}{SWR^2 + \tan^2 \theta} \quad (\text{Eq 10})$$

therefore

$$R_{IN}(SWR^2 + \tan^2 \theta) = SWR(Z_0)(1 + \tan^2 \theta) \quad (\text{Eq 11})$$

$$R_{IN}SWR^2 + R_{IN}\tan^2 \theta = SWR(Z_0) + SWR(Z_0)\tan^2 \theta \quad (\text{Eq 12})$$

$$R_{IN}\tan^2 \theta - SWR(Z_0)\tan^2 \theta = SWR(Z_0) - R_{IN}SWR^2 \quad (\text{Eq 13})$$

$$\tan^2 \theta (R_{IN} - SWR(Z_0)) = SWR(Z_0) - R_{IN}SWR^2 \quad (\text{Eq 14})$$

$$\tan^2 \theta = \frac{SWR(Z_0) - R_{IN}SWR^2}{R_{IN} - SWR(Z_0)} \quad (\text{Eq 15})$$

$$\tan \theta = \pm \sqrt{\frac{Z_0 - R_{IN}SWR}{\frac{R_{IN}}{SWR} - Z_0}} \quad (\text{Eq 16})$$

The selection of the correct sign for $\tan\theta$ presents no problem because when the load is purely resistive and less than Z_0 , the sign of $\tan\theta$ is always the same as the sign of X_{IN} .

Having established the value of $\tan\theta$, we can convert it to Smith-chart line length as follows:

$$\lambda = \frac{\tan^{-1}(\tan \theta)}{2\pi} \quad (\text{Eq 17})$$

if we are working in radians, or:

$$\lambda = \frac{\tan^{-1}(\tan \theta)}{360} \quad (\text{Eq 18})$$

if working in degrees. The Smith-chart line length given by Eqs 17 and 18 is in the format of the second definition given in the introduction and it will have a value within the range -0.250 to $+0.250$.

All of the foregoing has assumed a value of the terminating resistor that is less than the characteristic impedance of the line. If the terminating resistor's value is greater than the characteristic impedance of the line, we need only add 0.250 to the outcome of Eq 17 or 18. If at this stage, the value is negative, 0.500 is added to produce a positive value. Having established the Smith-chart line length, we can now proceed to the measurement of antenna impedance.

Stage 2: Determination of Antenna Impedance

As in Stage 1, the first point we have to decide on is how to correct for line loss. Points on a transmission line where the impedance is purely resistive correspond to Smith-chart line lengths of zero and 0.250. The mathematics of correcting the impedance of these for line loss are straightforward; but anywhere else, where there is a reactive component unless the line is perfectly matched, the correction is much more tedious. The approach taken here is to make the correction at the Smith-chart zero position. To do this, we must first establish the reflection coefficient and SWR at the transmitter end of the line. Then, by using a known value of line loss, we can de-

termine the reflection coefficient and SWR at the antenna end of the line.

Therefore, with the antenna reconnected to the transmission line, $R \pm jX$ readings are taken at the transmitter end of the line at the same frequency as was used for the determination of Smith-chart line length. Eqs 6 and 7 are used as in Stage 1 to determine values for reflection coefficient and SWR at the transmitter end of the line. With the known value of line loss, we can then calculate the reflection coefficient and SWR at the antenna end of the line as follows:

$$\begin{aligned} \rho_{ANT} &= \rho_{TX} 10^{\frac{2L}{20}} \\ &= \rho_{TX} 10^{\frac{L}{10}} \end{aligned} \quad (\text{Eq 19})$$

where

ρ_{ANT} = reflection coefficient at antenna

ρ_{TX} = reflection coefficient at transmitter

L = known line loss, in decibels

The SWR at the antenna is then derived using Eq 7.

A note of explanation is called for here since I was unable to find Eq 19 in any of the standard references on my bookshelf. The reflection coefficient is a function of voltage or current but not power, so the logarithm is divided by 20. When comparing reflection coefficients at the opposite ends of a transmission line, there is a two-way loss incurred, hence the $2L$ value in Eq 19.

You may be questioning why we should be working with a known value of line loss when the information required to calculate the actual line loss is available from the measurements made in Stage 1. The reason is that when this was tried in an earlier version of this spreadsheet, the results obtained did not agree with the known line loss. An investigation into why this might be so showed that the calculated loss is very sensitive to the actual value of the line Z_0 , which evidently varies somewhat from the values specified.³ I therefore decided that a better option would be to work with a known value obtained by one of the accepted methods.

The antenna impedance is now derived by first establishing the line length between the transmitter and Smith chart zero using Eqs 16 and 17. Note that for this part of the procedure, the SWR value is that at the transmitter end of the line. We can now derive the line length between the antenna and Smith chart zero by subtracting the Smith-chart line length from the

length between transmitter and Smith chart zero. The result is positive if the Smith-chart line length is less than the length between transmitter and Smith chart zero and negative if it is greater. This is important because Eqs 3 and 4, which we shall use to calculate antenna resistance and reactance, are directional. They are a mathematical representation of going round the Smith chart in a clockwise direction from the antenna to the transmitter. However, if the line length is entered as a negative value, which means that the sign of $\tan\theta$ is reversed, they work in the opposite direction. This permits the equations to deliver the correct answer for all possible values of line length between the antenna and Smith chart zero. It is helpful in the understanding of this rather confusing procedure to work a few typical examples on a paper Smith chart.

The line length between antenna and Smith chart zero has to be expressed as $\tan\theta$ in the Smith chart equations and is derived as follows:

$$\begin{aligned} \tan\theta &= \tan(2\pi_length) \text{ radians} \\ &= \tan(360_length) \text{ degrees} \end{aligned} \quad (\text{Eq 20})$$

We can now use Eqs 3 and 4 to derive antenna resistance and reactance. Starting first with resistance, we use Eq 3, which simplifies to the following because reactance is zero at Smith chart zero:

$$R_a = \frac{R_i(1 + \tan^2\theta)}{1 + \left(\frac{R_i}{Z_0}\tan\theta\right)^2} \quad (\text{Eq 21})$$

where

R_a = antenna resistance

R_i = resistance at Smith chart zero

Nevertheless, as we saw earlier, R_i is entered into the equation as Z_0 divided by the SWR at the antenna, so we get:

$$\begin{aligned} R_a &= \frac{Z_0(1 + \tan^2\theta)}{1 + \frac{\tan^2\theta}{\text{SWR}^2}} \\ &= \frac{Z_0(1 + \tan^2\theta)}{\text{SWR} + \frac{\tan^2\theta}{\text{SWR}}} \end{aligned} \quad (\text{Eq 22})$$

Similarly, to derive antenna reactance, X_a , we use Eq 4, which simplifies initially to:

$$X_a = \frac{\left(Z_0 - \frac{R_i^2}{Z_0}\right)\tan\theta}{1 + \left(\frac{R_i}{Z_0}\tan\theta\right)^2} \quad (\text{Eq 23})$$

Substituting $R_i = Z_0/\text{SWR}$ gives:

$$\begin{aligned} X_a &= \frac{\left(Z_0 - \frac{Z_0}{\text{SWR}^2}\right)\tan\theta}{1 + \frac{\tan^2\theta}{\text{SWR}^2}} \\ &= \frac{Z_0\tan\theta - \frac{Z_0\tan\theta}{\text{SWR}^2}}{1 + \frac{\tan^2\theta}{\text{SWR}^2}} \\ &= \frac{\text{SWR}(Z_0)\tan\theta - \frac{Z_0\tan\theta}{\text{SWR}}}{\text{SWR} + \frac{\tan^2\theta}{\text{SWR}}} \\ &= \frac{Z_0\tan\theta\left(\text{SWR} - \frac{1}{\text{SWR}}\right)}{\text{SWR} + \frac{\tan^2\theta}{\text{SWR}}} \end{aligned} \quad (\text{Eq 24})$$

That completes the derivation of antenna impedance, but we have all the information needed to calculate line loss at the actual SWR, which can be expressed in terms of both decibels and transmission-line efficiency.

$$\begin{aligned} \text{line efficiency} &= \frac{\text{power delivered to antenna}}{\text{power delivered by transmitter}} \\ &= \frac{\text{forward power at antenna} - \text{reflected power at antenna}}{\text{forward power at transmitter} - \text{reflected power at transmitter}} \end{aligned} \quad (\text{Eq 25})$$

but

$$\frac{\text{forward power at antenna}}{\text{forward power at transmitter}} = \frac{\text{reflection coefficient at transmitter}}{\text{reflection coefficient at antenna}} \quad (\text{Eq 26})$$

and

$$\text{reflected power} = (\text{forward power})(\text{reflection coefficient})^2 \quad (\text{Eq 27})$$

If we let the forward power at the antenna be equal to 1, then:

$$\begin{aligned} \text{line efficiency} &= \frac{1 - \rho_{\text{ANT}}^2}{\frac{\rho_{\text{ANT}}}{\rho_{\text{TX}}} - \frac{\rho_{\text{ANT}}\rho_{\text{TX}}^2}{\rho_{\text{TX}}}} \\ &= \frac{1 - \rho_{\text{ANT}}^2}{\frac{\rho_{\text{ANT}}}{\rho_{\text{TX}}} - \rho_{\text{ANT}}\rho_{\text{TX}}} \\ &= \frac{1}{\frac{\rho_{\text{ANT}}}{\rho_{\text{TX}}} - \rho_{\text{ANT}}} \\ &= \frac{1}{\frac{1}{\rho_{\text{TX}}} - \rho_{\text{TX}}} \end{aligned} \quad (\text{Eq 28})$$

This can be expressed in percent by multiplying by 100. The loss in decibels is then:

$$\text{loss} = 10 \log_{10} \left(\frac{100}{\text{line efficiency}\%} \right) \quad (\text{Eq 29})$$

That completes the description of the method and we can now turn our attention to the spreadsheet.

The Spreadsheet

The spreadsheet comprises two user screens, which occupy the first 24 rows of columns B to Y. The processing takes place in rows 26 to 56 of which only 22 are involved in arithmetic or logic, the remainder being either links to the user screens or headings. Screen 1, which is shown in Fig 1, provides for only one set of results but includes instructions on the use of the spreadsheet and is self-explanatory. Screen 2, which is shown in Fig 2, provides for eight columns of results but by the simple use of the drag handle is self-explanatory. This screen includes provision for entering frequency as column identification, but frequency is not involved in any of the calculations. Another reason for including frequency is that *Excel* provides for the graphical display of results, and it can be very useful to see the various antenna parameters plotted against frequency. Incidentally, the values displayed in Fig 2 relate to my own antenna and show that some tweaking of the gamma settings is called for.

All of the action takes place between rows 26 and 56. They are shown with a set of sample values in Fig 3 and with the formulae in Fig 4, which also shows the relevant equation numbers as they appear in the text. Again it is all largely self-explanatory, but the formulae in lines 32 and 43 are worthy of explanation. The tangent of 90° is infinity, which even *Excel* can't handle. The consequence of this is that if a reactance value of zero is entered together with a value of resistance higher than Z_0 , *Excel* can't handle Eq 16. The problem is overcome by using the logic function to change a reactance value of zero to 0.001Ω . This gives a very large—but finite—value for $\tan \theta$, which *Excel* can use. The error it introduces is at least 1000 times less than anything that might concern us.

I would recommend that for initial programming, the values shown in Fig 3 for cells J27, J28, J29, J30, J31, J41 and J42 are entered rather than the links to the user screen shown in Fig 4. Then as the formulae are entered into the remaining cells in the J column, the appearance of the values shown in Fig 3 will confirm that

	A	B	C	D	E	F	G	H	I	J	K	L	M
1													
2													
3													
4													
5													
6													
7													
8													
9													
10													
11													
12													
13													
14													
15													
16													
17													
18													
19													
20													
21													
22													
23													
24													

REMOTE ANTENNA IMPEDANCE MEASUREMENT USING RANDOM LINE LENGTH

1. TO ESTABLISH THE "SMITH CHART" LINE LENGTH

Disconnect the feeder from the antenna and terminate it with a resistive load to give an SWR of between 2:1 and 3:1. The value can be higher or lower than the feeder Z_0 . Take R+/-jX readings at the transmitter end of the line at the chosen frequency.

2. TO DETERMINE THE IMPEDANCE OF THE ANTENNA AND LINE LOSS AT ACTUAL SWR

Reconnect the antenna and take R+/-jX readings at the transmitter end of the line at the same chosen frequency.

For spreadsheet providing for up to eight sets of results use columns O to Y

Enter feeder Z_0	50.0 ohms
Enter known feeder loss	0.8 dB
Enter value of terminating resistor	120.0 ohms
Enter resistance reading	24.9 ohms
Enter reactance reading	-13.3 ohms
"Smith Chart" feeder length	0.197 λ

Enter resistance reading	22.1 ohms
Enter reactance reading	13.9 ohms
Antenna resistance	36.9 ohms
Antenna reactance	-49.2 ohms
SWR at antenna	3.08
SWR at transmitter	2.48
Feeder loss at this SWR	1.25 dB
Transmission line efficiency	75.0 %

compiled by g4jnh

Fig 1—Showing user Screen 1 with basic instructions and one column of results.

the formulae have been entered correctly.⁴ This part of the spreadsheet can be used as it stands without linking it to the user screen. That is a matter of personal choice, as is the layout of the user screens.

Using the Spreadsheet

To make meaningful use of the spreadsheet, it is necessary to make reasonably accurate measurements of resistance and reactance. I have managed to calibrate my own impedance bridge to an accuracy of $\pm 2 \Omega$ or better, for any combination from 0 to 150 Ω resistance and $\pm 60 \Omega$ reactance at frequencies up to 15 MHz. So far, I have found this adequate for my requirements. *The ARRL Antenna Book*, 17th Edition provides details of the design, construction and calibration of a suitable impedance bridge.⁵ An alternative approach is the admittance or parallel bridge, as it is sometimes called, which is generally accepted to be easier to calibrate than an impedance bridge. I would recommend to anyone contemplating constructing a bridge to study Caron's excellent article in *Communications Quarterly*.⁶

Unless you have access to a professional-grade network analyzer, it would be well worth your time to check very carefully the calibration of any measuring device to be used in conjunction with this spreadsheet. Make the checks with complex impedances as well as with pure resistance and reactance.⁷ The 17th edition of *The ARRL Antenna Book*⁸ lists several sources of error in using the Smith Chart for remote-antenna impedance measurement. This spreadsheet accounts for all such sources, except that relating to the characteristic impedance of the line, which in practical cables can evidently have a reactive component in addition to the resistive component differing to some extent from that specified. We saw earlier that it was not practical to use the known impedance values at both ends of the line to determine line loss. It was surmised that this may be due to the feeder's characteristic impedance being different from that specified. I decided therefore to make up a dummy antenna with precision components and measure its impedance at the remote end of a feeder. This would give some idea of the accuracy that could be expected using the specified rather than a measured value of the cable's characteristic impedance.

The dummy antenna comprised a 100- Ω , 1%, 0.6-W, noninductive metal-film resistor in parallel with a 150-pF,

	N	O	P	Q	R	S	T	U	V	W	X	Y	Z
1	LINE TERMINATED IN RESISTIVE LOAD TO GIVE AN SWR OF BETWEEN 2:1 AND 3:1												
2	Enter frequency	14.000	14.050	14.100	14.150	14.200	14.250	14.300	14.350	14.300	14.350	MHz	
3	Enter feeder Zo	50.0	50.0	50.0	50.0	50.0	50.0	50.0	50.0	50.0	50.0	ohms	
4	Enter feeder loss	1.0	1.0	1.0	1.0	1.0	1.0	1.0	1.0	1.0	1.0	dB	
5	Enter load res. value	20.0	20.0	20.0	20.0	20.0	20.0	20.0	20.0	20.0	20.0	ohms	
6	Enter R reading.	59.5	64.7	68.6	73.5	77.9	82.8	86.7	89.2	86.7	89.2	ohms	
7	Enter X reading	28.2	28.0	26.8	24.6	21.0	16.7	11.5	6.2	11.5	6.2	ohms	
8	"Sm. Cht." fdr. length	0.171	0.183	0.191	0.201	0.212	0.222	0.233	0.241	0.233	0.241	λ	
9	ANTENNA CONNECTED												
10	Enter antenna details G4JNH 3 element gamma matched monoband Yagi at 50 feet.												
11	Enter R reading.	70.4	69.0	65.2	60.4	54.9	47.0	41.5	34.4	41.5	34.4	ohms	
12	Enter X reading.	2.6	-4.8	-11.6	-16.4	-19.3	-19.9	-18.9	-16.5	-18.9	-16.5	ohms	
13	Antenna resistance.	36.2	38.4	41.3	43.6	45.8	50.9	54.8	64.1	54.8	64.1	ohms	
14	Antenna reactance.	12.7	14.4	17.3	20.0	22.8	26.7	30.1	37.3	30.1	37.3	ohms	
15	SWR at antenna	1.55	1.52	1.52	1.56	1.61	1.69	1.77	2.00	1.77	2.00		
16	SWR at transmitter	1.41	1.39	1.40	1.42	1.46	1.51	1.57	1.72	1.57	1.72		
17	Fdr loss at this SWR	1.08	1.07	1.07	1.08	1.09	1.11	1.13	1.19	1.13	1.19	dB	
18	Line efficiency	78.0	78.1	78.1	78.0	77.8	77.4	77.0	76.0	77.0	76.0	%	
19													
20													
21													
22													
23													
24													

Fig 2—Showing user Screen 2 with provision for up to eight columns of results and columns headed by frequency. Frequency is not involved in the calculations.

	A	B	C	D	E	F	G	H	I	J	K	L
25												
26												
27										50.000	ohms	
28										0.800	dB	
29										120.000	ohms	
30										24.900	ohms	
31										-13.300	ohms	
32										-13.300	ohms	
33										0.373		
34										2.192		
35										0.344		
36										-0.344		
37										-0.053	λ	
38										0.197	λ	
39										0.197	λ	
40												
41										22.100	ohms	
42										13.900	ohms	
43										13.900	ohms	
44										0.425		
45										2.475		
46										0.510		
47										3.085		
48										0.338		
49										0.338		
50										0.052	λ	
51										-0.145	λ	
52										-1.294		
53										36.870	ohms	
54										-49.244	ohms	
55										75.032	%	
56										1.248	dB	
57												

Fig 3—Showing the working lines for Screen 1 with values.

1%, polystyrene capacitor inside a PL-259 plug. At the test frequency of 14.150 MHz, the impedance is 36.0 $-j48.0 \Omega$. The feeder used for the test was a 30-meter length of UR67 (UK equivalent of RG-213) terminated at both ends with a PL-259 plug. Its loss as read from the standard loss graphs in the handbooks was taken to be 0.8 dB. The test to determine Smith-chart line length was conducted with terminations of both 20 Ω and 120 Ω . Both resistors were 1%-tolerance, 0.6-W noninductive metal-film units and both were incorporated into PL-259 plugs. A back-to-back double-male adapter was used to connect the PL-259 plugs containing the terminations to the PL-259 at the remote end of the cable. I realize that the PL-259s and the coupling introduce a potential source of error, but consider that the test should be representative of a practical situation in which this is the configuration most likely to be used. $R \pm jX$ readings were taken at the near end of the cable for each of the three terminations at the remote end and entered into the spreadsheet. The results are shown in Table 1.

The 120- Ω termination produced a slightly larger value for Smith-chart line length than the 20- Ω termination, although when expressed in terms of the physical length, it amounts to only 3.3 inches. The difference in Smith-chart line length produced a difference of a few ohms in the computed value of $R - jX$ for the dummy antenna. The errors relative to the known value are within what would be considered acceptable for amateur needs. If we average them, they are remarkably close to the known value: The known value is 36.0 $-j48.0 \Omega$, and the average of remote measured values is 35.6 $-j47.9 \Omega$.

It is tempting to surmise that the differences between the two derived values of Smith Chart line length were due to a difference between the specified and actual characteristic impedances of the cable or effects of the coaxial fittings. The attendant errors would be in opposite directions when one termination was lower than the characteristic impedance of the line and the other higher and that by averaging them the errors would cancel. There is room for a lot more experimentation here.

Conclusions

A spreadsheet for the remote measurement of antenna impedance has

	C	J	L
26			
27	FEEDER Zo	=K5	
28	FEEDER LOSS	=K6	
29	VALUE OF TERMINATING RESISTOR	=K7	
30	RESISTANCE READING	=K8	
31	REACTANCE READING	=K9	
32	ZERO REACTANCE IS CHANGED TO 0.001	=IF(J31=0,0.001,J31)	
33	REFLECTION COEFFICIENT AT TRANSMITTER	=SQRT(((J27-J30)*(J27-J30)+J32*J32)/((J27+J30)*(J27+J30)+J32*J32))	Eqn 6
34	STANDING WAVE RATIO AT TRANSMITTER	=(1+J33)/(1-J33)	Eqn 7
35	POSITIVE ROOT SOLUTION FOR TAN THETA	=SQRT((J27-J30*J34)/(J30/J34-J27))	Eqn 16
36	SELECT VALID ROOT FOR TAN THETA	=IF(J32>0,J35,-J35)	
37	"SMITH CHART" FEEDER LENGTH (-0.250 TO + 0.250 NOTATION)	=ATAN(J36)/2/PI()	Eqn 17
38	ADDS 0.25 TO FEEDER LENGTH WHEN LOAD RESISTOR >Zo	=IF(J29>J27,J37+0.25,J37)	
39	CHANGES FEEDER LENGTH TO ALL POSITIVE NOTATION	=IF(J38<0,0.0001,0.5+J38,J38)	
40			
41	RESTISTANCE READING	=K15	
42	REACTANCE READING	=K16	
43	ZERO REACTANCE IS CHANGED TO 0.001	=IF(J42=0,0.001,J42)	
44	REFLECTION COEFFICIENT AT TRANSMITTER	=SQRT(((J27-J41)*(J27-J41)+J43*J43)/((J27+J41)*(J27+J41)+J43*J43))	Eqn 6
45	STANDING WAVE RATIO AT TRANSMITTER	=(1+J44)/(1-J44)	Eqn 7
46	REFLECTION COEFFICIENT AT ANTENNA	=J44*POWER(10,J28/10)	Eqn 19
47	STANDING WAVE RATIO AT ANTENNA	=(1+J46)/(1-J46)	Eqn 7
48	POS. ROOT TAN THETA - TX TO SMITH CHART ZERO	=SQRT((J27-J41*J45)/(J41/J45-J27))	Eqn 16
49	SELECT VALID ROOT FOR TAN THETA - TX TO S. CH. ZERO	=IF(J43>0,J48,-J48)	
50	LINE LENGTH - TRANSMITTER TO SMITH CHART ZERO	=ATAN(J49)/2/PI()	Eqn 17
51	LINE LENGTH - ANTENNA TO SMITH CHART ZERO	=J50-J39	
52	TAN THETA - ANTENNA TO SMITH CHART ZERO	=TAN(J51*2*PI())	Eqn 20
53	ANTENNA RESISTANCE	=J27*(1+J52*J52)/(J47+J52*J52/J47)	Eqn 22
54	ANTENNA REACTANCE	=(J47-1/J47)*J27*J52/(J47+J52*J52/J47)	Eqn 24
55	TRANSMISSION LINE EFFICIENCY	=100*(1/J46-J46)/(1/J44-J44)	Eqn 28
56	FEEDER LOSS AT ACTUAL SWR	=10*LOG10(100/J55)	Eqn 29
57			

Fig 4—Showing the working lines for Screen 1 with formulae.

been presented together with the mathematical reasoning on which it is based. Line loss is fully accounted for in both determining Smith-chart line length and in deriving antenna impedance. When used in conjunction with an impedance bridge of reasonable accuracy, it removes the pain from what can be a tiresome procedure. The spreadsheet is compiled in MS *Excel* and the time invested in entering it should be repaid many times over by eliminating work with the small divisions on the Smith Chart and the risk of attendant errors. I would be pleased to hear the opinions of anyone who makes use of it.

Acknowledgments

I would like to thank Morrison, VK3BCY, and Albert, GW4DJW, for their continued interest and for stimulating discussion. As a newcomer to computing, I would also especially like to thank Mrs. Jackie Rawling for the excellent tuition I received in her IT classes at Lockton House College, without which I could not possibly have tackled this project.

Mr. Barker is a retired metallurgist and materials engineer. He never worked professionally in radio or electronics, but worked in the steel industry for 45 years. He has been interested in radio since his middle teens, but did not get a license until 1980.

Notes

¹R. D. Straw, N6BV, Editor, *The ARRL Antenna Book*, 17th edition, (Newington, Connecticut: ARRL), "Smith Chart Calculations," pp 28-1 to 28-14. The current edition (19th) also contains the information. It is Order No 8047 \$30. ARRL publications are available from your local ARRL dealer or directly from the ARRL. Check out the full ARRL publications line at www.arrl.org/shop/.

²B. Hale, KB1MW, Ed, *The ARRL Handbook*, 66th edition (Newington: ARRL, 1989), p 16-3.

³*The ARRL Antenna Book*, 17th edition, pp 27-27 (pp 27-28 in 19th edition).

⁴You can download this package from the ARRL Web <http://www.arrl.org/qexfiles/>. Look for BARKER0901.ZIP

⁵*The ARRL Antenna Book*, 17th edition, p 27-23 to 27-26 (pp 27-24 to 27-28 in 19th edition).

⁶W. N. Caron, "A Simple and Accurate Admittance Bridge," *Communications Quarterly*, Summer 1992, pp 44 to 50.

⁷When impedance measurements are made at the end of a transmission line, the change of reactance with frequency may

Table 1—Test-Load Results

Test Load

Terminating resistor value	20	120 Ω
Measured resistance	71.1	24.9 Ω
Measured reactance	j33.3	-j13.3 Ω
Smith chart line length	0.191	0.197 λ

Dummy Antenna

Measured resistance	22.1 Ω	
Measured reactance	j13.9 Ω	
Dummy antenna resistance	34.3	36.9 Ω
Dummy antenna reactance	-j46.6	-j49.2 Ω

or may not follow the normal rules depending on the particular situation. If you use an antenna analyzer that determines the sign of reactance from the way reactance changes with frequency, you need to verify the sign of the reactance with an

impedance bridge. The bridge need not be accurately calibrated since you will be getting all but the sign of the reactance from the analyzer.

⁸*The ARRL Antenna Book*, 17th edition, pp 27-28 (pp 27-30 in 19th edition). □□



SALE

Atomic Watch
hard mineral lens,
hi-tech polymer case
black leather band
\$109.95

ATOMIC TIME™

...self setting
...correct time
...atomic clock

World's most exact time...
atomic clocks, atomic watches
and weather stations

- for any time zone
- synchronized to the u.s. atomic clock in colorado
- accurate to 1sec. in 1 mil. years
- engineered in germany

complete line of atomic clocks
JUNGHANS MEGA CERAMIC Watch
JUNGHANS MEGA CARBON Watch
JUNGHANS MEGA CLOCKS
JUNGHANS SOLAR WATCHES
ATOMIC SPORTS WATCHES
ATOMIC SCHOOL/OFFICE CLOCKS
ATOMIC INDUSTRIAL CLOCKS
Oregon Scientific Weather Stations,
Weather Forecast, World Time, NOAA
Radios, Radio Controlled Clocks...

call for our FREE Brochure
or go to www.atomictime.com
credit card orders call toll free
1-800-985-8463
30 Day Money Back Guarantee
send checks incl. s&h \$6.95 to
ATOMIC TIME, INC.
1010 JORIE BLVD.
OAK BROOK, IL 60523



atomic dual alarm
clock w. temperature
day and date, black
3.5x4.5x2
\$29.95



atomic radio with
2 alarms and
temperature,
day, date, LCD
\$39.95



jumbo digit atomic
clock w. temperature
& day and date, wall
or desk 8.5 x8.5 x1
• \$49.95



NEW

Junghans atomic
carbon, stainless bezel,
sapphire lens LCD day,
date - carbon/leather
band • \$279.00



black arabic 12 wall
clock for home or
office • \$59.95
(wood \$69.95)

A Flat Impedance Bandwidth for any Antenna

For a single-band antenna, you can match across an entire band with a few components and eliminate a bulky and expensive general-purpose matchbox. Come see how.

By Grant Bingeman, KM5KG

I have been using a simple lumped-parameter technique in the commercial-broadcast industry for 20 years. It passively matches an antenna input impedance to the transmission-line impedance over a wide frequency range. We can call this the “no-tune antenna.” For example, the 80-meter Amateur Radio band extends almost $\pm 7\%$ about 3750 kHz. This article will show you how to design a passive network that can transform an existing SWR of greater than 2.0 to about 1.2 from 3500 to 4000 kHz. This eliminates the need to adjust an impedance matching box with every frequency change, or eliminates the

expense of an autotuner (of particular concern to QRO operators). The broadband matching technique also minimizes transmission-line losses and stress by maintaining a good match across the operating band.

To clearly demonstrate this broadband matching technique, assume the antenna has a relatively narrow impedance bandwidth, such as an electrically short vertical monopole. For the sake of simplicity, let’s ignore wire and ground losses, guy wires, insulators and so on. A 15-meter tall, 20-cm diameter, base-insulated monopole has the bandwidth characteristic shown in [Table 1](#), when resonated at the base with a 3.7- μH series-connected coil.

Note that the [Table 1](#) SWR is not equal at the band edges, relative to

3750 kHz. For the broadband matching technique to work best, we want to select a middle resonant frequency that will create equal band-edge SWRs. By inspection of [Table 1](#), we know that 3750 kHz is a little high (the upper-band-edge SWR is smaller than the lower-band-edge SWR), so let’s try 3725 kHz resonated with 3.8 μH . As shown in [Table 2](#), the actual band center of this particular antenna is a bit below both the arithmetic (3750 kHz) and geometric (3742 kHz) means of the band edges. The loaded Q of the antenna is only about $86.6/19.0 = 4.6$, but the band-edge SWR is quite sensitive to the resonating inductance (3.7 versus 3.8 μH when comparing [Tables 1](#) and [2](#)). This means that the success of any impedance broadband matching effort relies on the stability of the an-

1908 Paris Ave
Plano, TX 75025
drbingo@compuserve.com

tenna impedance and the components used to match it to the transmission-line impedance. For example, a wire antenna supported by a wandering balloon would not be a good candidate for impedance broadband matching.

After resonating, the next step in broadband matching this antenna is to match the band-center impedance to the transmission-line impedance, which we will assume is 50 Ω. Keeping in mind that we want to maintain symmetrical impedances at the input to the matcher, we will try a lagging 85° T network that is resonant at 3750 kHz (see Fig 1).¹ This will rotate the antenna impedances to the other side of the Smith chart as shown in Fig 2 and Table 3. The band-edge SWRs are not perfectly equal, but they are close enough. The input resistances to the T network are about equal, and the input reactances are about equal and opposite in sign. Thus they are balanced and symmetrical, which is necessary if we expect the broadband-matching technique discussed in this article to work well.

After impedance rotation, the last step in this process is to insert a special broadband matching L network in front of the T network that will flatten the overall system SWR considerably. This L network consists of a parallel-resonant tank circuit in shunt, and a series-resonant circuit between this shunt and the T network. This simultaneously forms a leading-phase-shift L network at 3500 kHz (Fig 3) and a lagging-phase-shift L network at 4000 kHz (Fig 4), while remaining essentially invisible at the resonant frequency of 3750 kHz. The desired L network reactances are listed in Table 3. The shunt arm of an L network is always on the high-resistance side of the impedance transformation; in this case, the left or 50-Ω side.

The broadband matching L network's shunt tank has a loaded Q of 13.6, and the series tank has a loaded Q of 5.9. Thus the circulating currents and voltages are quite high, and careful component selection and placement are necessary. Fig 5 indicates a total RF power loss of 4%. Adding the loss of 1% in the T network, the total loss is about 5%, which translates as a 2% reduction in radiated field intensity. This is a small price to pay for a no-tune antenna, especially when we consider the initial high SWR values.

Sometimes a better design for a parallel-resonant tank can be obtained by

using a series-resonant circuit transformed by a 90° network or transmission line. That is, an antiresonant (parallel-resonant) circuit looks like a series-resonant circuit displaced 90 electrical degrees (opposite sides of the Smith chart).²

All the circuit analysis in this article has assumed a coil Q of 800 and a capacitor Q of 1000, which can be obtained with 1.0-cm-diameter tubing coils and vacuum capacitors. The current in the shunt tank is quite high in a 1-kW system, and 2.0-cm tubing is recommended for its coil, which will actually turn out to be a short strap across the capacitor bank. Less expensive, lower-Q capacitors may be used with the understanding that efficiency will drop and the capacitance value may be sensitive to temperature. However, any additional losses only serve to improve bandwidth, so a few more watts lost may certainly be worth the money saved. Be sure to provide adequate air circulation to deal with the extra heat loss. Also, research the temperature coefficient of the specific capacitors you are considering.

I mention component Qs to remind you that not only do you need to be concerned about the voltage and current ratings of your components, but also the temperature ratings. If you are operating a broadband matching network in a high ambient air temperature or in direct sunlight, especially in

a weatherproof box, you may want to derate your components. RF voltage breakdown is inversely proportional to air temperature. A weatherproof box should be designed to allow some air circulation. A screened inlet port beneath the box and a rain-protected outlet vent around the topsides of the box provide a good solution.

Notice that the tank circuits have been designed around the average L network band-edge reactances. Some iteration of component values can yield a better impedance bandwidth overall than the situation described in Table 4, but this is best done during the adjustment process rather than on paper. As an exercise, the reader may wish to juggle component values to see how he or she can reduce the 3500-kHz SWR without compromising the middle- and upper-band SWRs listed below. This is a problem ideally suited to an iterative optimizer program, which could probably reach an excellent solution in a few seconds on a modern computer. Recall that we started with band-edge SWR values of 5.05 and 3.83 in Table 1, so we have already come a long way. If the initial SWR values had been lower, the tank circuits would have had lower Qs, lower circulating currents and voltages and so forth. However, I chose an extreme example to highlight the caveats

(Continued on page 17.)

Table 1—Antenna Resonated at 3750 kHz with 3.7-μH Series Coil

kHz	Input Z (Ω)	Resonated Z (Ω)	SWR	Antenna Height
3500	15.9 -j112.0	15.9 -j31.2	5.05	63.0°
3750	19.0 -j86.6	19.0 + j0.0	1.00	67.5°
4000	22.6 -j62.6	22.6 + j29.8	3.83	72.0°

Table 2—Antenna Resonated at 3725 kHz with 3.8-μH Series Coil

kHz	Input Z (Ω)	Resonated Z (Ω)	SWR
3500	15.9 -j112.0	15.9 -j28.3	4.50
3725	18.7 -j89.1	18.7 + j0.0	1.00
4000	22.6 -j62.6	22.6 + j33.1	4.40

Table 3—L-Network Reactances

kHz	Shunt X (Ω)	Series X (Ω)	T Input Z (Ω)	SWR
3500	26.4	-37.3	10.9 + j16.7	5.13
3750	infinity	0	49.6 + j0	1.01
4000	-28.9	39.8	12.5 -j18.1	4.55

¹Notes appear on page 17.

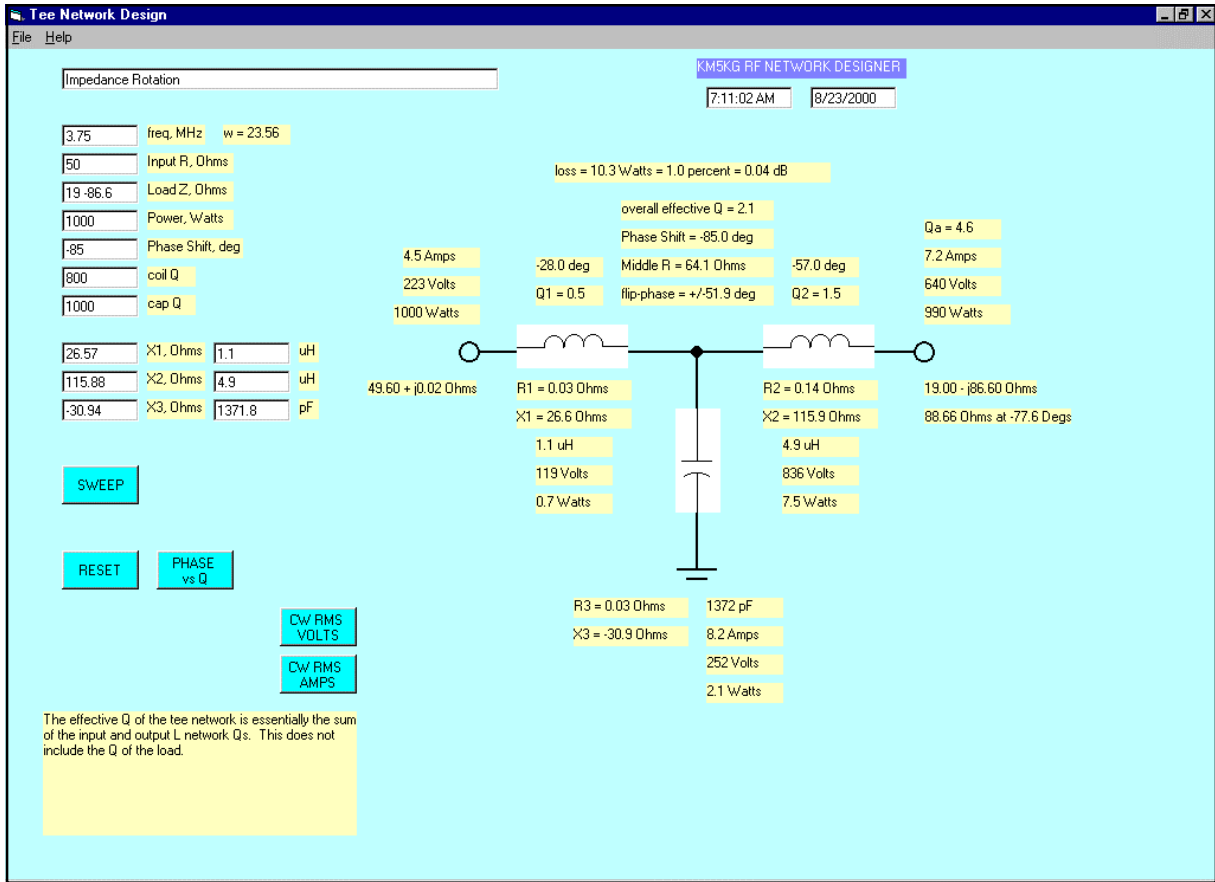


Fig 1—The “T-Network-Design” page of KM5KG’s RF-design program.

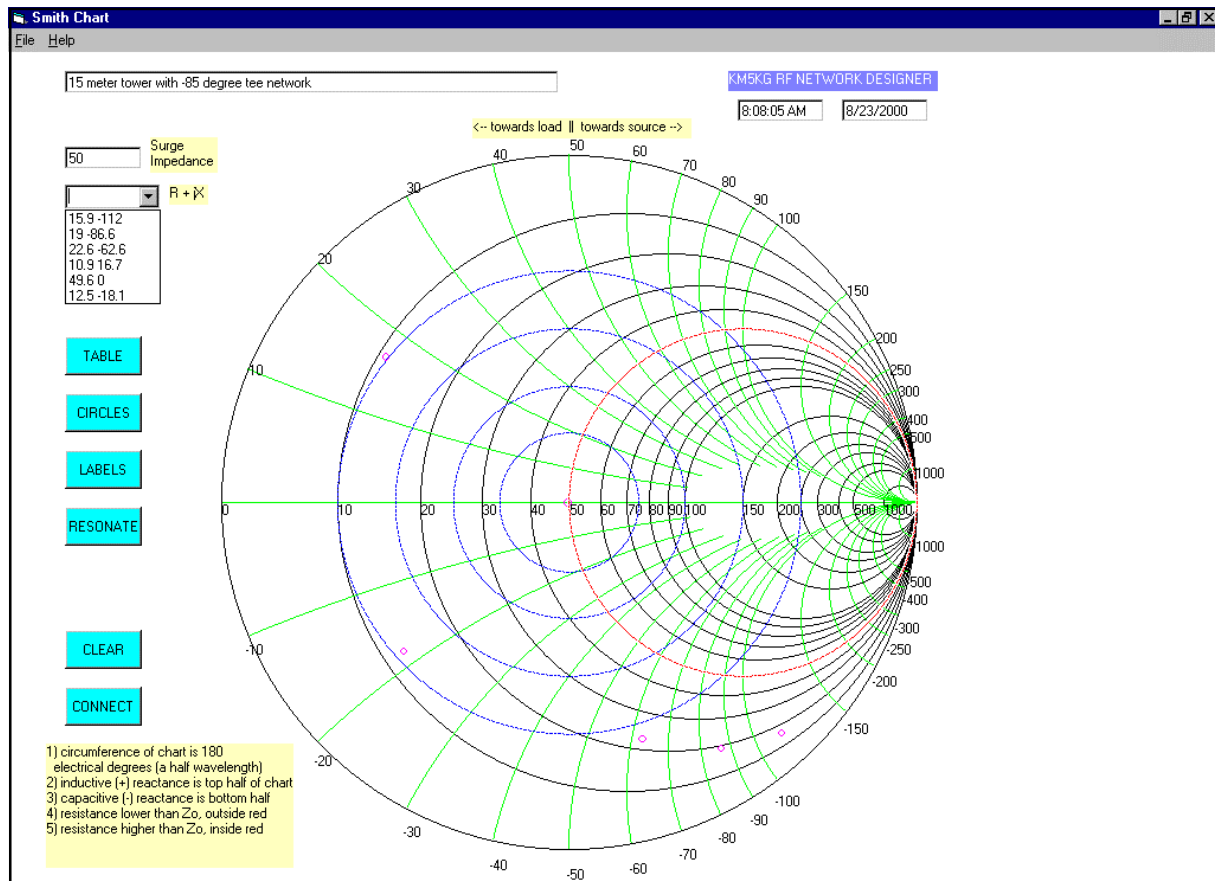


Fig 2—The “Smith-Chart” page of KM5KG’s RF-design program.

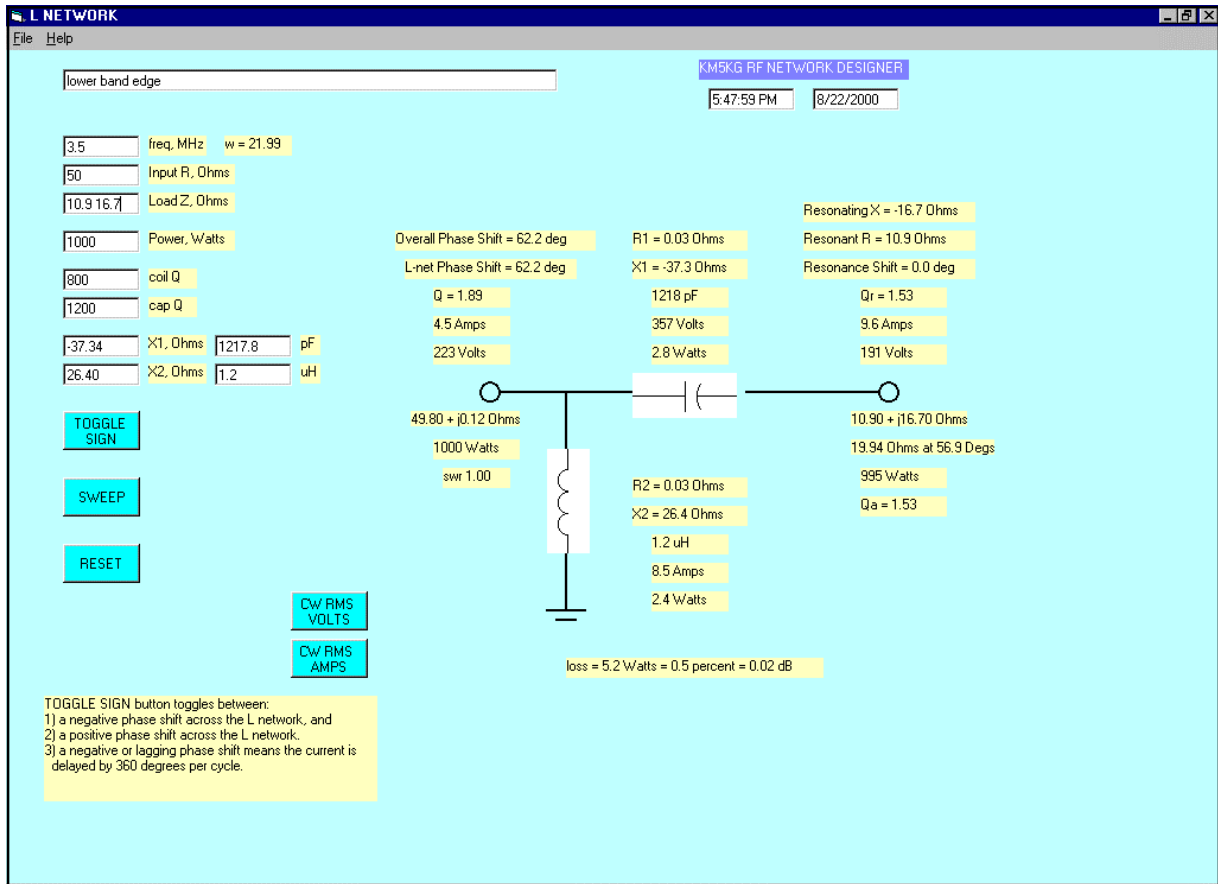


Fig 3—The “L-Network-Design” page of KM5KG’s RF-design program for the described network at 3.5 MHz.

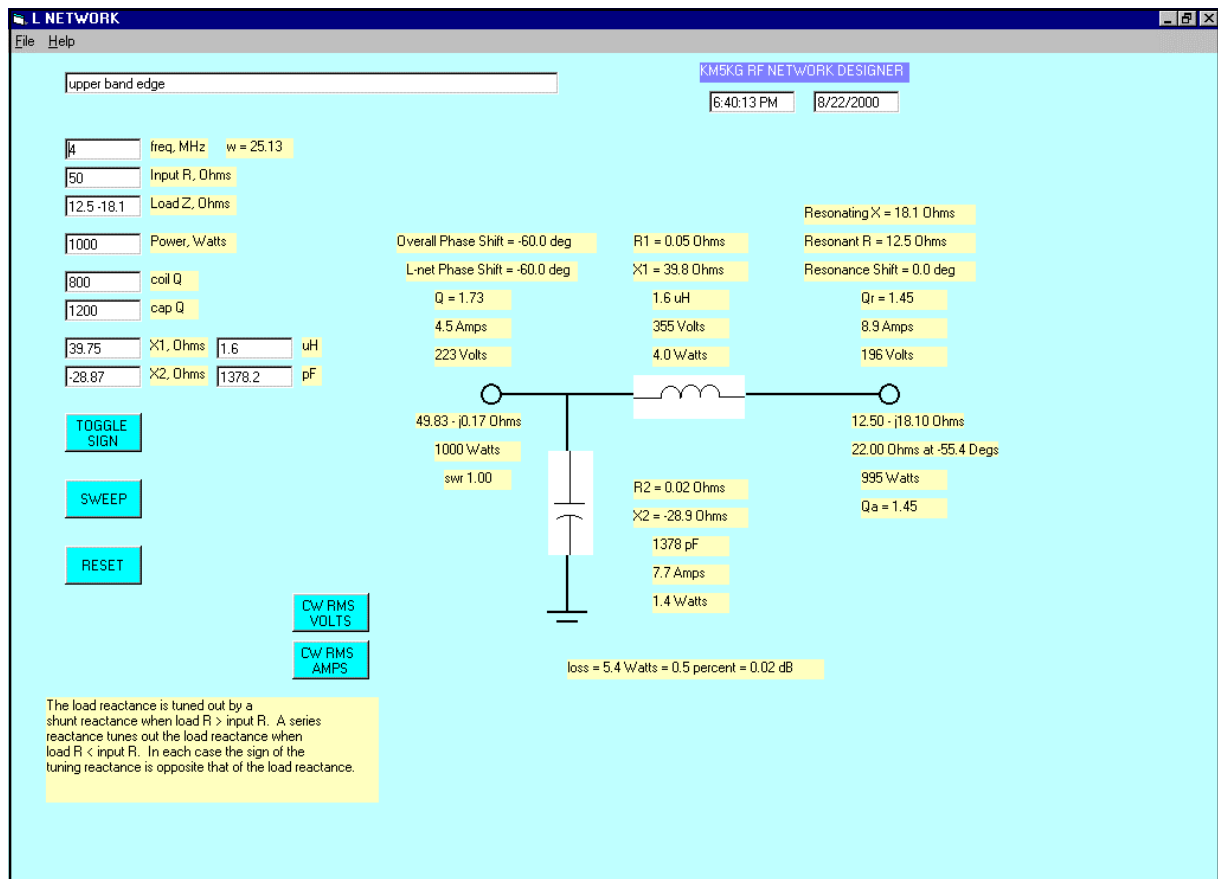


Fig 4—The “L-Network-Design” page of KM5KG’s RF-design program for the described network at 4.0 MHz.

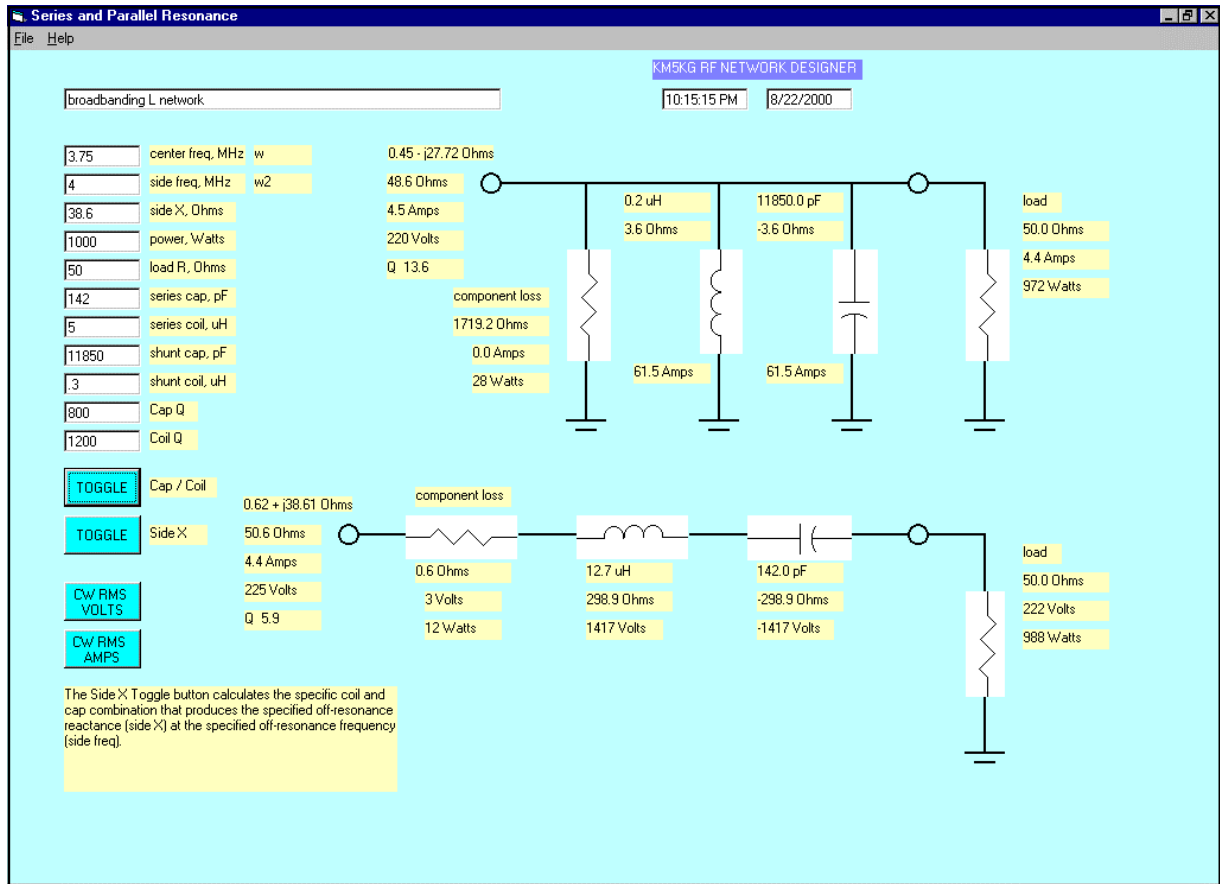


Fig 5—The "Series and Parallel Resonance" page of KM5KG's RF-design program.

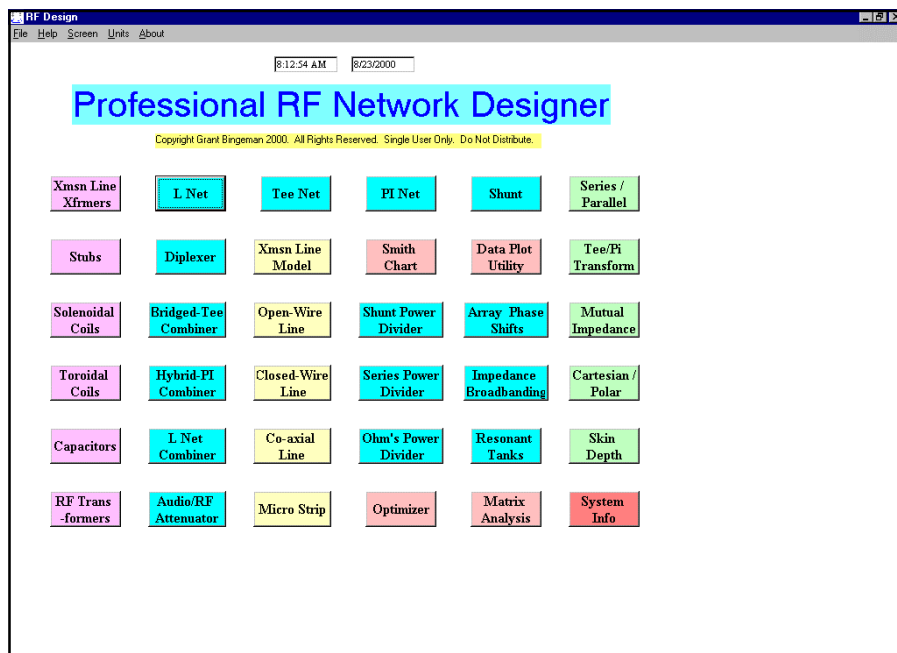


Fig 6—Functions available in KM5KG's RF-design program.

(Continued from page 13.)

of this broadband-matching scheme.

Radiated Power

When a transmitter delivers RF power to an antenna via some impedance-matching and transmission-line arrangement, it is that power (minus some small component losses) that gets radiated by the antenna regardless of the SWR of the system. This means that there is no such thing as an SWR "bottleneck" in an RF transmission system. So long as the transmitter is "happy" with the load it "sees," it doesn't matter if the SWR somewhere else down the line is less than ideal, since the power still gets radiated, less whatever heating losses may exist.

When an antenna is operated over a wide frequency range, its radiation efficiency may be greater at some frequencies than at others; but this is more of a pattern-bandwidth question, not so much an impedance-bandwidth question. The antenna example described in this article produces essen-

Table 4—System Overall Z

kHz	Input Z (Ω)	SWR
3500	$46.2 + j25.3$	1.69
3750	$47.0 + j9.2$	1.22
4000	$44.7 + j3.7$	1.15

tially the same field intensity from 3500 to 4000 kHz for a given power input. The practical reality is that this short monopole has a slightly greater efficiency at 4000 kHz, but earth losses are higher at this end of the band, so the effects oppose each other.

Summary

The resonant-tank L network technique for impedance broadband matching essentially eliminates the need for an adjustable matcher for antennas dedicated to a limited frequency band. High circulating currents and component voltages limit the practical range of the technique. First increase the bandwidth of the antenna using conventional means,

such as increasing the physical thickness of the antenna elements, or perhaps top-loading. In general, uncorrected antenna band-edge SWRs of as much as 5.0 can be accommodated, assuming a band-center SWR of 1.0. Naturally, component costs and stresses are lower when starting with lower uncorrected band-edge SWRs.

Notes

¹The stress analysis in Fig 1 is for 1000 W input, CW RMS voltage and current. A demonstration of the Windows98 RF-design program that generated the screens in this article is available at www.qsl.net/km5kg. The demo allows unlimited use of the L, T, π , shunt, resonant tank and Smith chart functions shown as in Fig 6.

²G. Bingeman and W. Jamieson, "Field Test Results of a New Phase/Amplitude Correction System for AM," 1984, NAB 38th Annual Broadcast Engineering Conference Proceedings.

[Editor's note: More information about antenna broadband matching techniques and generating the networks can be found in T. Cuthbert, Jr's *Circuit Design Using Personal Computers*, (New York: John Wiley & Sons, 1983). The book conveniently formulates work originally done by R. Fano—KF6DX] □□



Join the effort in developing Spread Spectrum Communications for the amateur radio service. Join TAPR and become part of the largest packet radio group in the world. TAPR is a non-profit amateur radio organization that develops new communications technology, provides useful/affordable kits, and promotes the advancement of the amateur art through publications, meetings, and standards. Membership includes a subscription to the *TAPR Packet Status Register* quarterly newsletter, which provides up-to-date news and user/technical information. Annual membership US/Canada/Mexico \$20, and outside North America \$25.

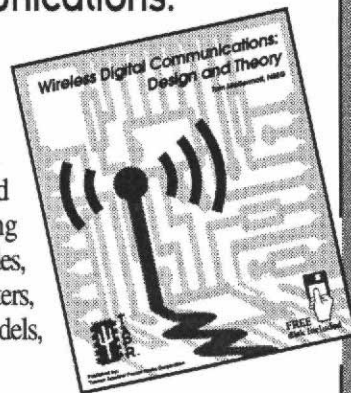


TAPR CD-ROM

Over 600 Megs of Data in ISO 9660 format. TAPR Software Library: 40 megs of software on BBSs, Satellites, Switches, TNCs, Terminals, TCP/IP, and more! 150Megs of APRS Software and Maps. RealAudio Files. Quicktime Movies. Mail Archives from TAPR's SIGs, and much, much more!

Wireless Digital Communications: Design and Theory

Finally a book covering a broad spectrum of wireless digital subjects in one place, written by Tom McDermott, N5EG. Topics include: DSP-based modem filters, forward-error-correcting codes, carrier transmission types, data codes, data slicers, clock recovery, matched filters, carrier recovery, propagation channel models, and much more! Includes a disk!



Tucson Amateur Packet Radio

8987-309 E. Tanque Verde Rd #337 • Tucson, Arizona • 85749-9399
Office: (940) 383-0000 • Fax: (940) 566-2544 • Internet: tapr@tapr.org www.tapr.org
Non-Profit Research and Development Corporation

160-Meter Propagation: Unpredictable Aspects

*Are you likely to work 160-meter DX today?
It's very difficult to say. Come learn why.*

By Robert R. Brown, NM7M

The sun is the main driving source of the ionosphere, through its ultraviolet (UV) radiation, which illuminates an entire hemisphere. A specific force is the solar wind, which interacts with the outer reaches of the geomagnetic field to form the magnetosphere. The geomagnetic field, however, is a major factor in organizing the ionosphere at lower altitudes. It controls the motions of ionospheric electrons on release by photo-ionization; and by its configuration, it shapes the global distribution of ionization, particularly at low latitudes.

The nighttime ionosphere results largely from geomagnetic control of ionization that remains after sunset, because of its low rate of recombination at high altitudes. There is also a forcing factor from the intermittent occurrence of aurora, with magnetospheric electrons accelerated to high energies going down the high-latitude field lines; those create ionization at E-region altitudes. At lower latitudes, F-region ionization decreases at night, but is maintained at low levels between the E-region and F-region peak because of UV in starlight, galactic cosmic rays and solar UV radiation scattered by the geocorona.

Communication on the upper-HF bands of the Amateur Radio spectrum is largely under direct solar control.

Propagation predictions are made using refraction calculations based on global ionospheric maps for the F and E regions, as in Figs 1 and 2. The F-region map shows geomagnetic control by the fact that the critical frequencies $foF2$ from the ionization are asymmetrical with respect to the geographic equator at the equinoxes. Also, there is the unusual distribution of critical frequencies in the F region, which shows that ionization extends

into the hours of darkness at low and equatorial latitudes.

Fig 2 shows the daytime critical frequencies that result from the distribution of ionization about the sub-solar point at E-region altitudes. That is of little consequence to propagation on the higher bands of the spectrum, as the operating frequencies there are large compared to the critical frequencies foE , as well as the electron-neutral collision frequencies F_c . The

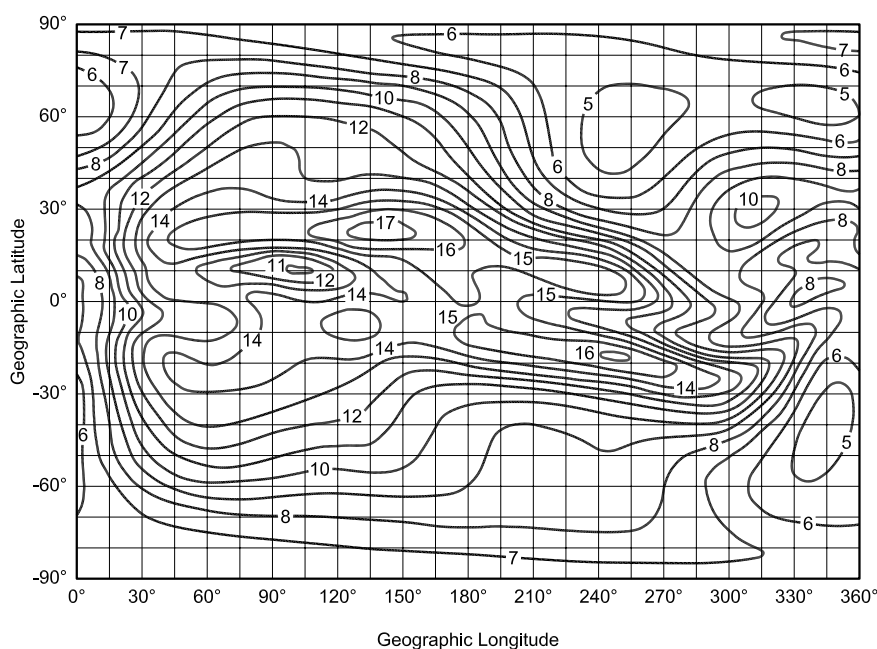


Fig 1—Global $foF2$ map for 0600 UTC, March 1979. (SSN-137, after Davies, Note 9).

result is that signals go through the E region with little deviation and only small amounts of ionospheric absorption along their paths.

All in all, HF propagation can be dealt with using only a few parameters: the sunspot number or a suitable surrogate, the planetary geomagnetic K-indices or their short-term estimates and the announcements of bursts of solar and magnetic activity. The first two of those parameters essentially give what can be expected on average and the update material provides additional guidance when conditions depart significantly from predicted averages.

The situation is quite different on the lowest band of the Amateur Radio spectrum, 1.8-2.0 MHz. There, signals propagate at altitudes around the E region, but operations occur only at night because of the heavy ionospheric absorption during daytime. Beyond that, there is more than enough ionization overhead to propagate signals in that frequency range, so critical frequencies or *MUFs*—so important at the top of the HF spectrum—are of no concern. Instead, signal propagation is considered limited largely by absorption and noise.

Even at the solar minimum, sunspot numbers are sufficient to guarantee propagation on the lowest band of the spectrum. There are second-order effects that result from the sunspot number: A small increase in the radiation angle that RF must have to penetrate past the E region to permit longer F-hops and ducting. In addition, there is a small increase in D-region ionization, which increases ionospheric absorption. Both of these effects are quite within the realm of prediction and thus are easily understood and dealt with.

Nonetheless, consideration of average parameters is something of an over-simplification of the situation, as it does not recognize various propagation modes possible at low frequencies for given parameters. They, in turn, can be affected by the dynamics of the neutral atmosphere. So, with propagation being a geometrical affair, rays are refracted as they travel through the ionosphere and anything that affects the geometry of ionospheric regions relative to the earth will have an impact on signal modes.

In that regard, the phrase “relative to the Earth” has a lot of meaning as the atmospheric motions are relative to the Earth, while the ionizing radiation comes from well outside the propagation region—say, auroral elec-

trons spiraling down relatively fixed magnetic-field lines, or solar photons on their straight-line paths from the distant sun. Thus, the level of ionization is more related to the amount of matter traversed by the incoming radiation and the neutral density, as distinct from geodetic altitude.

The atmosphere, being a target for such radiation, will present a different geometry relative to the Earth’s surface for wave refraction as air parcels in the target region are moved about by high-altitude winds. Those can be seen in the motions of visible trails and radar reflections from meteors, or expected from heating and vertical expansion of the atmosphere at sunrise. In addition, auroral energy will be transferred to the atmosphere as heat with the incidence of auroral ionization, say, during magnetic storms. Thus, levels of constant ionization density may move up or down or may even become tilted. All of those have an effect on the refraction process by bending rays vertically, to increase or decrease the lengths of paths, or horizontally, to skew them one way or the other, but away from regions of greater ionization. All those aspects of refraction can be expected to occur in the nighttime propagation of 160-meter signals, around the E region where E-hops, E-F-hops, F-hops and ducting can take place.

In addition to density changes at a given geodetic altitude from mass motions, there is the question of atmospheric composition, particularly the role of some minor constituents that are man-made. Among others, those in-

clude nitric oxide (NO), which is a by-product in the exhaust of jet engines and carbon dioxide (CO₂), which results from the widespread use of fossil fuels. Those minor constituents are created in specific locations, but their presence is related to transport through atmospheric circulation, making them highly variable in their concentrations.

Water vapor and ozone are two other trace constituents that are highly variable because of transport, but they are produced continually by the effects of solar radiation: heating of the oceans in the first instance and photodissociation of molecular oxygen, a major constituent of the atmosphere, in the second. Beyond its importance to atmospheric processes, ozone is of particular interest concerning the lower ionosphere, as it is transparent to visible radiation but opaque to UV. Thus, it limits the UV photo-ionization of the neutral atmosphere and photo-detachment of electrons, firmly bound to negative ions, at low altitudes around sunrise and sunset.

Ionospheric Variability

While 160-meter signals are propagated at heights between the bottom of the D region and the lower F region, it is of interest to first look at the variability found in measurements of parameters throughout the ionosphere and how they affect hop lengths and critical frequencies in the spectrum. Then we can consider how often observations are made related to those results in the ionosphere and compare them to observations for those aspects

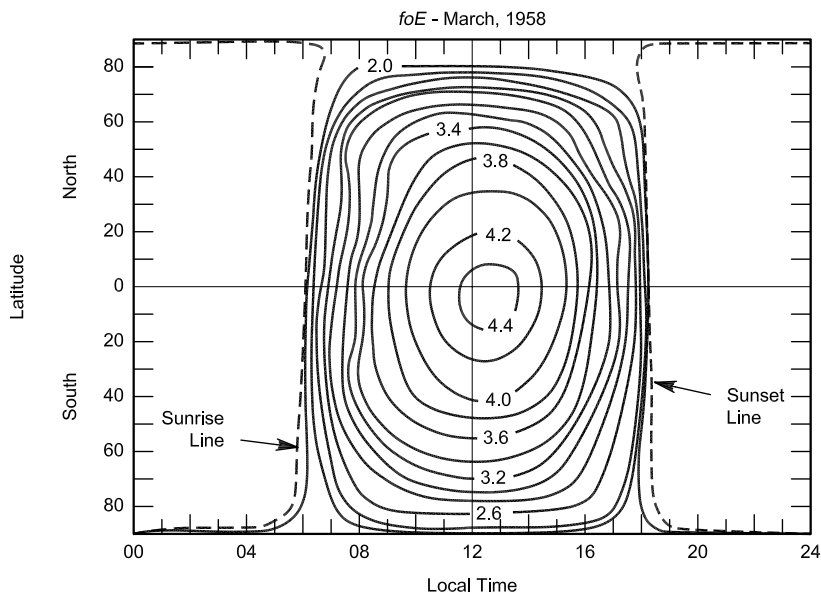


Fig 2—Global foE map at local noon, March 1958. (SSN-201, after Davies, Note 9).

of the neutral atmosphere that affect 160-meter propagation.

First, we note the principal ionospheric measurements that bear on Amateur Radio operations are critical frequencies, $foF2$ for the F region and foE in the E region. Concerning the F region, ionospheric variability is found in the records of ionosondes, as in Fig 3, which shows $foF2$ values for the hours of the day from ionosonde observations at Slough, England, in January 1969.¹ That figure shows the location of the median (50%) value of $foF2$ for each hour and the IONCAP prediction program makes use of the lower (90%) decile and upper (10%) decile values, which come from similar observations. Those are used with paths to predict the frequencies above which a path is open 27 days of the month (FOT) or only 3 days of the month (HPF), respectively, while the median (50%) value is used to find the MUF for the path.

Fig 3 shows there are departures of $foF2$ from the monthly median (50%) curve throughout a day. In that regard, observations show that the amount of departure from the median value varies not only with time of day but also with location and season, being the greatest in the middle of winter night. In addition, ionosonde records show that virtual heights $h'(f)$ of reflection for a given frequency f vary with location, sunspot number, whether it is day

or night, the season in the temperate zones as well as at low and high latitudes. While one of the IONCAP methods does give statistical values for FOT, MUF and HPF for any path, other statistical variations—say for the critical frequencies and virtual heights—are not given in the methods (1 and 2) of the IONCAP program, which deal with local ionospheric parameters.

Time Variations of Ionospheric Parameters

Another limitation of the IONCAP program is that it only gives predictions at hourly intervals. As a result, nothing is available for shorter periods and the predictions will not show if variations occur on a shorter time scale, say in one of the standard propagation parameters, MUF(3000), the maximum usable frequency for a 3000-km path centered on a given location. That information can be obtained from ionosondes by using shorter sounding intervals; Fig 4 shows soundings taken at five-minute intervals that would apply for the MUF on a 3000-km path centered at Brighton, Colorado, in February, 1981.²

The MUF(3000) variations in Fig 4 show oscillations with the MUF values having periods ranging from 20 to 30 minutes that would not be predicted from the hourly intervals in IONCAP and other prediction programs. Those variations may result from waves propagating through the ionosphere,

as suggested by the virtual-height data shown in Fig 5. There, ionosonde data at five-minute intervals, from fixed frequencies near the critical frequency $foF2$, show wave-like variations with the maxima and minima of virtual heights appearing later at lower frequencies (heights).

That particular data set suggests an apparent vertical downward velocity component of about 160 m/s, while the time variations in Fig 4 suggest a wavelength in the range 240 to 360 km. Taken together, the data in Figs 4 and 5 indicates that the main effects of those waves propagating through the F region are a variation of the layer height and—to a lesser degree—of the electron density.

As noted above, programs like IONCAP and the URSI and CCIR databases provide average values of ionospheric variables on an hourly basis. They are more indicative of the slow variations in the ionization levels from solar illumination as the earth rotates beneath it. Accordingly, they reveal none of the ionosphere's more dynamic aspects (which are of internal origin) and how they affect propagation. Since the sounding programs that provided the data on which they are based have long since been terminated, there is little chance to obtain further input to correct the shortcomings noted here.

Atmospheric Gravity Waves

The ionosonde data like those given

¹Notes appear on page 25.

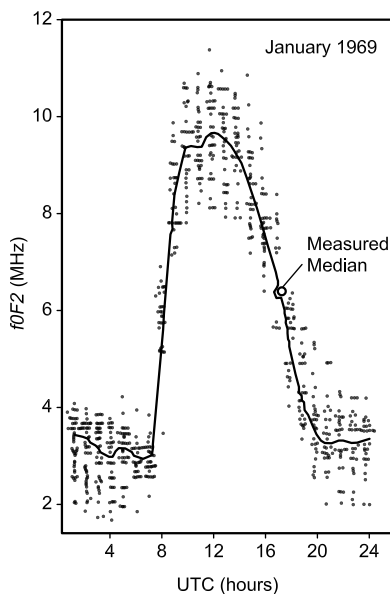


Fig 3—Ionospheric variability shown by $foF2$ soundings from Slough, England (after Piggott and Rawer, Note 1).

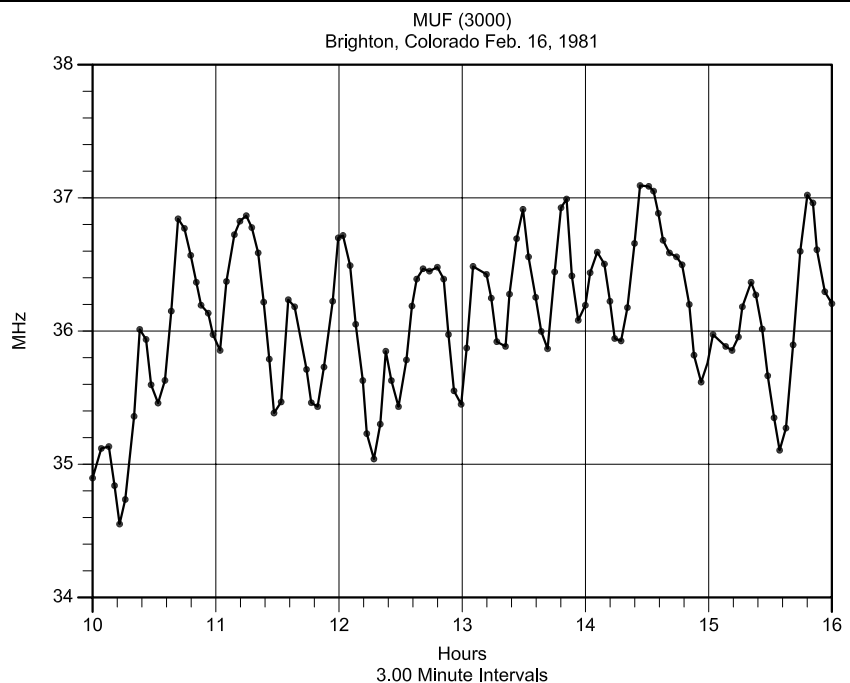


Fig 4—Temporal variations of MUF(3000) (after Paul, Note 2).

in Figs 4 and 5 support the hypothesis that F-region variations are caused by atmospheric gravity waves (AGW) with varying amplitudes, which are present all the time. Other data, from more singular events such as auroral substorms, show the presence of AGW at ionospheric heights in different ways, with equator-ward motions from the site of their origin along the auroral zone. Thus, virtual-height recordings in Fig 6 (from 10 ionosondes after the onset of an auroral substorm³) show the wave-like propagation of an F-region disturbance that advances from high latitudes in both hemispheres toward the equator. A linear-regression analysis of the first wave crest's advance gives equatorward speeds of 810 m/s and 790 m/s in the southern and northern hemispheres, respectively.

From standard magnetometer and riometer observations at the time of the auroral substorm in Fig 6, the observations were found to be consistent with large-scale traveling ionospheric disturbances (TID) that originated at auroral latitudes in both hemispheres and covered about 60° in longitude. While details of the mechanism at the source are unknown, it seems most likely that the origin of the TID was the AGW, from atmospheric heating with the deposition of energy at auroral heights by the influx of the energetic electrons at the onset of the substorm.

In regard to energy deposition by auroral particles, each pass of the NOAA-12 satellite gives a measure of auroral activity level as well as hemispheric power input (in gigawatts) that is deposited in the hemisphere's auroral zone. Such observations are available at www.sec.noaa.gov/today.html and cover the range from quiet (less than 1 GW) to major storm (greater than 500 GW). In addition, an array of sensors on the NOAA POES satellite displays the fluxes going down into the atmosphere, for electrons with greater than 30 keV, 100 keV and 300 keV. The more energetic electrons penetrate down to levels where 160-meter signals are propagated as well as into the lower D region⁴ and may affect the level of ionization there, depending on the level of auroral activity.

More generally, though, AGW are transverse waves that propagate in the neutral atmosphere and are maintained by gravity and buoyancy, but damped by viscosity. As shown above, they can be seen from the traveling disturbances (TID) they generate in the ionosphere. Sources of AGW⁵ include

not only heating from the precipitation of energetic electrons at auroral altitudes noted above, but also from other large expenditures of energy at lower altitudes. These include tropospheric turbulence, stratospheric winds from weather systems and geological events

such as earthquakes and volcanic eruptions.

The large-scale AGW, with periods from 1 to 3 hours and speeds of 500 m/s in the horizontal direction, seem to originate in auroral regions. The medium-scale AGW come up from

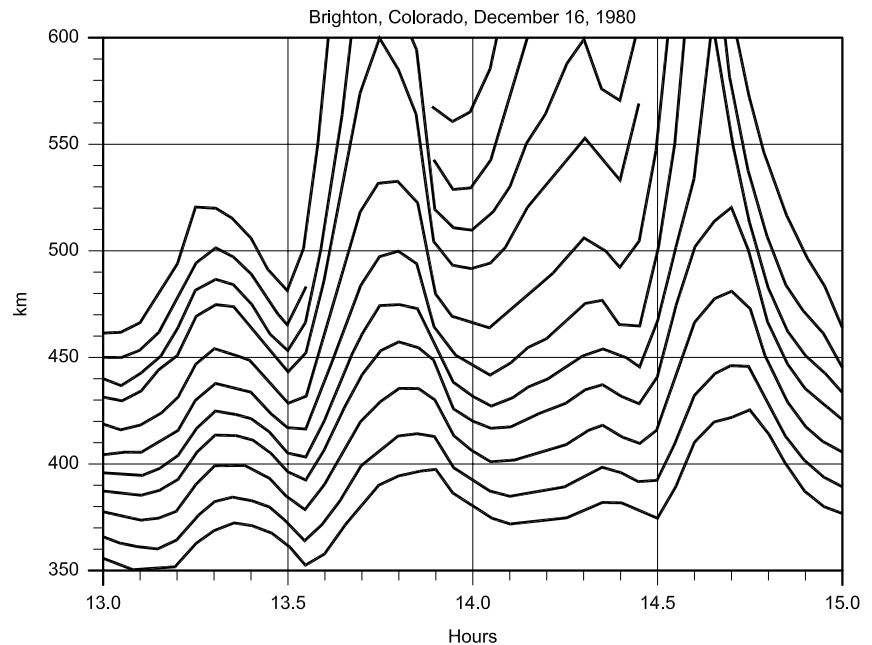


Fig 5—Virtual height variations at fixed frequencies (after Paul, Note 2).

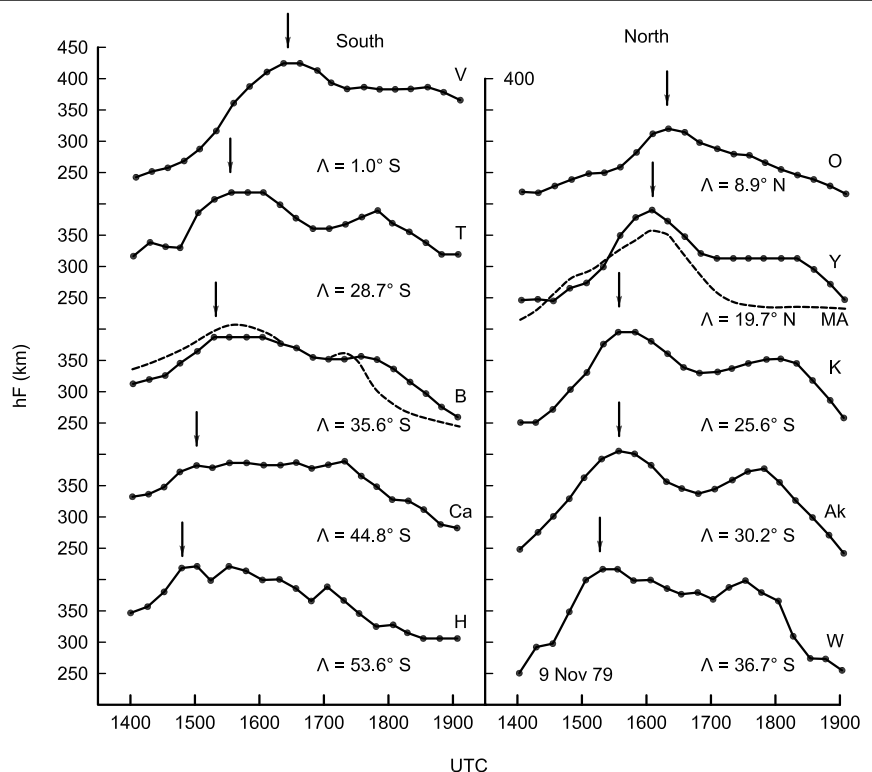


Fig 6—Variations in the virtual height of the F-region, following the onset of the substorm in the Southern and Northern hemispheres (after Hajkowicz, Note 3).

below the ionosphere, have periods between 20 and 45 minutes and speeds from 80 to 450 m/s. Small-scale AGW, with short periods (2-5 minutes) and speeds the order of 300 m/s, are associated with regions of wind shear and atmospheric turbulence. As shown by the virtual height data in Figs 5 and 6, large-scale AGW affect the height of higher ionospheric regions, thus having a significant effect on the geometrical aspects of HF wave propagation.

The same is probably true of the lower F region and the E region, where 160-meter and other MF signals are propagated. Thus, there will be variations in electron density levels at a given geodetic height, as well as density variations from AGW, which produce tilts of the surfaces of constant electron density. Those will contribute to the variability of ionospheric modes through changes in hop length as well as the initiation and termination of ducted signals.

Ionospheric Absorption

Beyond the availability of signals, which is more related to variations of propagation modes and the spatial distribution of ionization than the average electron densities, another matter is ionospheric absorption: a concern at the 160-meter and MF parts of the radio spectrum. Absorption results from collisions between electrons in the lower ionosphere and neutral constituents. For a given frequency, it depends on how the product of the electron density, N , and collision frequency, ν , vary with height. In that regard, an estimate of the effective collision frequency as a function of height is given in Fig 7.

While signal strength for a given frequency depends largely on the propagation mode—say, earth-ionosphere hops as compared to ducting—additional signal losses result from paths traversing the lower D region between ground reflections. At lower altitudes, Fig 7 shows the collision frequency varies as the neutral particle density and for 160-meter and MF propagation, the lower region is most important since the $N\nu$ product is the largest there. In addition, it is the most variable because of changes in the electron density from dusk to dawn, dawn being when signals reach their greatest strength.

The signal loss at a given height depends on the electron density in the lower D region and according to the International Reference Ionosphere (IRI90),⁶ that can differ by as much as a factor of two between dusk and

dawn. That serves to make the absorption greater at dusk by that factor. The IRI does not deal with details of the ionospheric processes, only the results of many years of ionospheric sounding.

The Role of Negative Ions

Conversely, laboratory data⁷ and observations of low-frequency propagation⁸ indicate a higher electron density at dusk compared to dawn. The lower electron density around dawn results from electron attachment to molecules, forming negative ions with a high electron affinity. The presence of atmospheric ozone serves to maintain negative-ion attachment until solar UV reaches the D region on rising above the ozone layer (see Note 8). Nothing similar is found at dusk, and the negative ions formed in the D region as the sun sets apparently have lower electron affinities and undergo detachment processes from visible light until in full darkness.

Now, current theoretical considerations indicate that the formation of negative ions depends on the series of ionic reactions summarized in Fig 8. There, we can see that it starts with electron attachment to molecular oxygen and then proceeds toward the right of that figure by processes which depend on minor atmospheric constituents. In that regard, for propagation purposes, the left-hand side of the figure can be considered as the start, at sunset. Electrons attach to molecular oxygen and ion reactions then proceeding toward the right-hand side, ultimately giving the final, stable ions

in the dawn ionosphere.

Close examination of the figure shows the various steps in which ozone (O_3), carbon dioxide (CO_2), nitric oxide (NO) and hydrogen (H) are involved. The actual availability of those minor constituents depends on vertical and horizontal transport processes in the atmosphere, starting from the photo-dissociation of molecular oxygen, vehicle exhaust, use of nitrogen fertilizer and the water vapor. Thus, in the course of a night, those molecules can combine with the simple negative ions of oxygen after sunset and develop into bicarbonate ions (HCO_3^-) and nitrate ions (NO_3^-), which hold their electrons closely.

It is possible that progress of ions from left to right in that figure may be subject to bottlenecks caused by a lack of one or more minor constituents. At one time or another, there may be a low density of ozone here or nitric oxide there, at one place or another. All that means that the lower ionosphere, where 160-meter propagation takes place, is not always a uniform region—either in composition or in ionization—during the hours of darkness. Indeed, going from the sunset terminator to the sunrise terminator, slow development of the negative ions that hold electrons closely has consequences for low-frequency and 160-meter propagation.

Thus, negative-ion species mutate from one with a low electron affinity (less than 0.5 eV) at sunset to another with a large electron affinity (greater than 4.5 eV) at sunrise. This means that kinetic detachment of electrons by

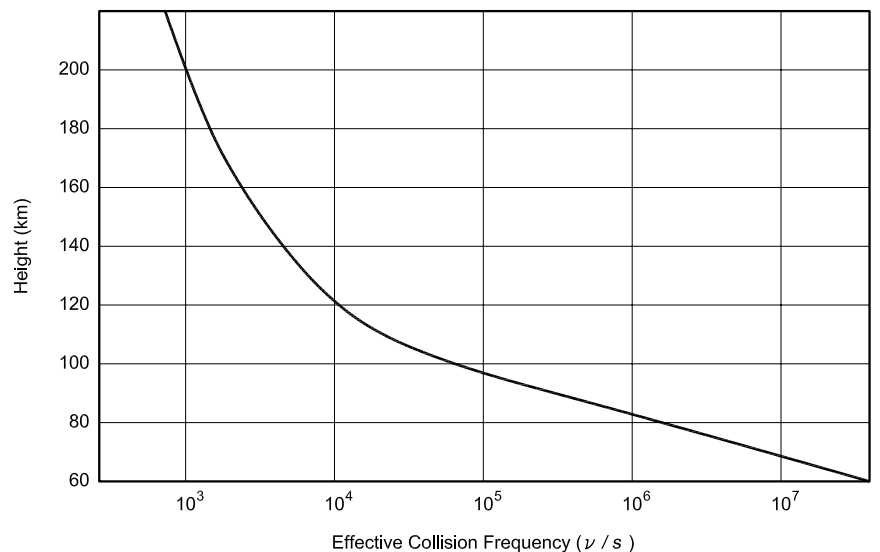


Fig 7—Effective electron-neutral collision frequency in the lower ionosphere.

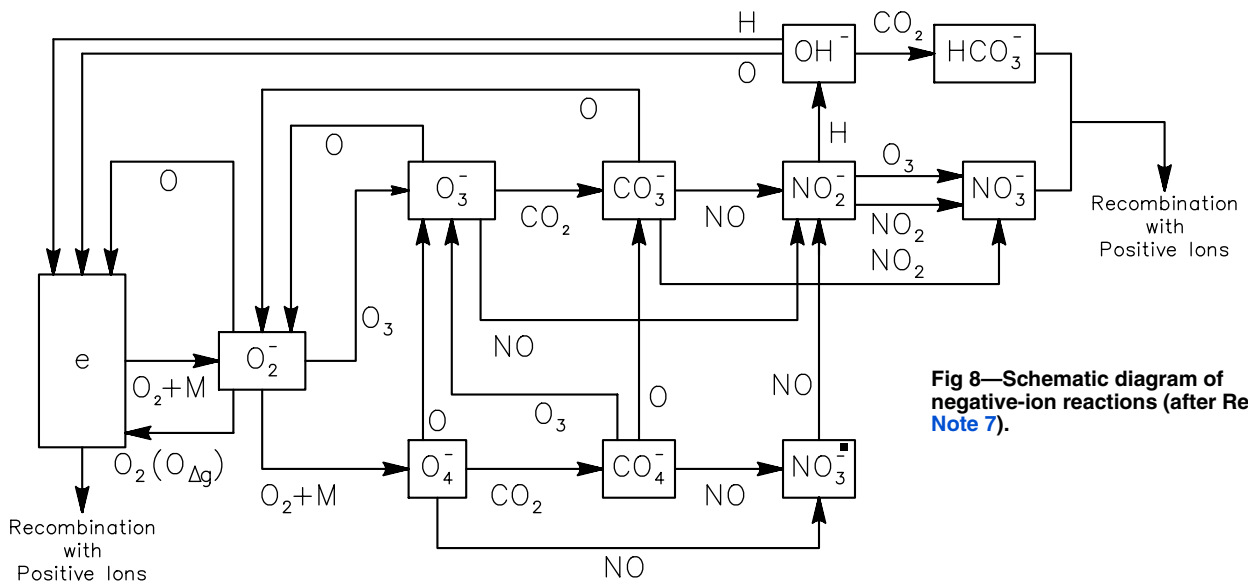


Fig 8—Schematic diagram of negative-ion reactions (after Reid, Note 7).

atomic oxygen at sunset would serve to yield a significant electron population in the D region. Only as atomic oxygen production comes to a halt after sunset would negative ions start to form, albeit slowly, and begin to decrease the electron density in the lower D region. Accordingly, signal absorption on 160 meters would be greater in the hours after dusk than sunrise.

Electron Detachment

There is one bright side to this picture, which is related to the greater electron affinity of negative ions near the sunrise terminator. It requires solar-ultraviolet radiation to photo-detach electrons from those negative ions at sunrise. Therefore, the sunrise on the D region with visible radiation is not effective in detaching electrons held by the negative ions. Studies of LF propagation (see Note 8) show that UV detachment is delayed about 15-20 minutes relative to sunrise with visible radiation, as the solar UV must surmount the ozone layer. That gives DXers a bump, as it were: DX signals last a bit longer before catastrophic D-region absorption sets in.

That was the good news; the bad news is that the ozone layer is quite variable in space and time, so one DXer could enjoy the benefit of the ozone delay, while another might not. That is also quite unpredictable, not only because of the variability of the ozone distribution, but also because the ozone layer, being concentrated at a lower altitude than the D region, casts its shadow on the traversal of

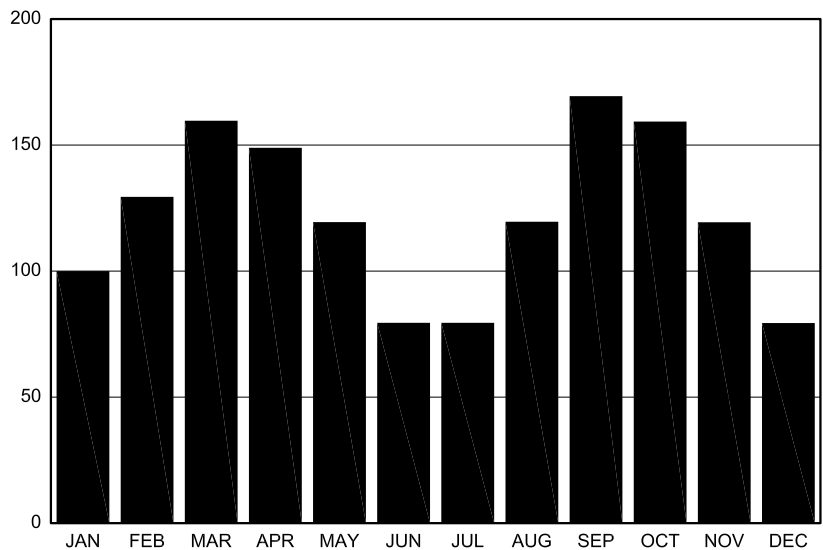


Fig 9—Monthly distributions of major magnetic storms from 1868 through 1992.

signals through the D region from a distance of several hundred kilometers away, in the direction of the rising sun. Atmospheric conditions at such distances would be completely unknown to the DXers and in addition, each path would have the sun rising on the D region at a rather different bearing, compounding the matter.

Seasonal Effects

DXing on 160 meters is done primarily in the winter months when there is a greater probability of darkness on paths of interest. Of course, that brings

up the question: Are there any seasonal effects that should be noted, predictable or otherwise? In that regard, long-term magnetic records show that magnetic storming is most probable at the equinoxes and least predictable at the solstices, as shown in Fig 9.

That is a statistical summary of magnetic disturbances, a result of observations over many decades. At any given time, the situation may depart from the average because of the current level of solar activity, coronal mass ejections (CME) and streams of solar wind from coronal holes or flares. So,

about the best guidance for 160-meter DXing is to log the indices of magnetic activity as they occur and look for a recurrence of the quiet conditions that go with low indices with the next solar rotation. Nevertheless, sporadic events may still disrupt DXing.

With meteorological factors affecting propagation, features of weather systems may be involved in the winter months. Wind shears and turbulence produce irregularities in the electron distribution up to 90 km in the D region, as noted by Davies⁹ concerning the forward scatter of VHF signals. Those irregularities would affect the distribution of ionospheric electrons in the region, one way or another and with all the predictability of weather.

Beyond D-region electron-density distributions, there are also effects of minor constituents in that region, which are affected by seasonal variations. In that regard, the negative-ion chemistry shown in Fig 8 is subject to the distribution or availability of minor constituents. Of particular interest are ozone (O₃) and nitric oxide (NO), which advance the ion chemistry reactions to the right toward more stable negative ions.

As noted earlier, transport processes play an important role in the distribution of ozone and, day by day, its distribution is quite dynamic. On the average, however, ozone has a seasonal maximum in the spring in the Northern Hemisphere.¹⁰ One type of dynamic event in winter is sudden stratospheric warming, and motions of the atmosphere during those events produce major rearrangements of chemical species such as ozone. In that regard, ozone flows from its site of production at low latitudes to middle and high latitudes, the flow sloping downward toward the pole. That flow is responsible, in part, for the increase in total ozone content at high latitudes.

The seasonal changes in the ozone distribution were quite evident in the LF study (see Note 8), which showed the importance of negative ions in the dawn ionosphere. The changes presumably play a significant role in negative-ion formation in the lower D region between dusk and dawn. The variation of negative ions from dusk to dawn serves to reduce the electron density in the D region. Thus, one can say that any increase in ozone density with a sudden stratospheric warming would decrease ionospheric absorption at night, not increase it.

Nitric oxide (NO) is another minor constituent of the atmosphere that is

involved in negative ion formation. There is also a seasonal variation in its formation and circulation, with NO being formed from atomic nitrogen released at E-region altitudes during auroral bombardment.¹¹ The NO is then carried pole-ward by meridional circulation; as it cools, it descends and the circulation returns it equator-ward. NO has a long lifetime around the dark, winter polar cap. With the return circulation, part of the NO spills out at mid-latitudes and is responsible for the “winter anomaly”¹² in absorption that is found on medium frequencies during daylight.

In that case, the NO becomes an additional target for solar UV and when ionized on illumination, serves to increase the electron density in the D region. There is a great deal of folklore about the negative effect of the winter anomaly on DXing in amateur circles. Unfortunately, those who continue to promulgate that idea fail to realize that it is an effect when the ionosphere is illuminated, not during darkness on paths when DXing is done.

Contrary to that negative aspect, circulation of additional NO would add to its role in the formation of negative ions with large electron affinities during time of darkness in the D region. Like the case with ozone, that would serve to reduce the electron density in the lower D region and serve to lessen any absorption rather than increase it.

The ideas dealing with meteorological aspects of 160-meter propagation cannot be related to many observations at the altitudes of interest. Instead, what measurements of the neutral atmosphere that do exist are for lower altitudes: ground-based observations of temperature, pressure and winds, or else satellite views of weather systems from cloud-cover and infrared data. In short, the features of 160-meter propagation where the neutral atmosphere comes into play are essentially unknown to DXers. Consequently, there is little to use in anticipating what propagation would be like. For that matter, even what constitute average conditions are essentially unknown: So the question as to the departure from normal conditions is moot.

At this time, the only method that works reasonably well applies to predictions on paths that go to high latitudes; it involves logging the level of magnetic activity and looking for recurrences. That is based on the effects of long-lived solar streams that sweep by the Earth. It works reasonably well from late in a solar cycle to the rise to-

ward greater solar activity in the next cycle. During the peak of solar activity, magnetic activity is more related to individual solar outbursts—say, coronal mass ejections (CME) and flares. So any propagation planning is strictly short-term in nature, using announcements from the NOAA Web sites on the Internet.

Summary

Propagation in the upper HF spectrum results from the ionization of the atmosphere on a global scale by the sun, which is a strong but variable source of radiation. In addition, the slow recombination of electrons and positive ions at high, F-region altitudes contributes to the duration of the ionization, while its distribution is largely controlled by the geomagnetic field, another agent of global dimensions. Those ideas are well understood and propagation resulting from them proves to be quite predictable when bursts of solar and magnetic activity are taken into account.

In contrast to that situation, propagation at the lower Amateur Radio spectrum results from steady but weak sources of ionization: UV in starlight, galactic cosmic rays and solar radiation scattered into the dark hemisphere by the geocorona. The distribution of that ionization near the E region is subject to altitude and density variations from two sources:

- Motions of the neutral atmosphere caused by atmospheric gravity waves
- Vertical and horizontal transport of minor constituents, which play a role in negative ion formation

The principal role of the geomagnetic field at the low end of the spectrum is to provide an efficient propagation mode by means of ducting in the ionization valley that develops just above the E region at night. Of course, magnetoionic theory shows that wave polarization is important there too, and non-reciprocity of paths becomes important because of polarization mismatches between waves and antennas.

Also, as another example, ray-tracing calculations (see Note 4) with the *PropLab Pro* software show that ducting is more likely on ray paths that are quasi-longitudinal. That is, close to the direction of the geomagnetic field lines, rather than on paths that are quasi-transverse to the field. Thus, signals from the lower magnetic latitudes may be ducted quite efficiently toward higher latitudes, while those in the return direction are more likely to be propagated as lossy earth-iono-

sphere hops because of the large magnetic dip angle where they originate. Along the same line, there can be large losses in getting waves in and out of the ionosphere, from mismatches in power coupling between antenna polarization and limiting wave polarizations on entrance to and exit from the lower ionosphere. That proves to be particularly important when using vertically polarized antennas for E-W propagation at low latitudes.¹³

Finally, in the HF case, the few parameters available and activity updates on solar-terrestrial conditions generally prove to be sufficient for the purpose of propagation predictions. At the low end of the spectrum, other than activity updates, the magnetic indices and satellite measurements of the power input by auroral electrons are about all that are available. They serve only to show when high-latitude paths might be subject to more absorption from auroral ionization, path skewing from that same source of ionization or the precipitation of radiation belt electrons at lower latitudes during magnetic activity.

However, perturbations of the neutral atmosphere from transport processes and atmospheric gravity waves along propagation paths affecting ionization density, heights or path geometry, cannot be predicted or dealt with. There are just no measurements being made that bear on the questions. In that regard, one is left with the conclusion that meteorological factors make 160-meter propagation even more unpredictable than the weather itself for the lack of observations, especially since not even average conditions are well documented.

Notes

- ¹W. R. Piggott and K. Rawer, *URSI Handbook of Ionogram Interpretation and Reduction, Report UAG-50*, World Data Center A for Solar-Terrestrial Physics, Boulder, Colorado, 1975.
- ²A. K. Paul, "Medium Scale Structure of the F Region," *Radio Science*, Vol 24, No. 3, 1989, p 301.
- ³L. A. Hajkovicz and R.D. Hunsucker, "A Simultaneous Observation of Large-Scale Periodic TIDS in Both Hemispheres Following an Onset of Auroral Disturbances," *Planetary Space Science*, Vol 35, No. 6, 1987, p 785.
- ⁴R. R. Brown, "Signal Ducting on the 160 Meter Band," *Communications Quarterly*, Spring 1998, p 65.
- ⁵R. D. Hunsucker, "The Sources of Gravity Waves," *Nature*, Vol 328, No. 6127, 1987, p 204.
- ⁶D. Bilitza, International Reference Ionosphere (IRI 90), NSSDC 90-22, National Space Science Data Center, Greenbelt, MD, 1990; nssdc.gsfc.nasa.gov/index.html.

- ⁷G. C. Reid, "Ion Chemistry of the D-region," *Advances in Atomic and Molecular Physics*, Vol 12, (San Diego: Academic Press, 1976).
- ⁸R. R. Brown, "Atmospheric Ozone, a Meteorological Factor in Low-Frequency and 160-Meter Propagation," *Communications Quarterly*, Spring 1999, p 97.
- ⁹K. Davies, *Ionospheric Radio*, (London: Peter Peregrinus Ltd, 1989).
- ¹⁰M. L. Salby, *Fundamentals of Atmospheric Physics*, (Academic Press, 1996).
- ¹¹R. R. Garcia, Susan Solomon, Susan K. Avery and G.C. Reid, "Transport of Nitric Oxide and the D-Region Winter Anomaly," *Journal of Geophysical Research*, Vol 92, 1987, p 977.
- ¹²E. V. Appleton and W.R. Piggott, "Ionospheric Absorption Measurements during a Sunspot Cycle," *Journal of Atmospheric and Terrestrial Physics*, Vol. 3, 1954, p 141.
- ¹³R. R. Brown, "Demography, DXpeditions and Magneto-Ionic Theory," *The DX Magazine*, Vol X, No. 2, March/April 1998, p 44.

References

- A. Brekke, *Physics of the Upper Polar Atmosphere*, (New York: Wiley & Sons, 1997).
 R. R. Brown, "Unusual Low-Frequency Signal Propagation at Sunrise," *Communications Quarterly*, Fall 1998, p 67.

Bob Brown was first licensed as WGPDN 1937-1941; he was KA6PTT 1981-1982; N7DGZ, 1982-1985 and became NM7M in 1985. He holds an AB (1944) and a PhD (1950) in Phys-

ics from the University of California.

He was an Instructor of Physics at Princeton University and then Professor at Physics at the University of California, 1950-1982. Bob retired from UC Berkeley in 1982. He has done research on high-energy cosmic rays, solar-proton and auroral-electron bombardment of the polar atmosphere, ionospheric absorption at high latitudes, auroral X-rays in conjugate regions of the geomagnetic field.

Bob's professional publications include over 80 scientific papers in refereed journals, from 1944 through 1982, and a review article, "Electron Precipitation in the Auroral Zone" Space Science Reviews, 1966. His ham columns are "Propagation and DX" in QRP Quarterly, "Over the Horizon," in The Canadian Amateur and "Propagation" in Worldradio. He has written numerous propagation articles for The DX Magazine, Communications Quarterly and the Low Band Monitor. Bob's "Long-Path Propagation," was published privately in 1992. "The Little Pistol's Guide to HF Propagation," was published by Worldradio Books in 1995. His current interest is the role of atmospheric effects in 160-meter propagation. □□

RIGblaster

rig to sound card interfaces

RIGblaster and a computer

the powerful replacement for old expensive adapters or TNC's.

PSK31

MFSK

MT63

RTTY (FSK or MFSK)

Club announcements

Repeater controller

CW (key or MCW)

Contest Voice Keyer

Voice or CW MS

Keyer

SSTV

Packet-APRS

Hellschreiber

AMTOR

Remote Base



New PLUS	\$119.95	
M8, M4, RJ	\$89.95	
NOMIC	\$34.95	

<http://www.westmountainradio.com>

West Mountain Radio de N1ZZ and K1UHF

18 Sheehan Avenue, Norwalk, CT 06854 (203) 853 8080

The Art of Making and Measuring LF Coils

Large, high-quality coils are an important factor in working the LF bands successfully. This short note on the specific art describes good quality-factor coils ($Q \approx 600$) for 136 kHz.

By Paolo Antoniazzi, IW2ACD, and Marco Arecco, IK2WAQ

The “new” band of 136 kHz in Europe and the “lower” 160-190 kHz band in the USA are to be considered a good mix between the old fascinating era of Marconi antennas (plus specific grounding topics) and the technologically advanced world of DSP and related high-precision spectrum and noise analysis. Combining modern PC processing capability with very interesting old-style experimentation on big coils and big vertical antennas with

capacitive hats, we can obtain unique results (see Ref 4). A very simple transmission circuit to start operation at 136 kHz is shown in Fig 1.

The circuit includes an audio power amplifier commonly used in high-quality TV sets: the TDA7265 made by STMicroelectronics.¹ The PC board and heat sink are shown in Fig 2 and complete technical information is available on the Web site (www.st.com). The typical output power of the amplifier at audio frequencies is 25 W with 4- Ω speakers; but at 136 kHz, the output power drops to 3-4 W, maximum. This power is more than adequate for LF system tests, generating up to 0.5 A of antenna current.² The transformer, T1, is constructed on a

standard FT101-43 one-inch toroid core and is used to match the specified 4- Ω load to the 16-20 Ω total resistance of the antenna system (antenna + coil + ground). To check the complete system, a relatively simple antenna is used, with a vertical (Marconi) rod of 7-10 meters isolated from ground using a plastic plate. About 40-50 meters (130-160 feet) of horizontal wires (hat) are connected atop the Marconi antenna to realize a 450 pF total antenna capacity. This establishes a near unity ratio between the top and base currents in the antenna (Fig 3). As you can see from the diagram (from Ref 1), the radiation resistance of our antenna at 136 kHz is very low: about 0.03 Ω . For comparison, the height for a similar antenna at 14 MHz would be 7-10 cm!

Paolo Antoniazzi, IW2ACD
cia Roma 18
Sulbiate (Milano), Italy
paolo.antoniazzi@st.com

Marco Arecco, IK2WAQ
Cia L. Einaudi, #6
20093 Cologno Monzese, Italy

¹Notes appear on [page 32](#).

More complete technical documentation on the big antennas is available in the paper of Ref 1 (Monster Antennas). The ground connection is another big problem at LF, but if you have a country house with a big garden, you don't normally have a ground problem. As is well known, earth is inherently a rather poor conductor, with normal resistivities in the range of 10-300 Ω per meter, and the conductivity of the metal constituting the grounding rod is not very important.

The ground resistance R_G can be pictured as the resistance resulting from a series of equally thick concentric earth shells around the ground rod. With a typical 3-meter rod, half of the resistance is contained within a cylinder of 12-cm radius around the rod (Ref 3). The only way to reduce the ground resistance is with the addition of multiple electrodes. Adding more ground rods reduces the grounding resistance, but the gain is less for each additional rod. That is, the final resistance for many rods is greater than the value obtained by simply dividing the resistance of a single rod by the number of parallel connected rods. A single 3-meter rod of 16 mm diameter driven into soil with 100 Ω /meter average resistivity will have a ground resistance (measured at 50-60 Hz) of 30-50 Ω . Using four parallel rods placed at 10-15 m in a square will give a final LF resistance of 10-15 Ω . At 136 kHz, the inductance of the connecting cables is not important, but we must use a big wire to avoid skin-effect resistances. As seen in Table 2 for 42x0.18 mm Litz wire, we have only a 0.0164 Ω /meter dc resistance (probably less than 0.5 Ω of RF resistance for a 10-meter connection cable).

When using four or more parallel ground connections, the resistance of the wires is not very important. In our tests, two 4-meter-deep rods and two 2-meter-deep rods were used at a distance from the common ground point (at the base of the Marconi vertical antenna) of 10-15 meters. The measured value of our ground resistance at 136 kHz is $R_G = 12-14 \Omega$. The system's total load resistance seen by the output transformer is:

$$R_L + R_G = 4.3 \Omega (\text{coil}) + 14 \Omega (\text{ground})$$

$$\approx 18 \Omega \text{ or about } 4 \Omega \text{ as an amplifier load}$$

(Eq 1)

The very poor efficiency of any short vertical Marconi system can be calculated simply using the expression :

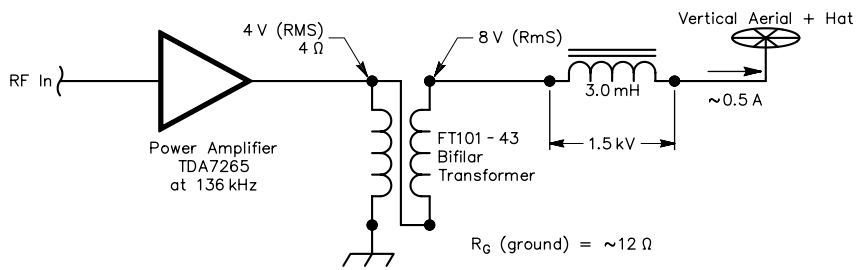


Fig 1—A simple 136-kHz linear amplifier using a low-cost monolithic IC.

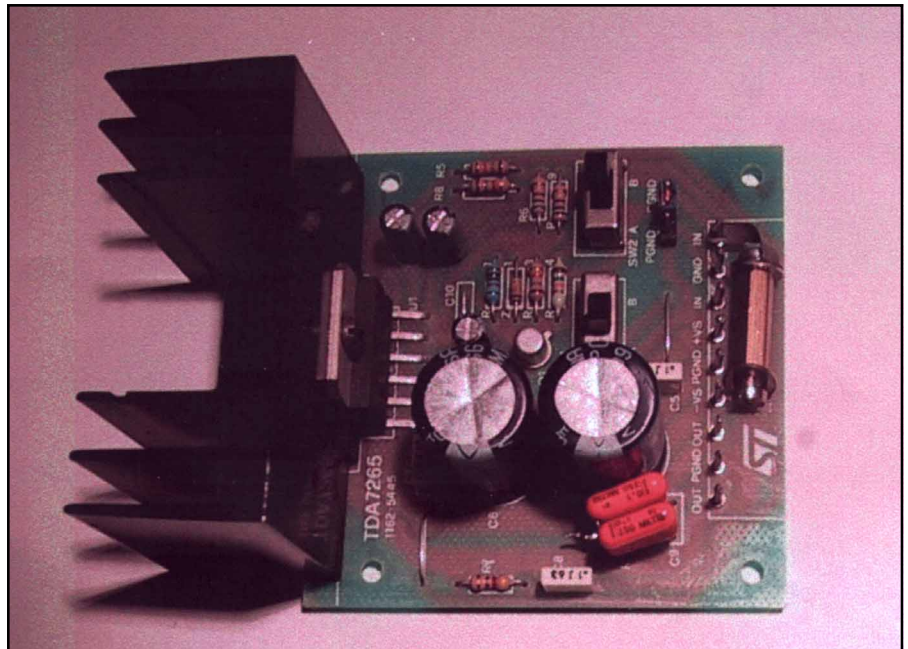


Fig 2—The ST board designed for 25-W stereo high-quality audio for TV (TDA7265).

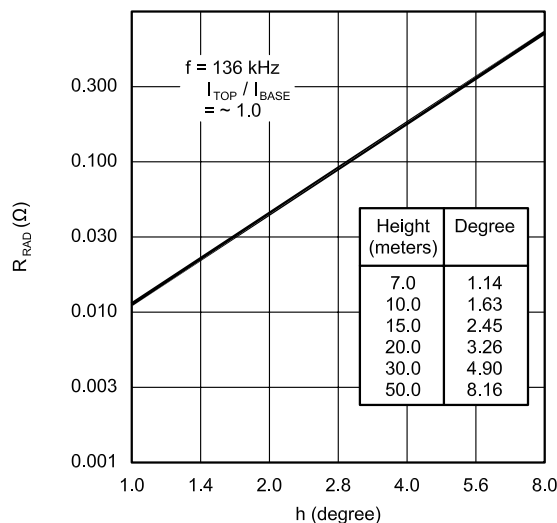


Fig 3—Radiation resistance versus height of Marconi vertical antennas plus capacity hat.

$$\text{Efficiency} \approx \frac{R_R}{(R_L + R_G)} \quad (\text{Eq } 2)$$

where

R_R = Radiation resistance (see Fig 3)

R_L = Coil resistance

R_G = Ground resistance

The Coils

The load coils used in LF transmitters must have a very high quality factor, Q , or a low equivalent series resistance (for example, $R_{AC} < 5 \Omega$) so as to reduce the transmission losses.

$$Q = \frac{(2\pi fL)}{R_{AC}} \quad (\text{Eq } 3)$$

where

f = frequency (kHz)

L = inductance (mH)

R_{AC} = LF equivalent series resistance (Ω)

As stated in the introduction, because of the very low antenna efficiency and the relatively high resistance of the Earth ($R_G \approx 10$ to 15Ω , see Fig 4), the use of low- Q coils is not practical.

The losses that affect the quality factor of LF coils are:

- Skin effect of wires
- Proximity effect between turns of winding
- Lossy dielectric of the distributed capacitance
- Lossy coil form material (such as gray PVC).

In the following, we will consider in more detail both the skin and the proximity effects in the RF windings. Now, we limit our discussion by writing that skin-effect problems are avoided by using Litz wire (which is many thin, insulated wires connected together at the ends). We take this opportunity to remind that, to manufacture some monster antennas, 3.5-inch Litz wire (9-cm diameter!) has been used. The dielectric losses are related to the material used to insulate the conductor—enamel, for instance—of the winding. In any case, this kind of loss is very small considering the total tuning capacitance for LF resonance.

During the beginning phase, we tried a gray PVC tube as a form. This tube is often employed in the manufacture of buildings. This was the worst case we found: Table 3 compares the Q of coil L01 with the other coils wound on wood and air.

The best case used a form of eight wooden dowels connected together by two wooden plates. This core minimizes the mass of material within the solenoid winding. An example of this arrangement is shown in Fig 8A,

where the core of coils L03 and L04 (of Table 3) is shown before the wire was wound. To verify the core material's quality, we made a hole in the center of the two wooden plates for the purpose of inserting a big, cylindrical mass of wood. No change in measured Q values was detected while performing this experiment.

To the contrary, a 30% drop of Q is verified when using gray PVC rods.

The LF coil-design goal is high performance, with:

- Wires able to sustain high RF currents
- Good insulation
- An inductance value of a few mH

To transmit adequate RF power, we need to produce a load-coil current of a few amperes. This means using a conductor of suitable cross section to carry the 1- to 5-A currents with low RF se-

Table 1—Wire Table including calculated R_{AC}/R_{DC} at 136 and 200 KHz

Diameter (mm)	Diameter (mils)	R_{DC} (Ω /meter)	R_{AC}/R_{DC} at 136 kHz	R_{AC}/R_{DC} at 200 kHz
0.050	1.97	8.9300	1.000	1.000
0.100	3.94	2.2330	1.000	1.000
0.180	7.09	0.6893	1.001	1.002
0.200	7.98	0.5583	1.002	1.004
0.300	11.80	0.2481	1.011	1.022
0.500	19.70	0.0893	1.075	1.149
0.900	22.86	0.0276	1.507	1.785
1.000	39.40	0.0223	1.650	1.962
2.000	78.80	0.0056	3.060	3.640

Table 2—Litz-Wire Table for typical Copper Wires

Diameter (mm)	Diameter (mils)	Litz Wire (number)	R_{DC} (Ω /meter)	R_{DC} Litz (Ω /meter)
0.051	2.010	100	8.510	0.0851
0.051	2.010	200	8.510	0.0425
0.051	2.010	600	8.510	0.0142
0.063	2.480	60	0.0031	0.0907
0.127	5.000	50	0.0127	0.0272
0.180	7.090	15	0.6890	0.0459
0.180	7.090	30	0.3445	0.0229
0.180	7.090	42	0.6890	0.0164
0.300	11.810	30	0.2480	0.0083

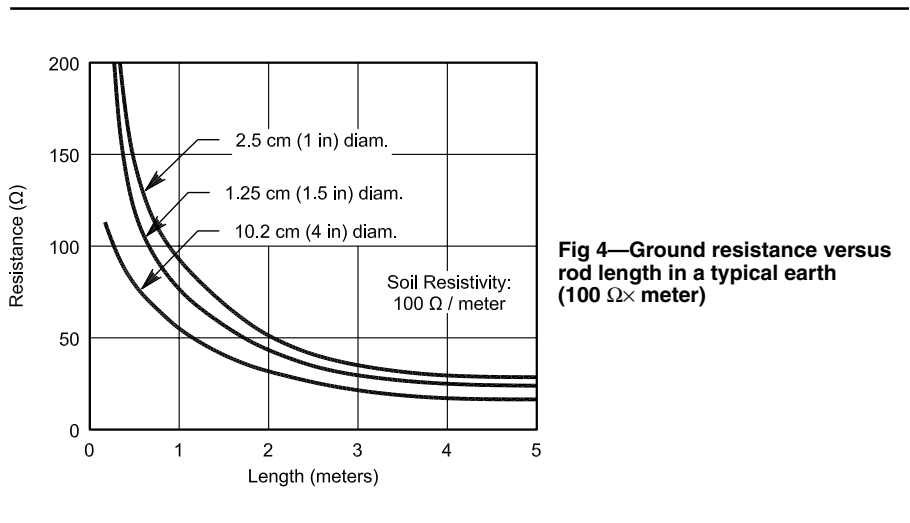


Fig 4—Ground resistance versus rod length in a typical earth (100 $\Omega \times$ meter)

ries resistance. For instance, if we have 3-mH coil in which a current of 1A flows, the voltage at the coil terminals is about 3000 V (3 mH is $+j2563 \Omega$ at 136 kHz and $+j3770 \Omega$ at 200 kHz). This is a very dangerous voltage. Moreover, it is necessary to consider the potential difference between two adjacent turns (25 to 40 V with 1 A of current flowing and proportionally higher with increasing current) to set requirements for dielectric strength of the conductor's insulation. The inductance of the coil, for LF purposes, can be calculated using the following equation, considering that it must resonate with the total antenna capacitance (vertical antenna plus top-hat capacity):

$$L = \frac{2.53 \times 10^7}{(f^2 \times C_A)} \quad (\text{Eq 4})$$

where

L = coil inductance (mH)

f = frequency (kHz)

C_A = vertical antenna + hat capacitance (pF)

At this point, it is necessary to find the number of turns (starting from the inductance computed with Eq 4) and the geometrical dimensions of the coil:

$$N = \frac{5.08 \times 10^5 Ldk + \sqrt{(5.08 \times 10^5 Ldk)^2 + 4.572 \times 10^5 LD^3}}{D^2} \quad (\text{Eq 5})$$

where

N = number of turns of solenoid winding

L = inductance (mH)

d = wire diameter (mm)

k = turns packing factor (greater than 1)

D = coil diameter (mm)

The above formula allows an accuracy of about 1% for a single-layer coil. This was confirmed by the obtained experimental results.

Before calculating the number of turns, N , it is necessary to minimize the proximity effect (see next paragraph). For this purpose, the factor k , which is greater than 1, has been introduced to consider when the distance between two adjacent wires (pitch) is greater than the diameter of the wire, d .

The diameter of the coil must be chosen to minimize the wire length in order to minimize the series equivalent resistance: By reducing R_{DC} , R_{AC} is also automatically reduced. In Fig 7, we show two graphs that are very useful for coil optimization. In the first graph, we have wire length versus form factor (D/Len); in the second, we have calculated wire length versus coil diameter.

Considering a maximum increase of the conductor length of 5%, with reference to best-case $D/Len = 2.5$, a maximum change in the coil form factor D/Len from about 1 to 4.8 can be accepted. On the second graph, we can find the coil diameter that we can put into Eq 5 to calculate the number of turns. For instance, considering spacing (pitch) between two adjacent turns of 2 mm, we can use a coil diameter between 260 and 570 mm to obtain a coil with 3 mH of inductance.

Fig 7 also shows the value relative to the final coil, L06, to show the optimization performed. The complete characteristics of the other coils are shown in Table 3.

Having chosen the value of coil diameter in the range reported above, the number of turns of the solenoid can be easily calculated. At the end of the theoretical calculations, we go to the practical realization of the load inductor. As already stated, Table 3 shows all the coils tested to verify the

optimization also from the practical point of view. L01, L04 and L05 coils have been manufactured using only enameled wire with a 0.9-mm diameter. The first inductor, on a gray PVC support, has the lowest quality factor ($Q = 205$ at 136 kHz and 187 at 200 kHz) because of the bad core material used. The second one has a higher Q (237 at 136 kHz and 230 at 200 kHz), which is related to the better support but affected by the proximity effect due to the closeness between the adjacent wires ($k \approx 1$). L05 has the highest quality factor of this coil group (318 at 136 kHz and 309 at 200 kHz) due to the increased distance between the subsequent turns ($k \approx 2$). This last result shows the big influence of the proximity effect on the equivalent series resistance (which we've already pointed out) in the LF range.

Remaining coils have been made using Litz wire: L02 with $2 \times 15 \times 0.18$ mm, L03 and L06 with 42×0.18 mm wires. The L02 inductor has a very good Q , but it is not useful for our purpose. It has only 1.4 mH of inductance and cannot resonate with the total antenna capacitance, which is estimated to be about 450 pF, considering both the vertical antenna and the top hat.

The best coil for our experimental LF transmitter is L06 (Fig 8B); it has a very high Q (597 at 136 kHz and 541 at 200 kHz) and a suitable inductance: 3 mH. For comparison, Table 4 shows some coils realized and measured by Bill Bowers (Ref 10). Apart from the reduced value of inductance for these coils (only 1 mH) and according to our experience, we believe that the author did not realize the real importance of the proximity effect with respect to high inductance quality factor.

Q s greater than 625 (over the Boonton Q-meter range) is related to two factors: the "distributed" turns and big Litz wire with 600 strands. Remember however that obtaining a Q of 600 at 3 mH is not so easy as with 1 mH! We think therefore that the use of Litz wire having 600 strands of 0.051-mm diameter is an unnecessary complication considering the skin effect. Also see Tables 1 and 2 and remember that $R_{AC}/R_{DC} = 1.001$ (!) with $d = 0.18$ mm at 136 kHz. At this frequency, the best Litz choice is probably 20 strands of 0.30-mm diameter. Where only direct current flows in a conductor, the resistance has the lowest value and the current density is uniform in the whole cross section of the wire.



Fig 5—A group of 136-kHz big coils realized for high quality factor (Q).

Table 3—High-Quality Coils Measured in the LF Range

Coil #	Core Material	Diameter (mm)	Wire Size (mm)	Litz Wires (n)	Turns (N)	Coil Length (Len mm)	D/Len	Wire Length (m)	L (mH)	R _{DC} (Ω)	136 kHz			200 kHz		
											(Ω)	Q*	R _{AC} (Ω)	XL (Ω)	Q*	R _{AC} (Ω)
L01	Grey PVC	160	0.90	none	175	176	0.91	88	3.12	2.43	2665	205	13.0	3919	187	21.0
L02	Air + wood	160	0.18	30	120	210	0.76	60	1.40	1.38	1196	513	2.33	1758	534	3.29
L03	Air + wood	200	0.18	42	157	272	0.73	99	2.70	1.63	2306	507	4.55	3391	435	7.80
L04	Air + wood	330	0.90	none	85	87	3.80	88	3.30	2.43	2818	237	11.9	4145	230	18.0
L05	Air + wood	330	0.90	none	85	165	2.00	88	2.50	2.43	2135	318	6.71	3140	309	10.16
L06	Air + wood	330	0.18	42	94	168	1.96	97	3.00	1.59	2562	597	4.29	3768	541	6.97

*Q = XL / R_{AC}

Table 4—Other Interesting Coils Measured by Bill Bowers¹⁰

Coil #	Diameter (mm)	Wire Size (mm)	AWG	Litz Wires (n)	Turns (N)	Coil Length (Len mm)	D/Len	Wire Length (m)	L (mH)	f = 200 kHz			
										XL (Ω)	Q	R _{AC} * (Ω)	R _{DC} (Ω)
B01	483	1.830	14	1	42	193	2.5	64	1	1256	325	3.86	0.53
B02	483	0.127	36	50	44	241	2.0	67	1	1256	300	4.19	1.82
B03	483	0.127	36	50	40	160	3.0	61	1	1256	400	3.14	1.65
B04	483	0.127	36	50	37	102	4.7	56	1	1256	345	3.64	1.53
B05	483	0.127	36	50	42	193	2.5	64	1	1256	410	3.06	1.73
B06	483	0.051	44	200	42	193	2.5	64	1	1256	430	2.92	2.71
B07	483	0.051	44	600	42	193	2.5	64	1	1256	>625	<2.01	0.90

*R_{AC} = XL / Q

$$R_{DC} = \frac{2.23 \times 10^{-2}}{d^2} \quad (\text{Eq 6})$$

where

R_{DC} = resistance for unit of length (Ω/meter)

d = wire diameter (mm)

For alternating current (RF), the current density is not uniform within the conductor cross section and the resistance increases. The current-density change can be explained by considering that the wire is composed of many tubular, concentric conductors. Because each tubular conductor is submitted to the external magnetic field, the inner elements link more magnetic flux than the outer ones. The consequence is an increase in inductance, and so of the reactance, in the part of the wire nearest the longitudinal axis. This is the reason why the alternating current flows mostly in the external surface of the conductor, which can be considered its skin. This effect already begins to be significant at LF (30- to 300-kHz frequency range) when using wires having a diameter that is large (≥ 3 – 4 times) compared to the skin depth.

The skin depth is the distance below the surface of the conductor where the current density drops to 1/e (≈37%) of its value at the surface. The following relation describes the decrease of current density versus the distance from the wire surface, x (Ref 9):

$$\frac{I_x}{I_s} = e^{\left(\frac{-x}{\delta}\right)} \quad (\text{Eq 7})$$

where

I_x = Current at depth x

I_s = Current at wire surface

e = Base of natural logarithms

δ = the skin depth defined by Eq 8

$$\delta = 10^3 \sqrt{\left(\frac{\rho}{\pi \mu f}\right)} \quad (\text{Eq 8})$$

where

ρ = wire resistivity (Ω-meter)

μ = wire material permeability

(Henries/meter)

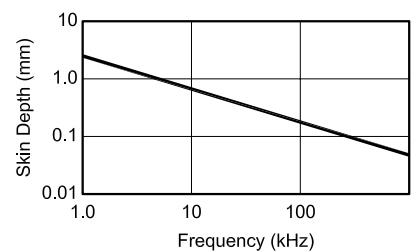


Fig 6—Skin depth versus frequency in copper-wires. At 136 kHz, the skin depth is 0.18 mm.

f = frequency (Hz)

Considering a copper wire at 20°C,

$\rho = 1.754 \times 10^{-8}$ Ω -meter

$\mu = 1.256 \times 10^{-6} \times \mu_r$ H/meter; $\mu_r = 1$

$$\delta = \frac{66.7}{\sqrt{f}} \quad (\text{Eq 9})$$

A graph of skin depth versus frequency is shown in Fig 6.

When the diameter of the wire is large compared to the skin depth (at least three times), the useful cross section becomes tubular and the alternating-current resistance can be described approximately by the following equation:

$$R_{AC} = \frac{8.374 \times 10^{-5} \sqrt{f}}{d} \quad (\text{Eq 10})$$

where

R_{AC} = alternating-current resistance for unit of length (Ω /meter)

The consequent ratio R_{AC}/R_{DC} , reported below, can be reduced using a tubular conductor with a wide periphery with respect to the cross section. For example, a copper conductor composed of many thin insulated wires can be used, such as Litz wire.

$$\frac{R_{AC}}{R_{DC}} = 3.750 \times 10^{-3} d \sqrt{f} \quad (\text{Eq 11})$$

The exact system to calculate the skin effect is reported in Ref 3 of the bibliography.

For the wires involved in our study, L_{en} values are reported in Table 1 both at 136 and 200 kHz. When two or more

nearby wires are carrying a current, the current distribution in every conductor is submitted to the magnetic field produced by the adjacent wires. This effect, named proximity effect, increases further the R_{AC}/R_{DC} ratio calculated by considering only the skin effect.

The proximity effect is very important in the LF coils, as we verified during the experimental phase of our work. If we consider the L04 and L05 coils (single 0.9-mm enameled wire) of Table 3, the R_{AC} is reduced simply by increasing the pitch between turns from 1 to 2 mm. The computation of the proximity effect can be performed only

on very simple cases that are very far from the single-layer solenoid. At this point, we believe that the better thing to do is to perform the measurements of the quality factor of the coils manufactured by considering all the above-mentioned effects together.

Q Measurements

Very few hams own a professional Q meter, and some old equipment (with difficulty) meets the measurement needs of our LF coils: very high quality factor with a few millihenries of inductance.

The first approach is to analyze the

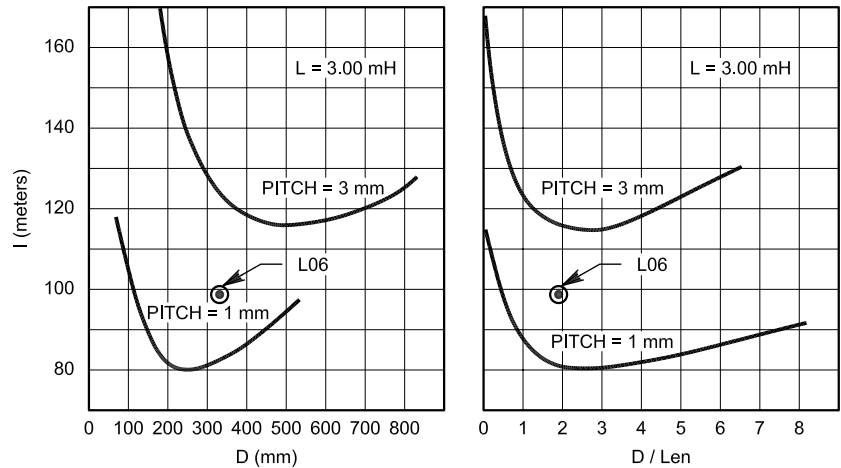
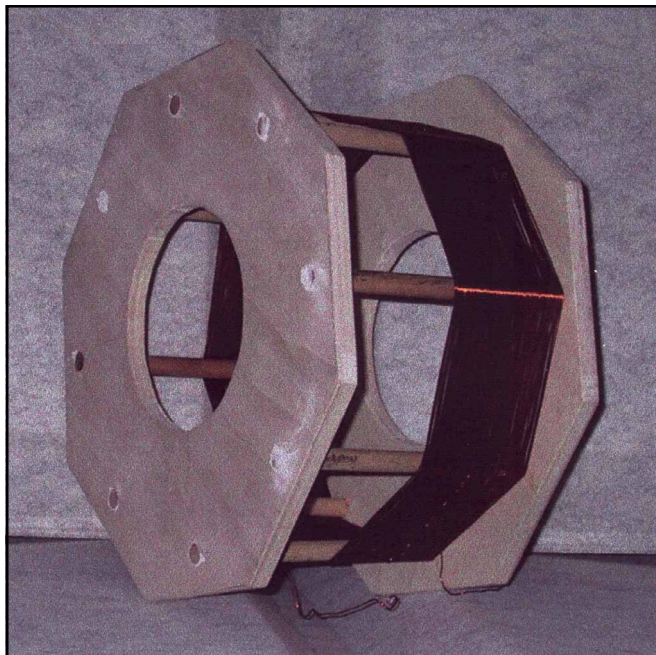
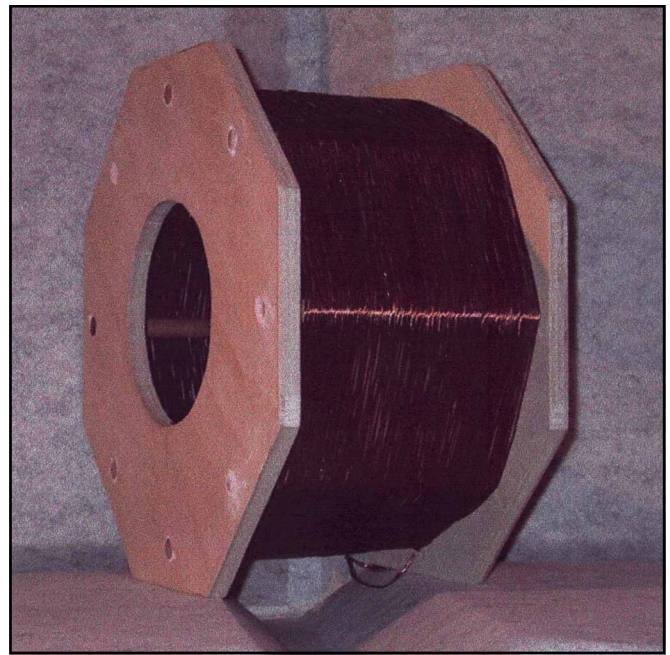


Fig 7—Minimum coil wire length versus coil diameter and D/L_{en} : a starting point to realize high-current and high-quality inductors



(A)



(B)

Fig 8—A, a simple wood support structure with no LF power loss. At B, the final load inductor (diameter = 33 cm, $Q \approx 600$ at 136 kHz).

possible errors in making the measurement in parallel using a small series resistance (0.5Ω) to inject RF into the resonant circuit and then measure the voltage at the coil terminals. To measure coils having a very high Q , it is necessary to consider the quality factor of all the components used in the measurement circuit: RF voltmeter, series resistance, capacitor and interconnections. If, for instance, we have a 3-mH inductance with $Q = 600$, the parallel resistance of the resonant circuit is greater than $1.5 \text{ M}\Omega$ ($2\pi fLQ$). An RF millivoltmeter with a $10\text{-M}\Omega$ input resistance changes the circuit by reducing the measured Q by about 14%.

The other thing that decreases the measured Q is the small series resistance used to introduce the RF signal into the resonating circuit. This effect, together with the RF millivoltmeter effect, reduces the measured Q by about 22%. Nevertheless, all the errors in the inductor quality factor just mentioned are well defined and computable, so the true Q can be calculated.

The last real problem of the parallel measurements is the capacitor loss that it is very difficult to measure because we used an air-variable capacitor. During our experiments, we used capacitors with different dielectric materials; but at the end, we decided to use only an air-variable capacitor for the following reasons:

- Easy tuning
- The very low dissipation factor (0.0001, or a $Q=10,000$).

These data have been found in the literature and not measured directly.

This uncertainty in the quality-factor measurement pushed us to find a better solution. The first idea was to use a toroidal transformer for the RF injection to drastically reduce the series resistance without decreasing the available signal too much. The second idea was to measure the series, rather than parallel, resonance to minimize the loading effects evident before.

The proposed circuit is shown in Fig 9. It was used for the measurements in Table 3. The main advantage of this new measurement concept is that it works at very low impedance levels and the R_{AC} can be evaluated by comparison with the series resistance ($R_S = 3$ to 10Ω). When the voltage, V_x , is one half of the voltage at the output of the transformer, the resistance is equal to R_{AC} and the relevant value (R_S) can be measured by a simple digital ohmmeter, available in any ham shack.

During these kinds of measure-

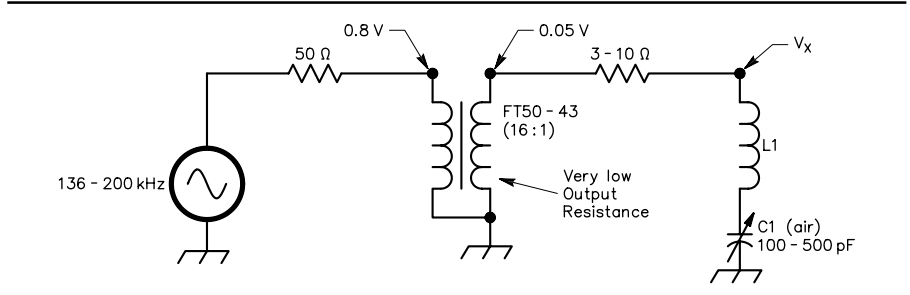


Fig 9—Circuit for simple and accurate measurements of the quality factor at 136 to 200 kHz.

ments, some shrewdness must be used to prevent possible mistakes. It's important to verify that the coil under test and its magnetic field are far from metallic surfaces and lossy materials (such as a wooden table) so that any such materials do not intercept the fields. Coils having such big dimensions, compared with those used in traditional radio applications, become loop antennas. So the measurements must be repeated, putting the winding in different positions and orientations to avoid possible errors.

Another consideration during the measurements is the distances among interconnection wires. They must be so far apart, in spite of the relatively low frequency involved, that they do not affect the result of the test.

Considering all these error sources, a possible suggestion is to find a reference inductor to verify the quality of the measurements performed. For this purpose, we used a shielded coil, manufactured by Boonton company and used in Q tests, having the following characteristics: $L = 2.5 \text{ mH}$, $Q = 170$. In Fig 5, this last (relatively small) coil is visible on top right together with the group of inductors realized in our LF operation.

Paolo Antoniazzi, IW2ACD, is a Technical Information Manager in the central IC marketing area of STMicroelectronics. He has more than 30 years of experience in RF and audio applications. Paolo is a member of IEEE, RSGB and the Audio Engineering Society. He was first licensed in the early 1960s. His amateur interests include narrow-band LF tests, FFT analysis and 2.4-GHz operations.

Marco Arecco, IK2WAQ, is an EPROM Product Engineering Team Leader at STMicroelectronics with more than 30 years experience in semiconductor manufacturing. He has been licensed since 1993, and his amateur interests include LF operation and VHF/UHF antenna tests.

Notes

¹STMicroelectronics, 1000 E Bell Rd, Phoenix, AZ 85022; tel 602 485 6100, fax 602 485 6102; us.st.com.

²A VLF band already exists in the US, but it's not an Amateur Radio allocation yet. A lot of "lower" (Low Frequency Experimental Radio) activity occurs in the 160 to 190-kHz region—the so-called 1750-meter band, authorized under Part 15 of the FCC regulations. Right now, you don't need a license to operate on 1750 meters, but there are severe legal restrictions on what you can put on the air there. For starters, you can't run more than 1 W input to the transmitter's final stage, and the entire length of the transmission line and antenna combined cannot exceed 15 meters (approximately 50 feet). That's not much antenna for a band where a half-wavelength antenna would be more than one-half mile long! Hams that operate on 1750 meters sometimes use just their call sign suffix as an ID.

References

1. W. J. Byron, W7DHD, "The Monster Antennas," *Communications Quarterly*, Spring 1996, pp 5-24.
2. W. J. Byron, W7DHD, "A Word About Short Verticals," *Communications Quarterly*, Fall 1998, pp 4-6.
3. M. Mardiguian, *Grounding and Bonding*, Vol 2, (Gainesville, Virginia: Interference Control Technologies, 1995) p 2.43.
4. P. Dodd, G3LDO, *The LF Experimenter's Source Book*, 2nd Edition, (Potters Bar, Hertfordshire, England: RSGB, 1998); www.rsgb.org/shop/acatalog/index.html.
5. P. Dodd, G3LDO, "Getting Started on 136 kHz," *RadComm* (RSGB), March 1988.
6. D. Curry, Basic 1750 m Transmitting Antenna; www.fix.net/~jparker/curry/1750mta.htm.
7. *Reference Data for Engineers*, 7th Edition, (New York: H. W. Sams & Co, 1989), p 6.4.
8. *The 1990 ARRL Handbook* (Newington, Connecticut: ARRL, 1989).
9. F. E. Terman, *Radio Engineer's Handbook*, (New York: McGraw-Hill, 1958).
10. B. Bowers, "Low Frequency Coil 'Q'," *The Lowdown*, Feb 1996. *The Lowdown* is the monthly newsletter of the Longwave Club of America (LWCA), 45 Wildflower Rd, Levittown, PA 19057, USA.
11. I. R. Sinclair, *Newnes Audio and Hi-Fi Handbook*, 2nd Edition, (Oxford: Butterworth-Heinemann, 1993), pp 748-752
12. M. Morando, 11MMR, "TX da 10 W a 137 kHz," *Radio Rivista* (Journal of the Associazione Radioamatori Italiani, Milan, Italy), Sep 1998, pp 52-53. □□

The Q of Single-Layer, Air-Core Coils: A Mathematical Analysis

*Exactly what is Q, and how does it affect
your circuits? Come along and see.*

By George Murphy, VE3ERP

During the past few years, in the process of writing software for *HAMCALC* (a collection of programs of interest to Amateur Radio enthusiasts),¹ I kept hoping that I would eventually come across a clear, concise definition of coil Q, complete with a simple equation or two. That did not happen, so I decided a more aggressive search through the available literature was in order. I was able to compile definitions and a series of equations (see the [Table of Equations](#)) from the following sources (abbreviated titles shown are used throughout this discourse; the full titles are given

in the Notes at the end of the article):

*The ARRL Handbook*²

*Radiotron Handbook*³

*Terman's Handbook*⁴

*Electronic Equations Handbook*⁵

The main purpose of my investigation was not to introduce any new theory or interpretations, but to see if I could determine a logical sequence and correlation between existing, proven equations. My original published findings dealing with true Q ⁶ have been expanded and more equations added for inclusion in this paper.

To preserve the integrity of the equations, they are presented in the [Table of Equations](#) as they appear in the original reference sources—some in metric units, others in imperial units. This may be a bother when doing calculations manually, for which I apologize, but it presents no problem in the

HAMCALC (version 50) computer programs where conversion is automatic.

Definitions of Q

*The 1997 ARRL Handbook*⁷ defines component Q as the ratio X/R , where X is the reactance of the component and R is the sum of all resistances associated with energy losses in the component. Terman defines two separate values of coil Q :⁸ true Q_t and observed Q_c . True Q_t ([Eq 3](#)) is a mathematical relationship between the radius and length of a “perfect” coil without losses, at a specific frequency when the turn spacing ([Eq 6](#)) is within the range of about 0.45 ([Eq 8](#)) to 0.70 ([Eq 7](#)) times the diameter of the conductor. Observed Q is the value observed by a Q meter.

The Radiotron Handbook (page 451) refers to Terman’s “observed Q ” as

¹Notes appear on [page 37](#).

“apparent Q .” Apparent Q_a (Eq 20), is less than true Q_t because of the presence of distributed capacity (Eq 10, Eq 11) and resistive losses within the coil that affect the reading of a Q meter.

Terman observes⁹ that with a given

inductance and coil diameter, Q is maximum when the length/diameter ratio of the coil is in the order of 0.5:1. Actually, some iterative calculation using equation Eq 3 will show the maximum Q increases rapidly with

L/d ratio, peaking in the L/d range of about 0.35:1 to 0.45:1, then decreases gradually with L/d ratio (see Fig 1). This is consistent with Terman’s popular rule of thumb, which probably includes a safety margin.

Table of Equations

$$L_\mu = \frac{d^2 n^2}{18d + 40L_{gth}} \quad (\text{Eq 1})$$

$$n = \frac{\sqrt{L_\mu(18d + 40L_{gth})}}{d} \quad (\text{Eq 2})$$

$$Q_t = \frac{\sqrt{f_{Hz}}}{\frac{6.9}{R_{cm}} + \frac{5.4}{L_{cm}}} \quad (\text{Eq 3})$$

$$L_{gth} = \frac{\frac{d^2 n^2}{40} - 18d}{L_\mu} \quad (\text{Eq 4})$$

$$L_o = 0.3937 \frac{5.4}{\frac{\sqrt{f_{Hz}}}{Q_t} - \frac{6.9}{R_{cm}}} \quad (\text{Eq 5})$$

$$S_w = \frac{L_{gth}}{n} \quad (\text{Eq 6})$$

$$W_{max} = 0.70S_w \quad (\text{Eq 7})$$

$$W_{min} = 0.45S_w \quad (\text{Eq 8})$$

$$S_d = \frac{S_w}{W} \quad (\text{Eq 9})$$

$$C_o = \frac{\pi d}{3.6} \times \cosh^{-1} \times S_d \quad (\text{Eq 10})$$

$$C_o = \frac{\pi d}{3.6} \log_n \left[S_d + \sqrt{S_d^2 - 1} \right] \quad (\text{Eq 11})$$

$$f_s = \sqrt{\frac{25330.29}{C_o L_\mu}} \times 10^9 \quad (\text{Eq 12})$$

$$C = \frac{25530.29}{f_{MHz}^2 L_\mu} \quad (\text{Eq 13})$$

$$R_{eq} = \frac{P_f (2\pi f_{MHz})^3 L_\mu^2 C_o}{10^8} \quad (\text{Eq 14})$$

$$R_{ac} = \frac{261 \sqrt{f_{Hz}} \times 10^{-9}}{2.54\pi W} \quad (\text{Eq 15})$$

$$R_{sk} = 2.54(\pi \cdot d \cdot n \cdot R_{ac} \cdot K_p) \quad (\text{Eq 16})$$

$$R_t = R_{eq} + R_{sk} \quad (\text{Eq 17})$$

$$L_a = L_\mu \left(1 + \frac{C_o}{C} \right) \quad (\text{Eq 18})$$

$$R_a = R_t \left(1 + \frac{C_o}{C} \right)^2 \quad (\text{Eq 19})$$

$$Q_a = \frac{Q_t}{\left(1 + \frac{C_o}{C} \right)} \quad (\text{Eq 20})$$

where:

C = added external capacitance required to resonate

C_o = distributed capacitance, in pF

d = coil pitch circle diameter, in inches

f_{Hz} = operating frequency, in Hertz

f_{MHz} = operating frequency, in megahertz

f_s = self-resonant frequency, in Hertz

K_p = 1.15 (proximity factor)

L_a = apparent inductance, in microhenries

L_{cm} = coil length, in centimeters

L_{gth} = coil length, in inches, as a function of inductance

L_o = coil length, in inches, as a function of frequency and Q

L_μ = true inductance, in microhenries

n = number of turns

P_f = 1 (assumed power factor)

π = 3.141593

Q_a = apparent Q of coil

Q_c = Q of coil due to self-capacitance

Q_t = true Q of coil

R_a = resistance due to distributed capacitance, in ohms

R_{ac} = RF resistance in ohms/cm.

R_{cm} = coil pitch circle radius, in centimeters

R_{eq} = equivalent series resistance of coil

R_o = equivalent resistance of Q_c , in ohms

R_{sk} = total skin-effect resistance, in ohms

R_t = true resistance, in ohms

S_d = winding pitch/conductor diameter ratio

S_w = winding pitch (center-to-center turn spacing), in inches

W = conductor diameter, in inches

W_{max} = maximum conductor diameter, in inches

W_{min} = minimum conductor diameter, in inches

Equation Sources

Eq 1: 1997 ARRL Handbook, page 6.22 equation 44.

Eq 2: 1997 ARRL Handbook, page 6.22 equation 45.

Eq 3: Radiotron Handbook, page 464 equation F.

Eq 4: Derived from Eq 1 or Eq 2.

Eq 5: Derived from Eq 3 and converted to inches.

Eq 6: Ratio of coil length, in inches, to number of turns.

Eq 7: Eq 8: Radiotron Handbook, page 463 (A), page 464

(B) (G), page 465 (G) (a), page 465 (H) (d).

Eq 9: Ratio of coil winding pitch to conductor diameter.

Eq 10: Electronic Equations Handbook, page 6 equation 1-38.

Eq 11: Eq 10 with cosh function re-phrased to suit calculation by computer.

Eq 12-13: Derived from the ARRL Handbook, page 6.35 equations 89 to 92.

Eq 14: Terman Handbook, page 34 equation 5.

Eq 15: Terman Handbook, page 35 equation 6.

Eq 16: Total conductor-resistance equation $R_{ac} \times$ conductor length, in cm.

Eq 17: Total resistance.

Eq 18-20: Radiotron Handbook, page 451 (I).

Effects of Distributed Capacitance on Q

Terman states:¹⁰ “The presence of distributed capacity causes a partial resonance that modifies the apparent resistance and reactance of the coil as viewed from the terminals. The apparent series resistances L_a and R_a . . . are related to the true resistance R_t and inductance L_μ according to the equations . . .” (The equations¹¹ that follow Terman’s statement are expressed in terms of the ratio [actual frequency]/[self-resonant frequency].

The *Radiotron Handbook* states:¹² “In all cases the self capacitance of a coil has an apparent effect on its resistance, inductance and Q, and at frequencies considerably below the self resonant frequency of the coil [are] . . .” Eqs 18, 19 and 20. These equations are expressed in terms of the ratio [self-capacitance of coil]/[external capacitance required to tune L_μ to resonance]. The equations (page 451) produce values identical to the Terman equations, which are not included in the [Table of Equations](#).

Losses

In addition to distributed-capacitance losses, Terman describes four other factors¹³ contributing to coil losses as:

- Skin effect¹⁴ (Eqs 15, 16)
- Proximity effect¹⁵ (the proximity

factor K_p used in the equations is assumed to be 1.15)

- Dielectric losses
- Eddy-current losses in neighboring objects

For purposes of mathematical analysis, the last two factors are ignored herein, as are the effects of component-lead wires, since these factors are variable and somewhat unpredictable, and they do not significantly affect the analysis.

Self-Resonance

At some sufficiently high frequency (Eq 12), inductors and capacitors become self-resonant. Just as in a tuned circuit, above that frequency, the capacitor will appear inductive and the inductor will appear capacitive.¹⁶ Because of this, coils are not usually designed for operation above their self-resonant frequency, and any calculated or measured Q above the resonant frequency becomes meaningless in most practical applications.

True Q_t versus Apparent Q_a

True Q_t , which has no losses, increases indefinitely with frequency. Apparent Q_a increases with frequency, peaks at a point appreciably less than the self-resonant frequency and then, due to distributed-capacitance effect and resistive losses, decreases until it reaches zero at the coil’s self-resonant

frequency. These relationships are shown graphically in Fig 2.

Choosing a True Q Value when designing a Coil

This is mostly a judgement call based on experience. Because there is little in the literature for guidance, and what little mention there is apparently refers either to apparent Q_a or to measurements made by a Q meter under unspecified conditions affecting the interpretation of the meter reading. As a rule, a high apparent Q_a is required for narrow bandwidth, minimum bandwidth noise and maximum efficiency.

A useful feature of the *HAMCALC Q Calculator* program is that as soon as the basic requirements (conductor diameter, inductance and frequency) are entered, it immediately computes and displays the approximate maximum true Q for those factors.

Coil Design

The tricky part in designing a coil with a specific Q_t is to arrive at a length and diameter where the length L_{gth} as a function of inductance (Eq 4) is equal to the length L_o as a function of frequency and true Q_t (Eq 5).

To design a coil with a specific true Q_t , using the equations here, determine five known factors:

1. Minimum conductor size required to carry the current

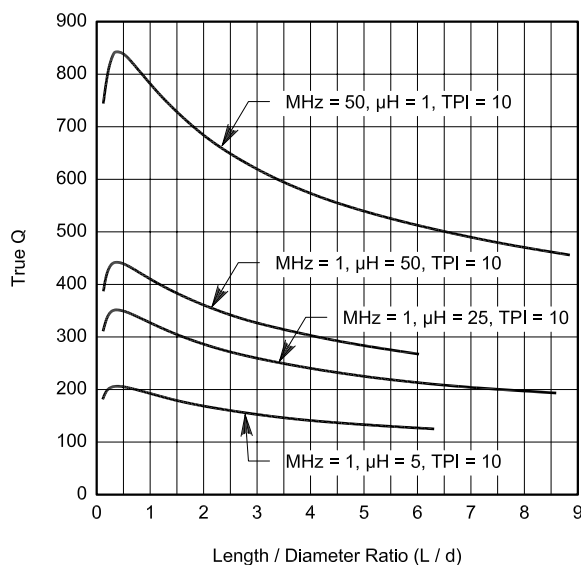


Fig 1—Maximum Q of typical coils.

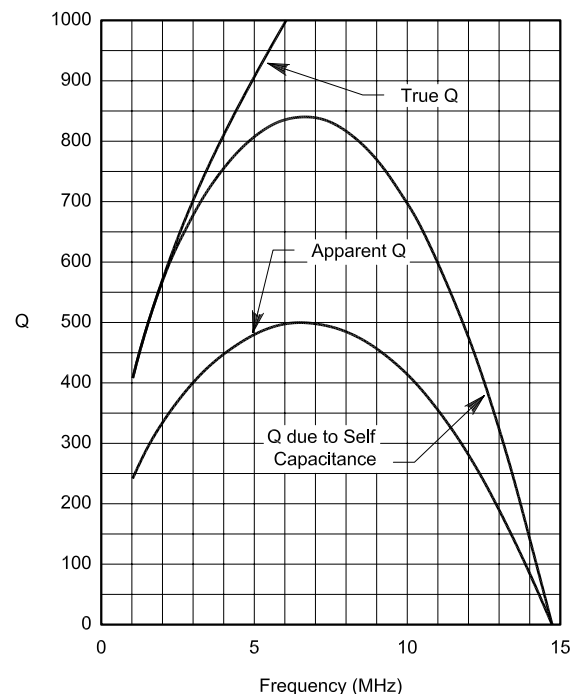


Fig 2 (right)—Values of Q for coil described in Fig 4: 34.7 μ H, 27 turns of #14 AWG at 8 turns per inch on a 3-inch diameter form. The coil is 3.375 inches long.

2. Required inductance
3. Operating frequency
4. Desired L/d ratio (lower L/d yields higher Q_t)
5. Desired true Q_t .

Proceed with the design calculations as follows:

1. Assume any very small pitch diameter, d , in inches.
2. Let $R_{cm} = 2.54d/2$. Calculate coil length L_o (Eq 5).
3. If L_o is equal or very close to $[d \times L/d \text{ ratio}]$ then proceed to Step 6.
4. If $L_o < [d \times L/d \text{ ratio}]$, increase d and return to Step 2.
5. If $L_o > [d \times L/d \text{ ratio}]$, decrease d and return to Step 2.
6. Calculate L_{gth} from Eq 4 and confirm that $L_o \approx L_{gth}$
7. Calculate number of turns (Eq 2).
8. Calculate winding pitch (Eq 6).
9. Calculate limits of conductor size (Eqs 7, 8).

10. If the specified conductor is within these limits proceed to Step 12.

11. Increase L/d ratio and/or decrease Q_t , and return to Step 1.

12. Calculate conductor circumference P , where $P = \pi d$.

13. Calculate other factors (Eq 9, 10, 11, 12, 13, 14, 15, 16, 17, 18, 19).

14. Calculate apparent Q_a (Eq 20).

Because of the iterative nature of the calculations, this can be a tedious manual operation. To design a coil with a specific apparent Q_t using a computer, decide four known factors:

1. Minimum conductor size required to carry the current
2. Required inductance
3. Operating frequency
4. Desired true Q_t .

With *HAMCALC* loaded in your computer, start the *Coil Q Calculator* program, and proceed as follows:

1. Select desired measurement units, either metric or inches.
2. Select menu item 1 "Coil Specifications for a Specific Q and Frequency."
3. Enter the wire diameter.
4. Enter the inductance.
5. Enter the frequency.
6. The computer will display the resultant approximate maximum true Q_t .
7. The screen will show a display similar to Fig 3. You have the option of changing any or all of the input data at this time.
8. Enter your choice of coil diameter within the range displayed. The computer will display complete coil specifications in a manner similar to Fig 4.
9. Refer to bar at bottom of screen and press 3 to return to the menu.
10. Select menu item 2 to make final minor adjustments to suit a standard

Conductor diameter.....	0.064 in.
Inductance.....	34.700 μ H
Frequency.....	1.800 MHz
True Q_t	549.640

L = length of coil, d = pitch circle diameter of coil			
Typical coils with these specifications			
L/d ratio	Lgth. (in.)	dia. (in.)	Wire diameter range
L/d= 0.40	L= 1.76	d= 4.40	0.12/ 0.19 cm = .048/.075 in.
L/d= 0.50	L= 1.98	d= 3.97	0.12/ 0.19 cm = .049/.076 in.
L/d= 0.62	L= 2.26	d= 3.62	0.13/ 0.20 cm = .050/.078 in.
L/d= 0.78	L= 2.61	d= 3.34	0.13/ 0.21 cm = .052/.081 in.
L/d= 0.98	L= 3.04	d= 3.12	0.14/ 0.21 cm = .054/.085 in.
L/d= 1.22	L= 3.59	d= 2.94	0.15/ 0.23 cm = .057/.089 in.
L/d= 1.53	L= 4.27	d= 2.80	0.16/ 0.24 cm = .061/.095 in.

Select ANY coil diameter (d) within the above range.
 RAISE frequency or LOWER Q for higher L/d ratios & smaller coil diameters.
 LOWER frequency or RAISE Q for lower L/d ratios & larger coil diameters.
 Enter 0 (zero) to try again or ENTER: Coil pitch diameter (in.)...?

Fig 3—Interim results from the *Coil Q Calculator* show possible coils for the specified conductor diameter, inductance and frequency.

COIL Q - True vs. Apparent		BY GEORGE MURPHY VE3ERP
True inductance.....	$L\mu =$	34.700 μ H
Number of turns.....	$n =$	26.994
Wire diameter.....	$W =$	0.163 cm. (0.064 in.)
Pitch (c.c. spacing of turns).....	$Sw =$	0.318 cm. (0.125 in.)
Coil pitch diameter.....	$d =$	7.620 cm. (3.000 in.)
Coil Length.....	$Lcm, Lgth =$	8.572 cm. (3.375 in.)
Coil Length/diameter ratio.....	$Ld =$	1.125:1
Self-Capacitance.....	$Co =$	3.376 pF
Frequency.....	$f =$	1.800 MHz
Self-Resonant frequency.....	$fs =$	14.704 MHz
True reactance.....	$X =$	392.448 ohms
Apparent reactance.....	$Xa =$	398.419 ohms
Capacity required to resonate @ f	$Cr =$	225.302 pF
External tuning capacitor.....	$C =$	221.926 pF
Apparent inductance.....	$La =$	35.228 μ H
True resis. (skin, proximity effects) $Rt =$		0.492 ohms
Apparent resistance.....	$Ra =$	0.507 ohms
Reactance at self-resonant frequency.....	$Xs =$	3205.797 ohms
True Q_t	$Qt =$	549.640
Observed Q due to self-capacitance.....	$Qc =$	541.403
Apparent Q due to all losses.....	$Qa =$	320.579

Fig 4—After selecting a coil diameter of 3.000 inches, *Coil Q Calculator* displays the various properties of that coil.

About Q Meters

The interpretation of readings displayed by Q meters is beyond the scope of this article. According to the manual I have for one of these instruments, there is a lot more to measuring coil Q than merely attaching a couple of test leads, pushing a button and getting an instant result. If anyone wants an article about how to read a Q meter, it won't be written by me—I don't even understand the manual!

wire type and size, a standard coil form diameter and to provide an integral number of turns. These small adjustments may slightly affect the true Q_t , which is displayed as each adjustment is made. The entire process takes only a few seconds or perhaps a few minutes if you engage in "what if" speculations in Step 7.

The *HAMCALC Coil Equation Calculator* may also be found useful in preliminary design and analysis of new or existing single-layer air-core coils. Given only a few of any known properties of a coil, it computes most of the other commonly sought proper-

ties, including true Q_t and apparent Q_a .

Summary

Nothing very new is presented in this paper, but I hope it may make life a little easier for the coil designer by presenting most of the pertinent equations in one place. Anyone interested in surfing the equations by computer can obtain a free program to do just that by e-mailing a request for *QSOLVE.BAS* to ve3erp@encode.com.¹⁷

Acknowledgments

Being a non-technical person whose

only contact with RF engineering has been through my involvement in Amateur Radio, I needed a lot of help and encouragement in conducting my investigation into the *Q* of coils. Both were provided in profusion by many knowledgeable people, especially Yardley Beers, W0JK; L. B. Cebik, W4RNL; Robert J. Dehoney, IEEEE; Bob Eldridge, VE7BS; Bob Tellefsen, N6WG; and Curt Thompson, VE3HML.

Notes

- ¹HAMCALC is free software on CD-ROM containing over 250 programs, obtainable from the author for a modest contribution to cover my costs of materials and airmail shipping anywhere in the world. Ask for Version 50 or later, and send US\$7.00 to George Murphy VE3ERP, 77 McKenzie St, Orillia, ON L3V 6V6, Canada.
- ²P. Danzer, N111, editor, *The 1997 ARRL Handbook for Radio Amateurs* (Newington, Connecticut: ARRL, 1996).
- ³F. Langford-Smith, editor, *Radiotron Designer's Handbook*, 4th edition, 1952, Wireless Press (Australia), reproduced and distributed in the US by the Tube Division, Radio Corporation of America, 1936.
- ⁴F. E. Terman, *Radio Engineer's Handbook*, (New York: McGraw-Hill, 1943).
- ⁵S. J. Erst, *Electronic Equations Handbook*, (Blue Ridge Summit, Pennsylvania: TAB Books, 1989).
- ⁶G. Murphy, "The Elusive Q of Single-Layer Air-Core Coils," *CQ Magazine*, May 1999, pp 24-31. In that article under the heading "Q Equations," the "*n* = ..." equation should read "*Q*_t = ..." as it does in Eq 3 of this article.
- ⁷*The 1997 ARRL Handbook*, p 6.21, equation 43.
- ⁸Terman, p 916 equation 15.
- ⁹Terman, p 74 paragraph 18, "Q of Single-Layer Coils."
- ¹⁰Terman, p 85.
- ¹¹Terman, p 85 equations 102 and 103.
- ¹²*Radiotron Handbook*, p 451, Section 2(i).
- ¹³Terman p 74 paragraph 18, "Factors Contributing to Coil Losses."
- ¹⁴Terman, p 35 equation 6.
- ¹⁵Terman, p 36 Fig 6. According to this graph, for current in the same direction in two wires spaced two diameters apart the proximity factor, *C*, is about 1.15.
- ¹⁶*The 1997 ARRL Handbook*, p 10.12, "Self-Resonance."
- ¹⁷You can download this package from the ARRL Web at www.arrl.org/qexfiles/. Look for Murphy0901.ZIP. Compaq computers require a software fix (file Fix50f.com) to run BASIC and HamCalc. I downloaded Compaq software pack SP2517, followed the instructions and was able to run HamCalc. To find the latest version of

the fix, search the Compaq support site (www.compaq.com/support/) for "Qbasic." The Compaq site says this fix is for Win95 and some other operating systems, but does not specifically mention Win98 (many programmers consider Win98 and Win95 functionally equivalent). Also, several pages on the Compaq site mention this package in various versions for various Compaq models.—Bob, KU7G

I am one of that very large group of amateurs who, with absolutely no training or experience in anything even vaguely connected with communications or electronics, decided in midlife to become an amateur because it sounded like fun. So it has been. I am

now retired, having spent most of my earning years as a professional musician and industrial designer. I hold a Canadian Advanced Amateur license, which I obtained in 1960. My main interest in Amateur Radio is teaching myself what it is all about. I believe the best way to learn anything is to teach it to someone else, which is my selfish motive for writing the articles I've had published over the years, and for the free HAMCALC software I produce and distribute. The only technical degree I hold is approximately 98.6°F when I am dressed appropriately for the weather. □□

EZNEC 3.0

All New Windows Antenna Software by W7EL

EZNEC 3.0 is an all-new antenna analysis program for Windows 95/98/NT/2000. It incorporates all the features that have made **EZNEC** the standard program for antenna modeling, plus the power and convenience of a full Windows interface.

EZNEC 3.0 can analyze most types of antennas in a realistic operating environment. You describe the antenna to the program, and with the click of a mouse, **EZNEC 3.0** shows you the antenna pattern, front/back ratio, input impedance, SWR, and much more. Use **EZNEC 3.0** to analyze antenna interactions as well as any changes you want to try. **EZNEC 3.0** also includes near field analysis for FCC RF exposure analysis.

See for yourself


The **EZNEC 3.0 demo** is the complete program, with on-line manual and all features, just limited in antenna complexity. It's free, and there's no time limit. Download it from the web site below.

Prices - Web site download only: \$89. CD-ROM \$99 (+ \$3 outside U.S./Canada). VISA, MasterCard, and American Express accepted.

Roy Lewallen, W7EL phone 503-646-2885
P.O. Box 6658 fax 503-671-9046
Beaverton, OR 97007 email w7el@eznec.com

<http://eznec.com>

ICOM IC-756 PRO



The impressive **IC-756 Pro** covers HF plus 6 meters. The high resolution 5 inch TFT color display provides more operating information than ever, including a spectrum scope. The 32 bit floating point DSP provides crisp, clear reception with 41 built-in filters. The "Pro" is the choice for serious DXers and contesters.

IC-746 ✓ 160 to 2 Meters!



The **IC-746** covers 160-10 meters plus 6 and 2 meters with 100 watts on all bands. Call or visit our website for further details and pricing on this and other ICOM radios.

Universal Radio
6830 Americana Pkwy.
Reynoldsburg, OH 43068
◆ Orders: 800 431-3939
◆ Info: 614 866-4267
www.universal-radio.com



universal radio inc.

Build this Simple, High-Resolution DC Voltmeter

Here's an easy-to-build, computer-read, six-digit voltmeter based on a new ADC chip and a precise voltage reference.

By Ron Tipton, ex-K5UJC

Last year, Linear Technology Corporation¹ introduced a single-chip, 24-bit analog-to-digital converter (ADC), the LTC2400. I requested a demo board to see what it would do. This project and article are the results.

Although the chip has 24-bits of resolution, it isn't really a 24-bit converter. The specification sheet says the typical output noise is 1.5 μV RMS. Gaussian random noise has a crest factor (peak divided by RMS) of about five so $1.5 \times 5 \times 2 = 15 \mu\text{V}$ pk-pk. At 5 V full scale, the least-significant bit is just 0.3 μV so the

converter noise effectively "uses up" the lower five bits; at best we have a 19-bit converter, which is really quite good for an SO-8 IC!

Selecting a Voltage Reference

However, we also need to find a voltage reference for the converter that adds minimum noise. Since the ADC and reference noise will be uncorrelated, the noise powers add directly. The noise voltage, therefore, will increase as the square root of the sum of the squares of the individual noise voltages, that is, the RMS sum. The demo board uses an LTC1236A 5-V reference chip for the converter reference and for the converter supply voltage. The LTC1236A "spec" sheet lists an initial uncertainty of $\pm 2.5 \text{ mV}$, a temperature coefficient of 5 ppm/ $^{\circ}\text{C}$,

and a maximum output noise of 3.5 μV rms. The RMS sum of 1.5 μV and 3.5 μV is 3.8 μV or about 38 μV pk-pk (assuming a crest factor of five).

Using an input of +2.000 V from a voltage reference, I measured an output variation about the mean of about 60 μV pk-pk. See the graph in Fig 1. This is greater than the predicted 38 μV pk-pk, but the 2-V input contributes some noise, too, so these numbers are in the right ballpark. Even so, I thought I could do better with a quieter reference supply. Thaler Corporation² makes a precision 5-V reference IC, the VRE305A, that I've used in other projects.³ Its specs are quite good. The initial voltage uncertainty is only $\pm 0.5 \text{ mV}$, the temperature coefficient is 0.6 ppm/ $^{\circ}\text{C}$, and the output noise is typically 3 μV RMS without

¹Notes appear on [page 43](#).

the optional external noise-reduction capacitor. The only drawback to this chip is its need for a 13.5 to 22 V supply, but I deemed this a worthwhile trade for its superior performance.

An output noise level of 3 μV RMS is pretty good, but what about summing the outputs of several references and dividing each reference output by the number being summed? The total noise voltage decreases and the dc output remains constant at 5 V. By summing three outputs, the initial uncertainty of the 5 V may decrease, too, since it's equal to the average of the three references. Using 3 μV RMS from the specification sheet, we get the curve in Fig 2 for multiple references. Three references looked like a good compromise, as

the improvement becomes increasingly smaller beyond four or five. Three is manageable in cost, circuit-board space and summing-resistor values. Another look at Fig 1 shows a decrease to about 30 μV pk-pk variation for the three-reference voltmeter, which I'm calling a model 251. The result is a solid 6-digit meter—not bad for a cost of about \$150!

Comments on the Circuit Diagrams

The circuit diagram is shown in Figs 3, 4 and 5. Let's take a look at how it works. In Fig 3, U1 is a very-low-noise, chopper-stabilized op amp connected for non-inverting operation. Slide switch S1 sets the input gain to 0.1, 1 or 10 for full scale ranges of 50, 5 and

0.5 V. The circuit-board common is not internally connected to the case, as this makes it easier to control ground loops. You may get more stable operation by placing a low-resistance jumper between the black and green (case) binding posts. The ADC uses an internal conversion oscillator and digital filter to reject either 50- or 60-Hz input signals. For 50-Hz rejection, pin 8 is connected to +5 V; it is grounded for 60-Hz rejection. The demo board and my board have jumpers to make this selection.

Input Protection

Resistor R2 and diode D1 protect the ADC from negative input voltages on the 50-V and 5-V ranges. The voltage drop across R2 from positive-voltage leakage current is measurable, but the error is so small I consider it negligible. There is no negative input protection on the 0.5-V range because of the gain of 10 in U1. You can connect a Schottky diode (such as a 1N5817) in parallel with R7 with the cathode end on U1, pin 6. This protects the ADC but the positive voltage leakage current causes a -0.4% error at +5 V into the ADC. I consider this unacceptable, but it would protect the ADC from destruction.

The 5-V range is the most accurate because U1 is just a voltage follower, and there are no resistor tolerances to worry about. On the other two ranges, gain-setting resistors are used. Although they are 0.1%-tolerance units, there will be a small gain uncertainty.

Serial Interface

The serial data interface to the computer copies the demo-board interface except I added optocouplers to isolate computer common from voltmeter common. That gives another option for controlling ground loops. A common interface was intentionally included so that the demo software would also

Resistor Matching

You can use stock 0.1% resistors for the whole project, but you can get better performance by matching them when same-valued sets or pairs are needed (see the [Parts List](#)). In these cases, the specific values are not as important as the degree to which the values match. This matching can be easily done with another digital multimeter (DMM). In fact, the DMM need not be very accurate, as long as its readings are stable. A 4^{1/2}-digit meter gives you a resolution of 1 Ω (0.01%) at 10 k Ω and 5^{1/2} digits is 10 times better. You can easily determine stability by rechecking matched pairs after 30 minutes or so.

The 0.1% resistors from Mouser Electronics have a temperature coefficient (TC) of ± 25 ppm/ $^{\circ}\text{C}$. This amounts to ± 0.25 Ω / $^{\circ}\text{C}$ for a 10-k Ω resistor. So matching to better than $\pm 0.01\%$ is probably useless because of the resistance change with temperature. Inexpensive 1% metal-film resistors could also be matched in this way, but their TC is ± 50 ppm/ $^{\circ}\text{C}$, so we should avoid the temptation to save money this way.

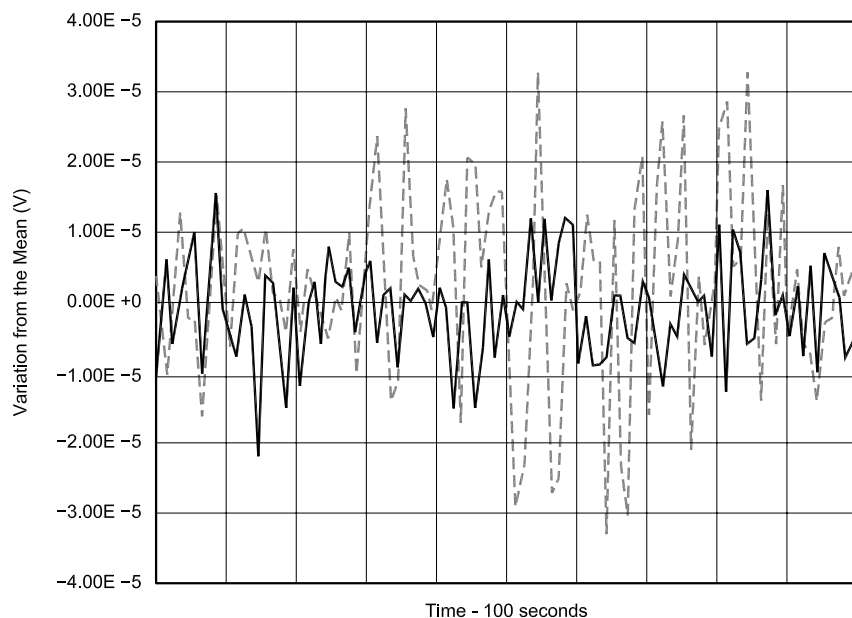


Fig 1—Comparison of short-term variation in voltage reading. The solid line is for the model 251 voltmeter and the dashed line is for the LTC2400 demo board. Input voltage was 2.000 V in both cases.

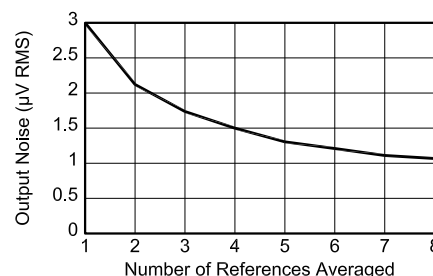


Fig 2—Total noise decreases as the number of uncorrelated sources increase. Three sources seems a good compromise between performance and circuit complexity.

work with this circuit. Remember, though, that the computer display will always be zero to +5 V, so you will have to mentally correct the decimal point unless you are on the $\times 1$ scale. The demo software is for *Windows95* and *98*, so I have written a companion *MS-DOS* program to also display the voltage and record data files.⁴ This could give new life to that old laptop computer gathering dust in your closet.

Reference

Fig 4 shows the 5-V reference circuit. The outputs of three Thaler VRE305As are summed by op amp U7 and then inverted back to +5 V by U8. These are very-low-noise chopper op amps; don't substitute another type. R11 through R16 are 10-k Ω , 0.1% metal-film resistors matched to 0.01% (see the sidebar "Resistor Matching"). Performance will be somewhat poorer with stock 0.1% resistors, so use a matched set if you can. To help with this, I'm making matched sets available.⁵ Actually, these resistors seem to group quite well. Fig 6 shows the results of matching the resistors I had on hand.

C11, C12 and C14 are the optional external noise-reduction capacitors, suggested on the VRE305A datasheet. Charge-storage capacitors C16, C17, C19 and C20, as well as C3 and C4 have polypropylene-film dielectric; for best performance, do not substitute another type.

Power Supply

The power supply is shown in Fig 5. The incoming low-voltage ac is rectified by U17 and filtered by C22. The resulting dc voltage is then split by power op amp U9 into ± 17 V. The +15 V regulator, U10, must be a low-drop-out-voltage type. The regulated +5 V powers the ADC and interface logic and the ± 6 V goes to the op amps. Using separate regulators provides high isolation between the digital and analog parts of the circuit, and the low ac power supply voltage minimizes 60- and 120-Hz feedthrough.

Construction

All components, except the connectors, are on one double-sided circuit board as shown in Fig 7.⁶ Fig 8 is the parts location diagram, while Figs 9 and 10 show how the connectors are mounted. Enclosure drilling and circuit board layout drawings can be

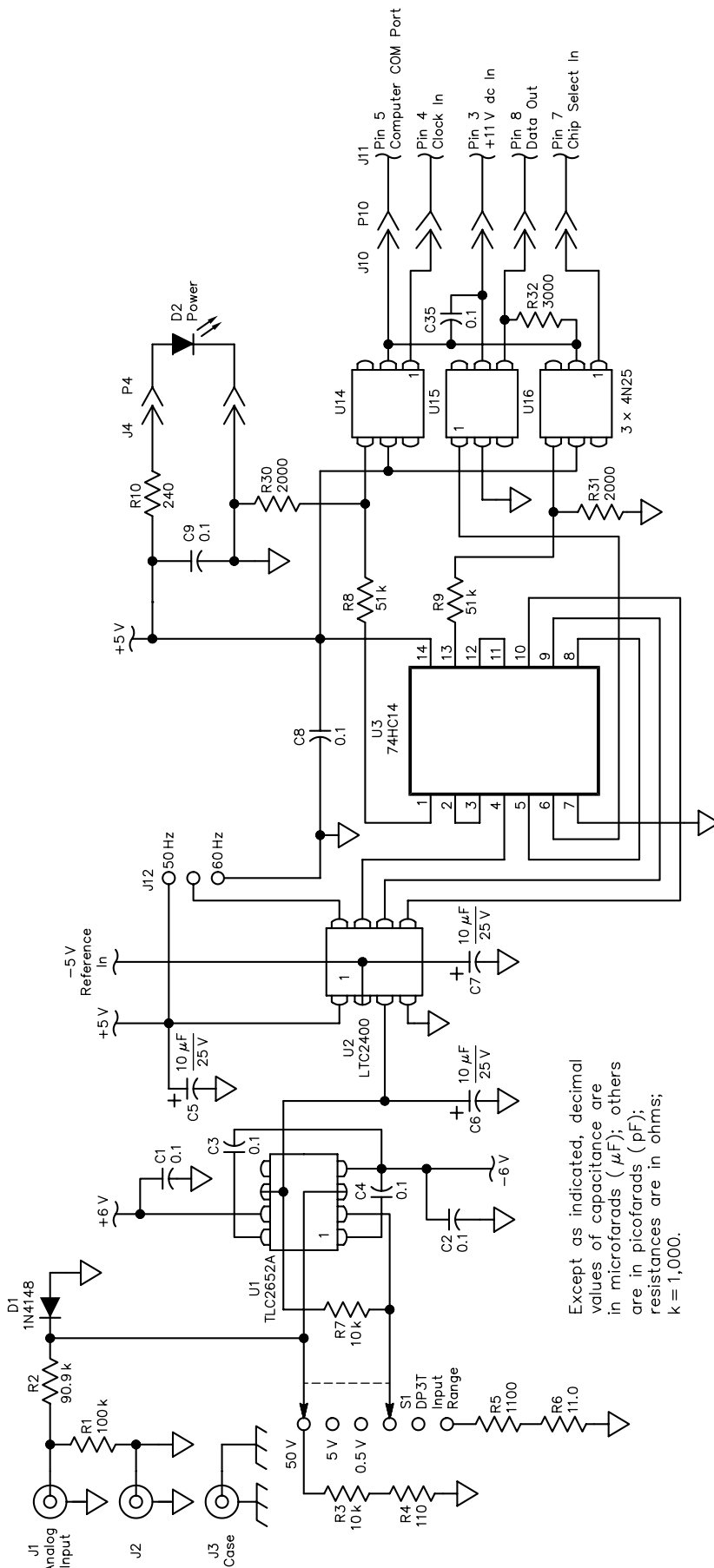


Fig 3—Input amplifier, ADC and serial data interface. U1 is an eight-pin DIP, but U2 and U3 are surface-mount devices.

downloaded; see [Note 4](#).

Although most of the ICs are somewhat expensive, don't use sockets. The added (and variable) contact resistance will degrade accuracy and long-term stability. It's also better to use solder from the same roll for the whole board as this, too, can affect accuracy.

I used a cast-aluminum enclosure to provide electrical shielding and a reasonably constant temperature for the whole voltmeter. The power op amp, U9, and +15 V regulator, U10, are connected to one of the enclosure walls through an aluminum bracket so their heat isn't dissipated inside the case.

Surface leakage on the circuit board can also degrade performance, so clean off the flux and oily fingerprints before mounting it in the enclosure. Mechanical stress on the board can produce cyclic variations as the board reacts to changes in its environment. To minimize this effect, I kept board mounting as simple as I could. The heat-sink bracket is attached to the case wall with two #4-40 machine screws and nuts. The other, output-end corner is supported by a 3/8-inch-long nylon snap-in post that attaches to the enclosure bottom with a sheet-metal screw, but just snaps into an oversize hole in the circuit board. The voltage-input end of the board is supported by two 3/8-inch nylon spacers that aren't attached to the enclosure bottom.

Operation

Plug the "wall wart" transformer

into any convenient outlet and attach its cord to the power-input connector. Connect the DB9 connector to your computer's serial port. Turn on the voltmeter's power and start the computer program (*Windows* or *MS-DOS*

version). You should see the input voltage displayed on the screen.

Software

Both versions of the software let you select either COM1 or COM2. Both

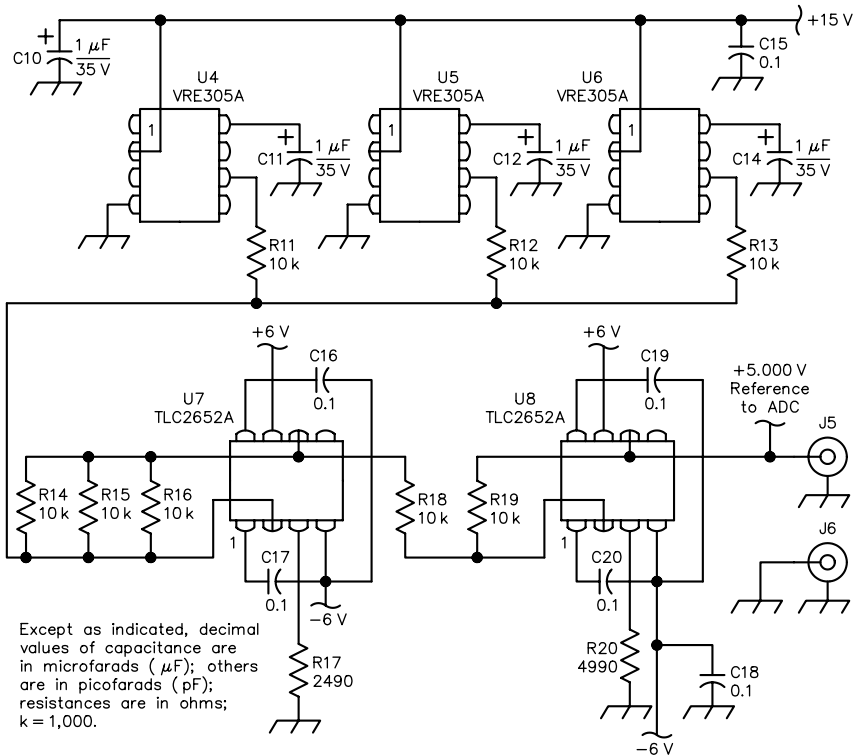


Fig 4—The 5-V reference supply averages three outputs to reduce short-term variations. The op amps are chopper-stabilized with very little output noise.

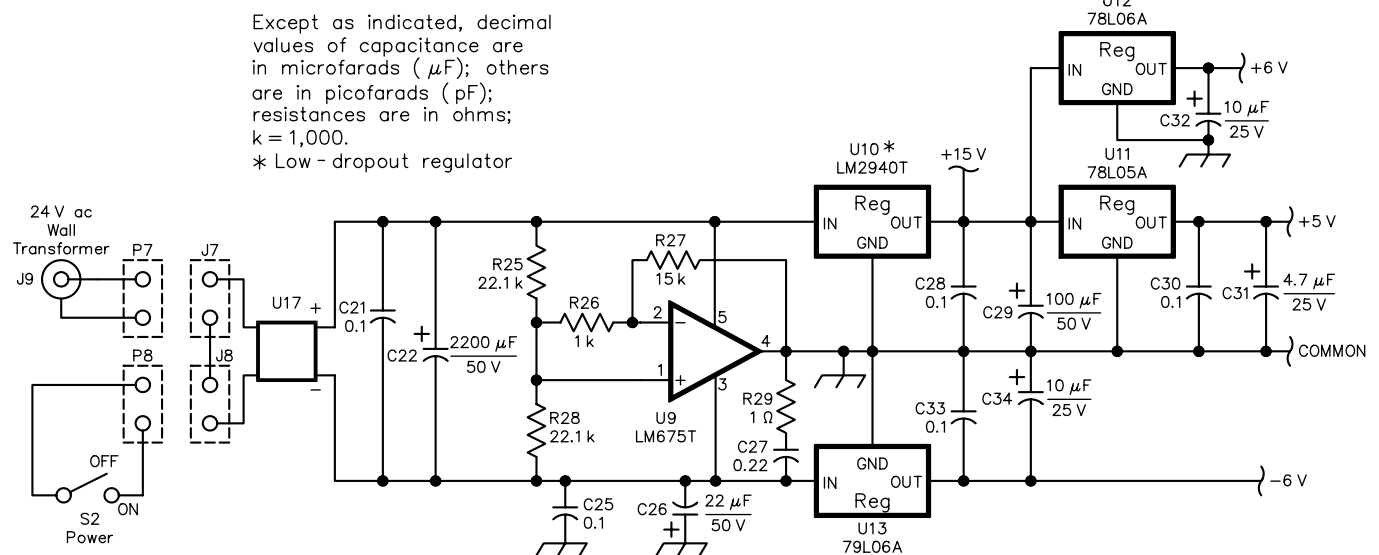
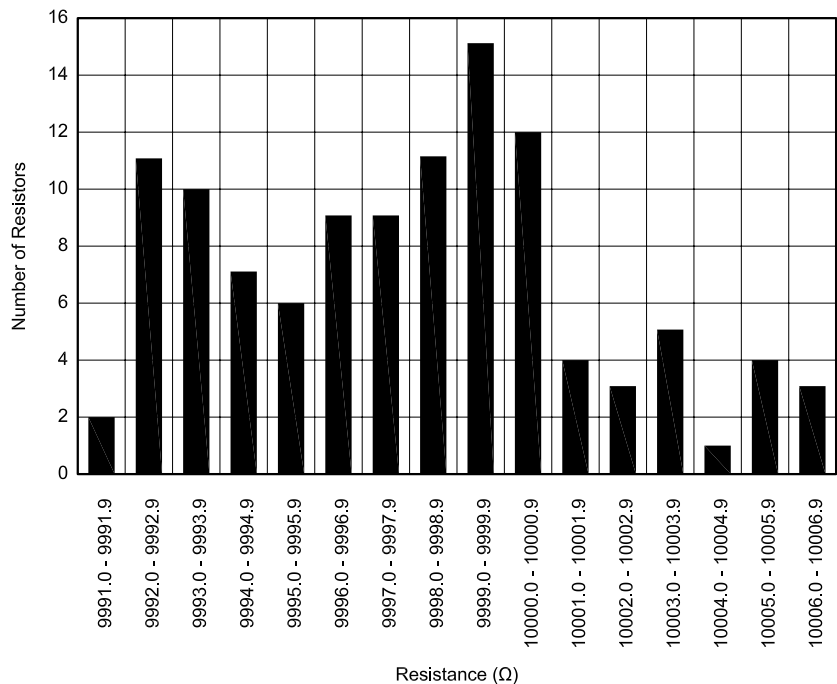


Fig 5—The LTC2400 voltmeter power supply. U9 splits the dc to +17 V and -17 V. U10 is a low-dropout voltage regulator.

versions let you do an *N*-point running average if you want to. Both versions also let you record a data file. The recorded data format uses ASCII numbers separated by tab and new line characters, so the files are easy to import into a spreadsheet or math program. For the *MS-DOS* version to work correctly you must have *ANSI.SYS* or an equivalent loaded. That is, you need a line in your *config.sys* file that reads: `DEVICE=C:\DOS\ANSI.SYS` (or wherever the file is located).

I wrote the *MS-DOS* program in *MIX Software PowerC*,⁷ and I used a serial-communications library from MarshallSoft named *PCL4C*.⁸ The source code is included in the *SVMETER.ZIP* file (see [Note 4](#)). The

Fig 6 (right)—This graph shows the result of measuring 112 10-k Ω , 0.1% metal-film resistors. The resistors in each “bin” are matched to 0.01%.



Parts List

C1, C4, C8, C9, C15, C18, C21, C23, C25, C28, C30, C33, C35—0.1 μ F, 50 V ceramic (Jameco 25523)
 C3, C4, C16, C17, C19, C20—0.1 μ F, 50 V, 5% polypropylene film (Mouser 1429-1104)
 C5-C7, C32, C31, C34—10 μ F, 25 V tantalum electrolytic (Jameco 94078)
 C10-C12, C14—1 μ F, 35 V, tantalum electrolytic (Jameco 154860)
 C13—not used
 C22—2200 μ F, 50 V electrolytic (Jameco 93841)
 C24, C26—0.22 μ F, 50 V polyester film (DigiKey P4667)
 C29—100 μ F, 50 V, low-ESR electrolytic (Mouser 140-ESRL50V100)
 D1—1N4148 silicon diode
 D2—Panel-mount red LED (Mouser 35MP062)
 J1, J5—Binding post, red (Mouser 164-4205)
 J2, J6—Binding post, black (Mouser 164-4201)
 J3—Binding post, green (Mouser 164-4204)
 J4, J7, J8—2-pin, 0.1-inch header (DigiKey WM4000)
 J9—DC power jack, insulated, to mate with the connector on the wall transformer (Mouser 163-4303)
 J10—5-pin, 0.1-inch header (DigiKey WM4003)
 J11—Panel-mount, female DB9 connector (Jameco 15780)
 J12—3-pin, 0.1-inch header with shorting jumper (DigiKey 929834-02-36)
 P10—5-pin terminal housing with pins (DigiKey WM2014)
 P4, P7, P8—2-pin terminal housing with pins (DigiKey WM2011) pins are (DigiKey WM2200)
 R1—100 k Ω , 1/4 W, 1% metal film (Mouser 271-100K)
 R2—90.9 k Ω , 1/4 W, 0.1% metal film (Mouser 279-90.9K)
 R3, R7—10 k Ω , 1/4 W, 0.1% metal film (Mouser 279-10K)
 R5—110 Ω , 1/4 W, 0.1% metal film (Mouser 279-110)
 R6—11.0 Ω , 1/4 W, 0.1% metal film (Mouser 279-11)
 R8, R9—51 k Ω , 1/4 W, 5% carbon film (Mouser 291-51K)
 R10—240 Ω , 1/4 W, 5% carbon film (Mouser 291-240)
 R11-R16—10 k Ω , 1/4 W, 0.1% metal film matched to 0.01% or better (Mouser 279-10K)
 R17—2940 Ω , 1/4 W, 0.1% metal film (Mouser 279-2.94K)

R18, R19—10 k Ω , 1/4 W, 0.1% metal film matched to 0.01% or better, see sidebar (Mouser 279-10K)
 R20—4490 Ω , 1/4 W, 0.1% metal film (Mouser 279-4.49K)
 R21 to R24—not used
 R25, R28—22.1 k Ω , 1/4 W, 1% metal film (Mouser 271-22.1K)
 R26—1000 Ω , 1/4 W, 1% metal film (Mouser 271-1K)
 R27—15 k Ω , 1/4 W, 1% metal film (Mouser 271-15K)
 R29—1 Ω , 1 W, 5% carbon film (Mouser 294-1.0)
 R30, R31—2000 Ω , 1/4 W, 1% metal film (Mouser 271-2K)
 R32—3000 Ω , 1/4 W, 1% metal film (Mouser 271-3K)
 S1—DP3T PC-mount slide switch (Mouser 10SL008)
 S2—SPST mini toggle switch (Jameco JMT113)
 T1—24 V ac, 500 mA or higher wall transformer (Mouser 412-224034)
 U1, U7, U8—Texas Instruments TLC2652ACP low-noise chopper op amp (Newark 08F9048)
 U2—Linear Technology LTC2400IS8 24-bit ADC (DigiKey LTC2400IS8)
 U3—74HC14AFN hex inverter (DigiKey TC74HC14AFN)
 U4, U5, U6—Thaler Corp VRE305A +5 V reference (Thaler VRE305AD)
 U9—National Semiconductor LM675T power op amp (Jameco120926)
 U10—LM2940CT +15 V low-dropout voltage regulator (DigiKey LM2940CT-15)
 U11—78L05A +5 V regulator (DigiKey NJM78L05A)
 U12—78L06A +6 V regulator (DigiKey NJM78L06A)
 U13—79L06A -6 V regulator (DigiKey NJM79L06A)
 U14, U15, U16—4N25 optoisolator (DigiKey 4N25QT)
 U17—Bridge rectifier, 50 V, 1 A (Jameco 103000)
 Enclosure—cast aluminum 6.8 \times 4.7 \times 2.2-inch (Mouser 400-4593)
 Heat sink for LM675T power op amp
 Circuit board—See [Note 6](#)
 Hardware
 Bumpers (stick-on rubber feet) (DigiKey SJ5523-0)

Linear Technology demo program records data at a fixed rate, but my program lets you select the time—up to 3000 seconds in one-second steps.

Wrapping It Up

The +5 V reference, which is brought out to its own set of binding posts, is good enough to be used as a reference for other instruments. It might be worthwhile to add an input inverter to measure negative voltages; but for its cost, this is useful meter.

Ron got his Technician class license at age 16 as WOMNP and was active on 2 meters. His call became K5UJC when he moved to New Mexico in 1956. He now has degrees in electrical engineering from New Mexico State University and is retired from an engineering position at White Sands Missile Range. In 1957, he started Testronic Development Laboratory (now TDL Technology Inc) to do consulting and electronic product development. He is still the TDL president and keeps busy in "retirement" doing consulting and technical writing.

Notes

- ¹Linear Technology Corporation, 1630 McCarthy Blvd, Milpitas, CA 95035-7417; tel 408-432-1900; www.linear-tech.com.
- ²Thaler Corporation, 2015 N Forbes Blvd, Tucson, AZ 85745; tel 800-827-6006; www.thaler.com.
- ³R. Tipton, "An Improved AC-DC Voltage Reference," *Nuts and Volts* magazine, Jan 2000.

⁴You can download this program along with the circuit-board layout and enclosure drilling drawings from www.zianet.com/tdl. Click on Magazine Article Reprints and select SVMETER.ZIP. After unzipping the file, look at contents.txt for information on the other files. You can also download this package from the ARRL Web www.arrl.org/qexfiles/. Look for SVMETER.ZIP.

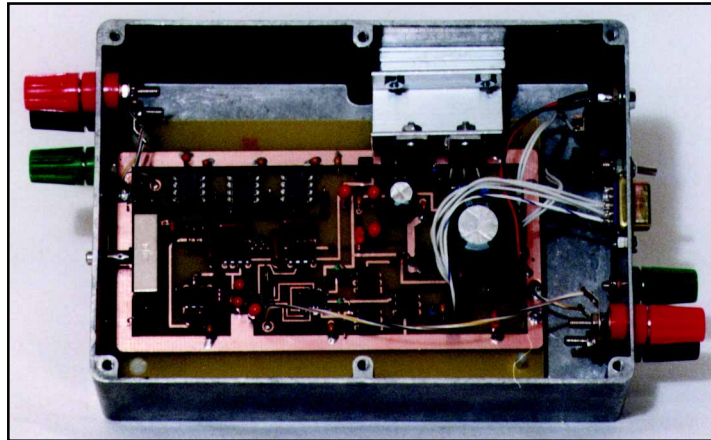


Fig 7—Photo of the circuit board in its enclosure. The heat-sink bracket is a 2-inch length of aluminum channel with two 2-inch lengths of $1/8 \times 1/2$ -inch bar and one 2-inch length of $1/16 \times 1/2$ -inch bar as spacers to the enclosure wall. Remember to use insulators and heat-sink compound.

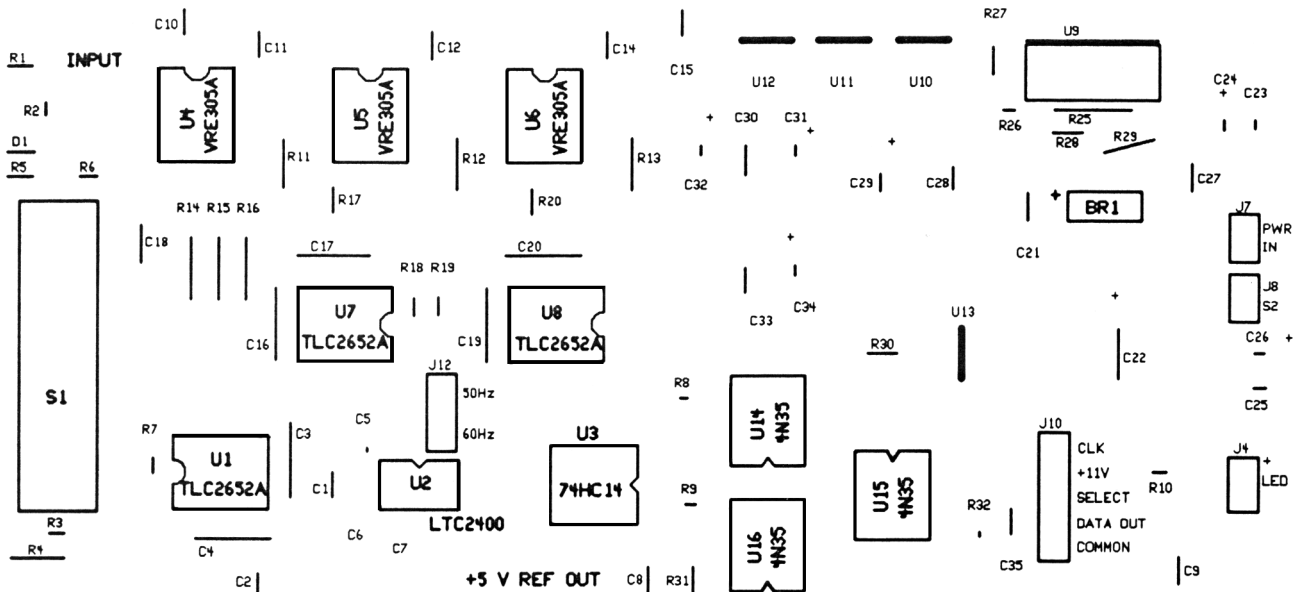


Fig 8—A parts-placement diagram for the LTC2400 voltmeter. All off-board connections use connectors except for the input and reference output.

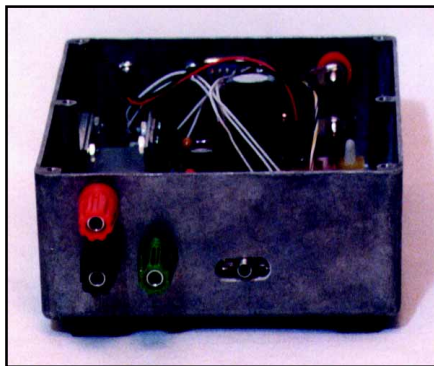


Fig 9—The voltage-input end. The slide switch (gain control) lever extends about a 1/4 inch through a slot in the enclosure wall.



Fig 10—The power-supply end. The wall-wart-input connector, LED and power switch are on the right. The binding posts on the left are for the +5 V reference-voltage output.

⁵A kit of eight matched 10-k Ω , 0.1% resistors is available from the author for US \$12 (postpaid in the US and Canada).

⁶The circuit board is available from FAR Circuits, 18N640 Field Ct, Dundee, IL 60118-9269; tel 847-836-9148 (voice and fax); www.cl.ais.net/farcir/. The boards are \$14 each plus \$1.50 shipping for up to four boards. VISA and MasterCard accepted with a \$3 service charge. This is a solder plated, double-sided board, but the holes are not plated through, so a few component pins must be soldered on both sides. There are also six *vias*, where short pieces of wire are inserted and soldered on both sides.

⁷MIX Software Inc, 1132 Commerce Dr, Richardson, TX 75081; tel 800-333-0330; www.mixsoftware.com.

⁸MarshallSoft Computing Inc, PO Box 4543, Huntsville, AL 35815; tel 256-881-4630; www.marshallsoft.com.

Parts Distributors

Digi-Key Corporation, 701 Brooks Ave South, Thief River Falls, MN 56701-0677; tel 800-344-4539; www.digikey.com.

Jameco Electronic Components, 1355 Shoreway Rd, Belmont, CA 94002-4100; tel 800-831-4242; www.jameco.com.

Mouser Electronics, 958 N Main, Mansfield, TX 76063-4827; tel 800-346-6873; www.mouser.com.

Newark Electronics, 1919 S Highland Ave, Lombard, IL 60148-6119; tel 800-463-9275; www.newark.com. □□

Ready to make some waves?

Denny & Associates, P.C. is a consulting engineering firm serving the broadcast and wireless industries. The firm, based in suburban Maryland just outside the Beltway, has a well-established reputation for providing its clients with innovative solutions to complex engineering problems.

The firm offers communications engineers a career with variety, flexibility, stability, and an exceptional opportunity for advancement. As a communications engineer, you will prepare coverage predictions, allocation and interference studies, and FCC and FAA filings using state-of-the-art software tools and participate in the design of a wide variety of communications facilities. Positions are open at all experience levels. Station experience, BS in electrical engineering or an equivalent technical degree, EIT or PE are considered pluses, and good oral and written communication skills are important.

Please contact Human Resources



Denny & Associates, P.C.
Consulting Engineers

6444 Bock Road, Oxon Hill, MD 20745-3001
Fax: 301.768.5620 E-mail: jobs@denny.com
www.denny.com

Deconvolution in Communication Systems

The title contains a fancy name for a DSP process that can reveal details of wave propagation paths without prior knowledge of their nature. Multipath and other distortions may be detected and corrected to some extent with this technique. It's also useful in DSP filter design. Come discover how it's done.

By Doug Smith, KF6DX

Multipath distortion is the enemy of many radio communicators, whether they are interested in moon-bounce, terrestrial microwave or HF. Multipath may be generally described as a situation in which radio signals take many different routes between transmitter and receiver. Those routes quite often have different lengths, so received information consists of a multitude of superposed copies of the transmitted information, smeared over time.

It might seem at first that there is nothing DSP or any other technology can do about that distortion, since it is caused by physical phenomena beyond

our control. But where knowledge exists beforehand about the nature of the transmitted signal, it turns out something often can be done. I'll try to explain what I've learned about that.

Modeling Multipath Environments

Imagine you're standing just inside the Taj Mahal (Fig 1). The clack of shoes meeting tile and the hush of whispers bounce lightly from the walls and ceiling. Your friends entered just moments ago. You scan the foyer; they aren't in sight. You call out to them. Your voice echoes through the halls and chambers of that place for what seems like an eternity—until security personnel come and tell you not to do that!

Your friends, having reached a distant part of the building by now, hear

the sound; but it doesn't sound much like you. In fact, it sounds more like a dull roar because your voice has taken so many paths to their location. All the echoes overlap so much that words and even syllables are indistinguishable. You are in a *reverberant environment*.

Your friends begin walking toward you. As they come closer, you speak again. This time, they understand you and reply. The number of paths and the differences in their lengths have now decreased; the time smearing and overlap of echoes are now little enough to allow you to be intelligible. You have demonstrated a useful model for reverberant environments: many discrete paths, each with its own transit time or delay and each with a particular attenuation. See Fig 2.

In the figure, multipliers h_n have

values less than unity and represent the attenuation on paths whose delays are proportional to n . Notice that no signal propagates directly from the input to the output; the output is derived only from delayed signals. That indicates the usual situation: Your friends are some finite distance from you, even when in view. So even on a direct path, there is always a positive, non-zero propagation delay. The model also applies when your friends are around the corner; they cannot hear your voice directly, but only the sound that is bouncing off the walls, floor and ceiling.

When the delays z^{-n} in the model are spaced apart by the same amount of time, which we shall call the *sampling period*, the set of attenuation constants h_n is referred to as the *impulse response* of the system. In fact, Fig 2 is exactly the same as the block diagram of a *finite-impulse-response (FIR) filter*, a common construct in DSP.¹ While it is perhaps strange to think of the Taj Mahal as a filter, that is indeed what it is. When the constants h_n are chosen strategically, the system may be made into almost any filter shape imaginable. When they are undefined, as in the case of sounds propagating through buildings or radio signals through whatever medium, the transfer function (frequency response) is also undefined.

If the impulse response of a system can be found (the model), then another system may be built having a transfer function that is the inverse (the inverse model) of the original system. When the two systems are cascaded, the final output is a restored version of the input signal (the desired). For the Taj Mahal or a set of radio propagation paths, the hard part is discovering the original impulse response. When the environment is known and fixed (as in the Taj Mahal), the impulse response may be discovered by modeling the structure and doing ray-tracing experiments on a computer, for example. When the environment is unknown (a radio path), we must resort to *inverse modeling* to get a clue about the corrupting system's impulse response.

That is fairly easy when the unknown environment is fixed. When it is changing, it is much more difficult. Even then, though, DSP provides weapons to combat the enemy. Follow me into a discussion of how those two cases are generally handled.

Inverse Modeling

When performing the operation
¹Notes appear on page 51.

shown in Fig 2, the output is the sum of all the delayed, attenuated signals. That sum is called a *convolution sum*; the input signal is said to be *convolved* with the impulse response. A convenient notation for the convolution sum is:

$$r_t = \sum_{n=0}^{L-1} h_n x_{t-n} \quad (\text{Eq 1})$$

where r_t is the output at discrete time t , x_{t-n} is the original input signal at time $t-n$, and L is the length of the finite-impulse response. The transfer function of that system may generally be found by taking the discrete Fourier transform (DFT) of the impulse response, h_n :

$$H_\omega = \sum_{n=0}^{L-1} h_n e^{-j\omega n} \quad (\text{Eq 2})$$

Where ω is the angular frequency in radians/s. The goal of inverse modeling is to discover the system that has a transfer function equal to the reciprocal of H_ω . Were a copy of the original input signal, x_t , available, that would be easy to do, as shown in Fig 3. The corrupted signal r_t forms the input to the inverse filter, whose coefficients are adjusted in some way based on a comparison between the original input signal, x_t and the doubly processed output of the inverse filter, y_t . When the error signal e_t goes to zero, the inverse filter's frequency response G_ω is the reciprocal of the corrupting system's:

$$G_\omega = (H_\omega)^{-1} \quad (\text{Eq 3})$$

Inverse filter G is said to "*deconvolve*" the original input signal and the

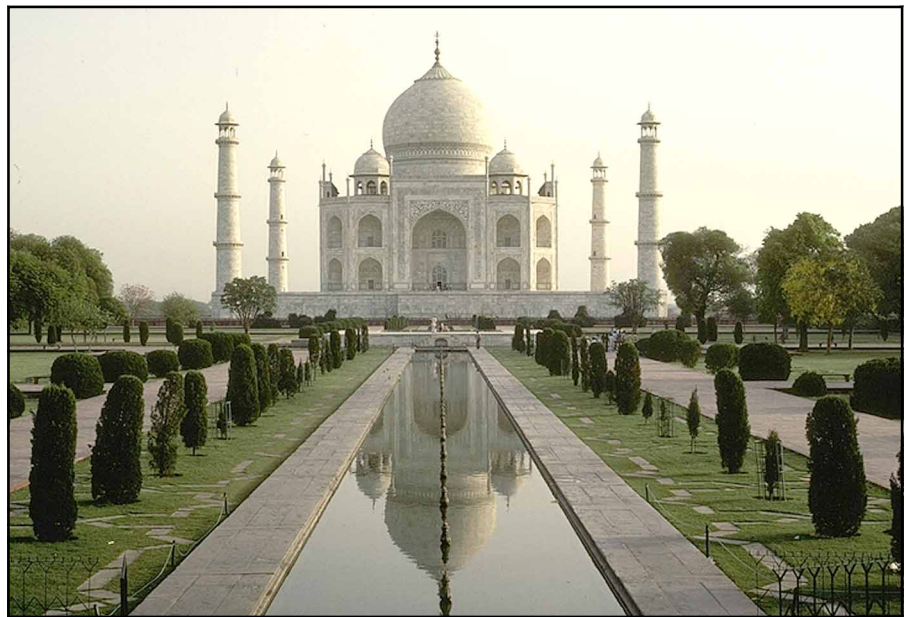


Fig 1—A reverberant environment.

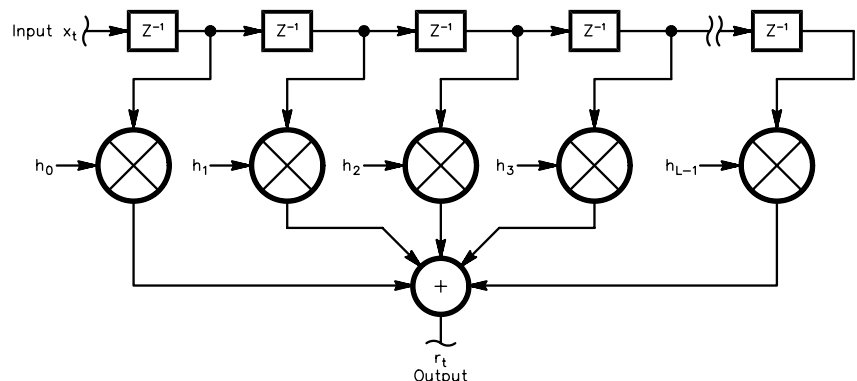


Fig 2—An FIR model of a reverberant environment.

corrupting filter's response, restoring the original signal. In the steady state, the inverse filter performs the operation:

$$y_t = \sum_{n=0}^{L-1} g_n r_{t-n} = x_t \quad (\text{Eq 4})$$

The transfer function of the cascaded system is a single, unity-amplitude impulse. A fixed delay is used in the upper path of the original input signal to compensate the delay through the two filters.

It's perhaps surprising that impulse response g_n is not necessarily the inverse DFT of G_ω , although that has sometimes been stated, incorrectly. The proof of that is a bit more complex than what I want for this article. Oppenheim and Schaffer take up the subject briefly.²

Now it's time to mention how impulse response g_n is adjusted during inverse modeling to efficiently achieve the desired result. The most popular method is called the least-mean-squares or LMS algorithm. It was published by Widrow and Hoff in 1960³ and it's the same as algorithms currently used for adaptive noise reduction and automatic notches in radio receivers.

In the LMS algorithm, each value or *coefficient* of the impulse response is adjusted at each sample time according to:

$$g'_n = g_n + 2\mu e_t x_t \quad (\text{Eq 5})$$

for L values of n , where μ is a constant chosen to alter the speed of convergence and the amount of error in the steady-state solution. Additional details of the behavior of adaptive filtering systems may be found in the Amateur Radio literature⁴ and will not be treated further here.

You may be questioning how the methods described above can be useful, since they require a copy of the signal originally sent. One application is found in the suppression of echoes on telephone circuits. Another is found in DSP filter design.

Telephone-Line Echo Suppression

On a two-wire, full-duplex telephone circuit, hybrids are used at each end to segregate transmitted and received signals. The hybrids must achieve significant isolation between the two signals lest a signal transmitted at one end arrive at the other end to be retransmitted toward the sender. The result is a series of echoes. When termination impedances are not perfect on the line or imbalance exists, those echoes are always present. They

are most discomfiting to the talker—and perhaps also to the listener—especially over lengthy, overseas paths having transit times of 300 ms or more. This sort of thing can also be a problem in speakerphones.

The system of Fig 3 may be employed to eliminate the echoes, since copies of both transmitted and received signals are present at the transmitter. That is, in fact, what telephone companies currently do to handle the situation. I notice some long-distance companies need to check the operation of their echo cancelers. Echoes were rampant in the early days of long distance, then the problem seemed to have virtually disappeared for a long time; but now, I regularly get reports of its reappearing.

LMS Filter Design

This example is one of direct modeling rather than inverse modeling, so it's a little different from what we've covered so far; but it's still useful because it shows something about the underlying concepts of system modeling in general.

Imagine we want to find the finite impulse response corresponding to some particular filter shape—say, a low-pass. First, we must characterize the desired transfer function, H_ω , completely by both its amplitude and phase responses. Amplitude versus frequency is more important at this stage than phase; we dream up a *pseudo-filter* having the desired response. FIR filters generally have linear phase responses; the phase versus frequency plot is a straight line. We place this pseudo-filter into the modeling system shown in Fig 4. Notice that the pseudo-filter need not actually exist as an FIR filter; it is just a block that replicates the transfer function we want, and we may perform that function in any way.

To make the adaptive filter, G , in Fig 4 converge to match the pseudo-filter's response, the generator signal

x_t 's spectrum must contain energy at all frequencies of interest. White noise is a good first choice for this signal source. Start the thing going and when the LMS algorithm has minimized the error e_t , the adaptive filter will have converged on the impulse response most closely matching our desired response.

Depending on the length (L) of the adaptive filter, it may be difficult to achieve the desired response at certain frequencies exactly. That may be addressed in LMS filter design by changing the amplitude-versus-frequency content of the generator, x_t . A large relative amplitude of the generator's content at some particular frequency allows the filter to more closely meet its specification at that frequency.

When a Desired Response Is Not Available

For radio signals, the telephone scenario above is not particularly relevant. The question becomes "How can we use inverse modeling when a copy of the original signal is not available?" The answer is that the signal x_t used to compute error signal e_t and used in the LMS algorithm need not be an exact copy of the original; it need only be a reasonable approximation of that signal. Any information about the original is useful in nudging the algorithm toward convergence at the start of adaptation; we then get a better deconvolution that, in turn, helps the next iteration toward the optimal solution. Let's look at some examples that illustrate how to make inverse modeling work without an exact copy of the original signal.

Adaptive Equalization of a Dispersive Medium

A *dispersive* medium is one in which different frequencies travel at different velocities. That is, the *group delay* is not constant. To grasp these terms, let's say we have a medium or channel with frequency response H_ω . Response H_ω may be completely characterized

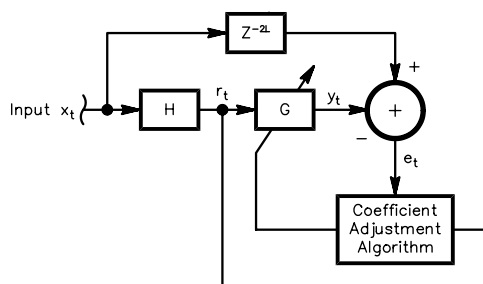


Fig 3—Block diagram of an inverse-modeling system.

by its amplitude response, A_ω , and its phase response, ϕ_ω :

$$H_\omega = A_\omega e^{j\phi_\omega} \quad (\text{Eq 6})$$

The time delay (or phase delay) through the channel is:

$$t_{\text{prop}} = \frac{-\phi_\omega}{\omega} \quad (\text{Eq 7})$$

and the group delay is equal to the differential time delay:

$$t_g = \frac{-d\phi_\omega}{d\omega} \quad (\text{Eq 8})$$

A medium is said to be dispersive if the group delay is not a constant function of frequency; that is, if:

$$\frac{d^2\phi_\omega}{d\omega^2} \neq 0 \quad (\text{Eq 9})$$

Dispersive propagation is very similar to multipath, since it also implies that received information is smeared over time. Now let's say that we have a dispersive medium that is not horribly so. We also stipulate that noise levels are reasonably low, so as not to be a problem in demodulation of the data signal we're going to send through the medium. To further simplify what follows, let's also say the channel has a very large bandwidth.

Adaptive equalization may conveniently be discussed by considering the case of a single carrier, modulated by a single binary signal. While that is not a common situation on telephone lines, the format is still used over radio quite a bit. In any case, it is the simplest instance, and study of m -ary or multiple-carrier systems stems from it.

Now a simple data transmitter encodes a binary one as a transition of one polarity; a binary zero is encoded as a transition of the opposite polarity. That is true no matter the modulation format. FSK, PSK and other traditional formats may employ rapid polarity transitions that, unless otherwise limited, may cause the signal to occupy a rather large bandwidth. Even through a channel of large bandwidth, dispersion alters the shape of the transitions received because the carrier and modulation sidebands propagate at different velocities. That ultimately limits the data rate that may be supported.

Let's look at what happens when a very sharp one-zero transition passes through our dispersive channel (see Fig 5). What started out as an instantaneous state reversal now becomes smeared in time; its shape is determined by the impulse response of the channel. The group-delay-induced distortion makes recovery of the data more difficult. We can say that the

received signal is the convolution of the original signal and the impulse response of the channel. Its spectrum is the product of the spectrum of the original signal and the transfer function of the propagating medium. In other words, convolution in the time

domain is equivalent to multiplication in the frequency domain.⁵

Forward Equalization

It is often desirable to equalize the channel so that it can support higher data rates. The goal of an equalizer is

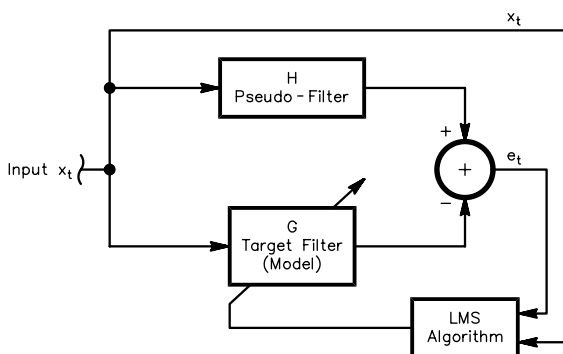


Fig 4—Block diagram of an LMS filter-design algorithm.

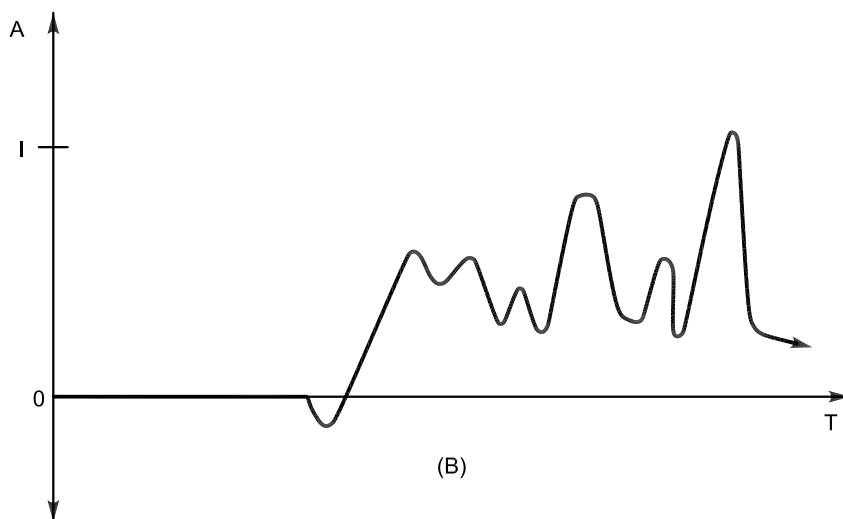
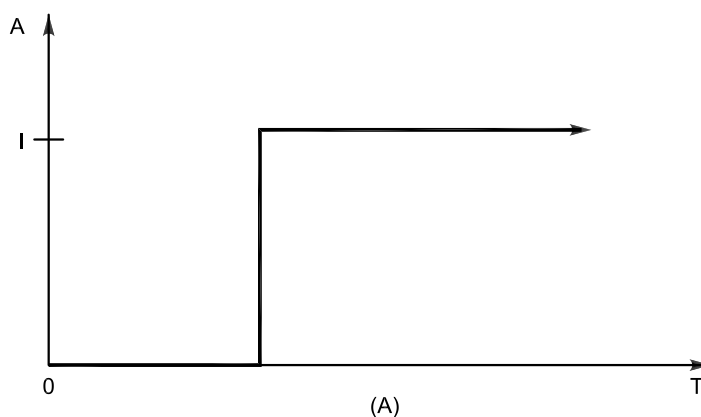


Fig 5—A: A sharp data-state transition. B: Transition as received through a dispersive medium.

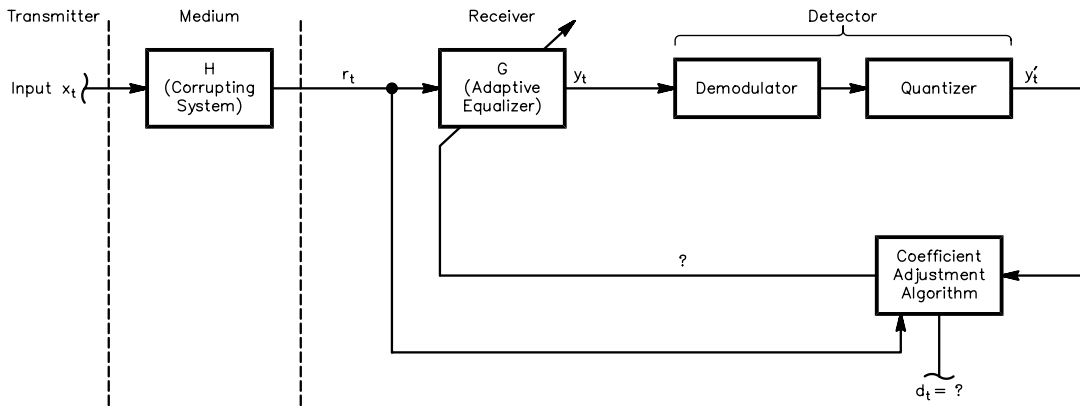


Fig 6—Block diagram of forward equalization.

to achieve a constant group delay and a flat frequency response. To equalize a channel, insert an FIR filter (G) into the data path and add a demodulator and *quantizer* at its output, as in Fig 6. So how do we decide how to adjust the equalizer? Well, one way is to arrange for a known *training sequence* to be transmitted and to compare the equalized signal with a locally generated copy of that sequence. The LMS algorithm may be used to adapt the equalizer. Then the block diagram is as shown in Fig 7. That system is fine for channels whose conditions do not change rapidly, as long as retraining can be tolerated periodically.

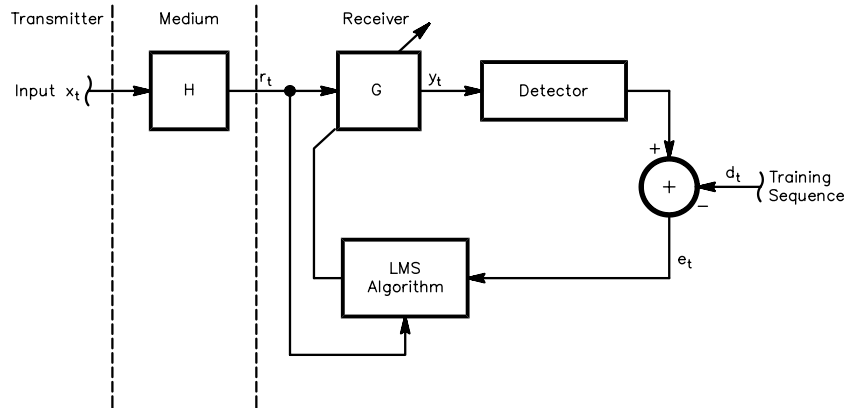


Fig 7—Forward equalization using a training sequence.

Decision Feedback Equalization

A method for deriving d_t using only the adaptive filter's output was discovered by R. W. Lucky of Bell Laboratories,⁶ obviating the need for a *priori* knowledge of the original signal. Lucky (an apt name!) found that d_t could be approximated by the demodulated signal itself, as shown in Fig 8. The bet is that if the dispersion is not severe, the demodulator generates bit decisions that are close to correct, and the adaptive filter moves toward the correct solution.

As it happens, this system works well when not much noise is present and when the dispersion is mild. Performance is improved when the sampling rate is increased beyond just once per bit.

That is fine for digital signals, but what about analog signals? The decision-making process is much tougher in that case; but the processes of *linear prediction* and *autocorrelation* may be used to steer the algorithm. Details of that are beyond the scope of

this paper. For more information, refer to Widrow and Stearns.⁷

Homomorphic Deconvolution

Now that is an esoteric phrase, but what does it mean? Well, it's a method of deconvolution that uses nonlinear transforms of signals, which are manipulated algebraically. More specifically, the nonlinear transform used is the logarithm. I'll show how a useful property of logarithms reduces multiplicative systems to simple superposition and why that is useful in deconvolving signals.

As mentioned before, convolution in the time domain is equivalent to multiplication in the frequency domain. When a signal passes through a propagation medium, the spectrum of the convolved signal is the product of the original signal's spectrum and the frequency response of the medium.

For an input signal x_t having spectrum X_ω and a medium having impulse response h_n and frequency response H_ω , a convolved signal y_t has spectrum:

$$Y_\omega = X_\omega H_\omega \quad (\text{Eq 10})$$

Now for that useful property of logarithms, which is:

$$\log(ab) = \log a + \log b \quad (\text{Eq 11})$$

If we take the logarithm of Y_ω , we have:

$$\begin{aligned} \log(Y_\omega) &= \log(X_\omega H_\omega) \\ &= \log(X_\omega) + \log(H_\omega) \quad (\text{Eq 12}) \\ &= C_{x_\omega} + C_{h_\omega} \end{aligned}$$

Taking the inverse Fourier transform of Eq 12 therefore results in the sum of two time-domain sequences:

$$c_{y_t} = c_{x_t} + c_{h_t} \quad (\text{Eq 13})$$

c_{y_t} is called the *cepstrum* of y_t . That term and a bunch of other funny terms were coined in a paper by Bogert,

Healy and Tukey.⁸ The block diagram of a system that produces it is shown in Fig 9.

Eq 13 is a useful result since, in many reverberant environments, the two cepstral components c_{xt} and c_{ht} are easily separated because they are so different. For example, let's say that most of the energy in c_{ht} lies at low values of t and most of the energy in c_{xt} lies at high values of t . That might be the case for a voice bouncing around in the Taj Mahal. Simple window functions may segregate the individual energy contributions. Then each cepstral component may be transformed back to a regular time sequence using a process that is the inverse of Fig 9. That inverse system is shown in Fig 10 for one of the components, c_{xt} . Its output is a deconvolved (restored) version of x_t .

Homomorphic deconvolution requires minimal information about the nature of the original signal and of the propagation medium. The basic requirement is that the significant length of the medium's impulse response be considerably different from the rates of change in the original signal. Where echoes are spaced at a constant period, the contribution of c_{ht} may be removed with a window that looks like a notch filter, removing only those samples that fall within a small range of values of t . In that last case, though, a less-complex method may exist for *de-reverberation*.

A Sigma-Delta Method for De-Reverberation

In the special case where all echoes are spaced apart in time by a constant amount and those echoes decay in amplitude geometrically, a more straightforward method may be used to recover the original signal. Such reverberant environments may be found in radio communications systems and in public-address venues like large baseball or football stadia, for example. You may hear the announcer get on the public-address system and say, "Now batting, batting, batting...number nineteen, nineteen, nineteen...Tony Gwynn, Gwynn, Gwynn!"

The sound you hear is the sum of the direct signal and an infinite series of regularly spaced echoes declining in amplitude exponentially. The situation may compactly be represented as a summation:

$$y_t = \sum_{k=0}^{\infty} \mu^k (x_{t-nk}) \quad (\text{Eq 14})$$

where x_t is the input signal, μ is a positive constant less than unity and n is the number of sample times between

echoes. This is clearly a causal system since output depends only on present and past samples. The original signal may be recovered using "first-differencing" (discrete differentiation):

$$y_t - \mu y_{t-n} = \sum_{k=0}^{\infty} \mu^k (x_{t-nk}) - \mu \sum_{k=0}^{\infty} \mu^k (x_{t-nk-n}) = x_t \quad (\text{Eq 15})$$

This is approximately the difference between samples of the corrupted signal spaced one echo-time apart; but this method ignores all echoes but the first. We obviously have to wait for that first echo to occur to retrieve its energy. The system introduces a delay of n sample times before producing the desired output. Additional energy contained in all subsequent echoes is lost with this algorithm.

The total signal amplitude contributed by any particular original sample is the sum of the direct signal and all its echoes, which, assuming the original signal is of unity amplitude, is:

$$E_{\text{total}} = \sum_{k=0}^{\infty} \mu^k = 1 - \frac{\mu}{\ln \mu} \quad (\text{Eq 16})$$

That means that when $\mu=0.93$, less than one tenth of the total energy is recovered by using only the first echo—a lot of the energy is in the other echoes. Signal-to-noise ratio (S/N) would be degraded by about 20 dB. In this case, it's clearly worth an additional wait to improve our lot.

To recoup the energy in all echoes would take an infinitely long period, so

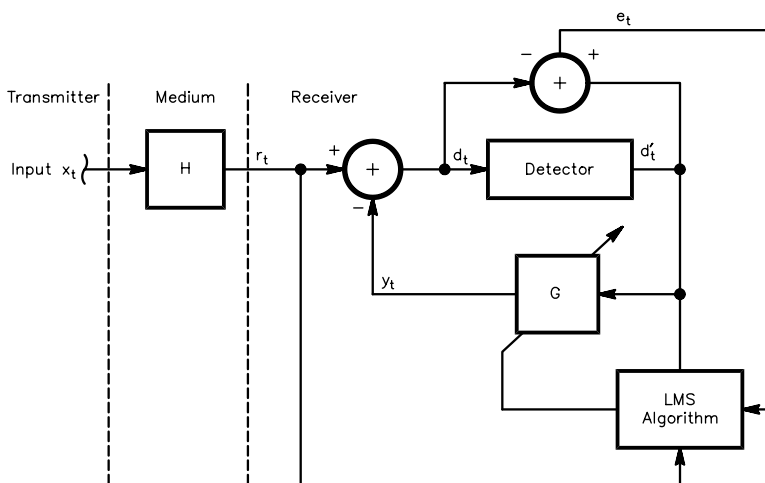


Fig 8—Decision feedback equalization using the received data as a desired signal. In this method, an adaptively filtered copy of the detected signal is subtracted from the unmodified received signal to cancel intersymbol interference. D' is the output. Feedback equalization is typically used in concert with feed-forward equalization. For more detail, see Reference 7.

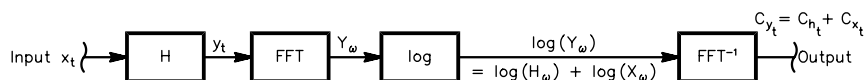


Fig 9—Block diagram of a cepstral transform.



Fig 10—Block diagram of an inverse cepstral transform.

we can only regain the energy over some number of echoes, L , for which we are willing to wait. The delay incurred is nL sampling periods. To recover the energy contained in echoes beyond the first, consider taking "second-differencing," or the weighted difference between samples two echo times apart. We have:

$$\begin{aligned}
 y_t - \mu^2 y_{t-2n} &= \sum_{k=0}^{\infty} \mu^k (x_{t-nk}) - \mu^2 \sum_{k=0}^{\infty} \mu^k (x_{t-nk-2n}) \\
 &= x_t + \mu x_{t-n} \\
 \therefore \mu x_{t-n} &= y_t - \mu^2 y_{t-2n} - x_t
 \end{aligned}
 \tag{Eq 17}$$

where x_t is determined by Eq 15 above. x_{t-n} was x_t n samples ago, and is added to the result of Eq 17 to yield $x_{t-n} + \mu x_{t-n}$. A similar operation may be performed for $y_t - \mu^3 y_{t-3n}$, $y_t - \mu^4 y_{t-4n}$, and so on, continuously, to build energy from echoes as they get older. In that way, almost all the energy can be regained from a reverberant environment having a single, uniform echo.

Performance of the Sigma-Delta Method

Over a finite number of echo intervals, L (during which we wait nL sample times), the energy recovered is not as much as in the infinite summations. It is only:

$$\begin{aligned}
 E_L &= \sum_{k=0}^{L-1} \mu^k \\
 &= \left(1 - \frac{\mu}{\ln \mu}\right) + \frac{\mu^L}{L \ln \mu}
 \end{aligned}
 \tag{Eq 18}$$

If $\mu=0.93$ and $L=8$, the S/N degradation would be about 1 dB, since about 88% of the energy would have been recovered.

The algorithm counts on absolute frequency and phase accuracy between transmitter and receiver. Serious phase distortion or frequency errors would render the sigma-delta method unusable. It is not well suited to SSB operation, therefore, without a pilot carrier and a synchronous (phase-locked) receiver, or other suitable demodulators.

The algorithm is also quite sensitive to phase noise in the local oscillators of radio transceivers and to dispersive

propagation—the thing so similar to the problem it attempts to solve! So this algorithm turns out not to be a very good pick at all, but it is relatively simple compared to homomorphic processing.

Summary

This article showed convenient modeling methods for reverberant and dispersive environments. Systems for deconvolution were discussed that correct for multipath and dispersion; they even produce a model of the corrupting system in most cases. In some instances, the model of the corrupting system may be the thing that is sought. That is the case in ionospheric studies or in planetary science, where the impulse response of the model represents a map of the atmosphere or planetary surface, respectively. Deconvolution systems are sometimes adaptive and thus are capable of handling changing propagation conditions. Homomorphic deconvolution is generally not adaptive and relies on some knowledge of the differences between the desired signal and the nature of the medium.

Research is ongoing to use adaptive receiving arrays and homomorphic processing on weak, convolved signals. Moonbounce (EME) modes are a particular target of that research.

Notes

1. C. Hutchinson, Editor, *The 2001 ARRL Handbook*, p 18.5.
2. A. Oppenheim and R. Schaffer, *Digital Signal Processing*, (Englewood Cliffs, New Jersey: Prentice-Hall, 1975).
3. B. Widrow and M. Hoff, Jr., "Adaptive switching circuits," *IRE WESCON Convention Records*, Part 4, IRE, 1960.
4. S. Reyer and D. Herschberger, "Using the LMS Algorithm for QRM and QRN Reduction," *QEX*, Sep 1992, pp 3-8.
5. M. Frerking, *Digital Signal Processing in Communications Systems*, (New York: Van Nostrand-Reinhold, 1994) p 11.
6. R. Lucky, "Techniques for Adaptive Equalization of Digital Communications Systems," *Bell Systems Technical Journal*, volume 45, pp 255-286, Feb, 1966.
7. B. Widrow and S. Stearns, *Adaptive Signal Processing*, (Prentice-Hall, 1985).
8. B. Bogert, M. Healy and J. Tukey, "The Frequency Analysis of Time Series for Echoes: Cepstrum, Pseudo-autocovariance, Cross-Cepstrum and Saphe Cracking," *Proceedings of the Symposium on Time Series Analysis*, (New York: John Wiley and Sons, 1963) pp 209-243. □□





VARI-NOTCH® DUPLEXERS

FOR 2 METERS



The TX RX Systems Inc. patented Vari-Notch filter circuit, a pseudo-bandpass design, provides low loss, high TX to RX, and between-channel isolation, excellent for amateur band applications. TX RX Systems Inc. has been manufacturing multicoupling systems since 1976. Other models available for 220 and 440 MHz, UHF ATV and 1.2 GHz.

MODEL 28-37-02A
144-174 MHz
92 dB ISOLATION AT 0.6 MHz SEPARATION
400 WATT POWER RATING

TX RX SYSTEMS INC.
8625 INDUSTRIAL PARKWAY, ANGOLA, NY 14006
TELEPHONE 716-549-4700 FAX 716-549-4772 (24 HRS.) e-mail: sales@txrx.com

A MEMBER OF THE BIRD TECHNOLOGIES GROUP



19" RACK MOUNT

Despite its lower output power, the SMALL it provided more volume with less distortion—wattage isn't everything! The TPA2000D2 operates at 5 V with a quiescent current of 8 mA. By contrast, the LM4835 (a modern surface-mount 2-W stereo linear amplifier) also operates at 5 V but uses 15 to 30 mA. The popular LM386 only puts out 0.13 W and needs 3.5 to 7 mA quiescent current with a 5-V supply.

What Is Class D?

Descriptions for various amplifiers are given in *The ARRL Handbook*.⁴ The *Handbook* descriptions apply to tuned RF amplifiers, but we can use them as a general guide.

Class-A amplifiers are linear circuits that accurately reproduce the input signal with the greatest fidelity and least distortion. This is at the expense of poor power efficiency. A typical efficiency for class A is 25%, the remainder of the energy is dissipated as heat.⁵ A bias current runs in the amplifier at all times, and the input signal is used to vary that current.

Class-B amplifiers are biased so that no power supply current flows in the absence an input signal. The waveform

looks like a half-wave rectified signal. While it is suited for some RF applications, the distortion would be intolerable for audio work. Efficiency is 60%.

Class-AB amplifiers are biased between A and B, and they gain some of the benefits of each operating class. Maximum efficiency typically exceeds 50%.

Class-C amplifiers are saturated amplifiers, and current only flows in narrow pulses corresponding to peaks of the input signal. Efficiency can be 80% but due to their extremely nonlinear nature, they are not used as audio amplifiers.

Class-D amplifiers work as saturated switches controlled by the input signal. They are not commonly used in amateur applications. The harmonic-rich output needs careful filtering, and the amplifiers require sophisticated design and adjustment techniques. They are seldom used in amateur projects because the additional complexity and cost rarely justifies their use.

The ARRL Handbook is not the only source that until recently excluded applications for class-D amplifiers that are now becoming practical. Consider this from *TRIPATH*:⁶ "The audio qual-

ity of class-D PWM amplifiers is inferior because of fundamental problems with the PWM approach. The output transistors are not perfect switches and are not perfectly matched, and this causes distortion. The switching of the transistors causes 'ground bounce,' which adds noise. There is crossover distortion caused by the dead time between when one of the output transistors turns off and the other turns on (like a Class-AB amplifier). Finally, all the energy of the triangular waveform cannot be removed from the audio band with a simple low-pass filter, and what remains is distortion."

My home-built class-D stereo amplifier, using a TPA2000D2, sounds better than my expensive home stereo—there is no distortion that I can hear. If you suspect I am an electronic genius skilled at designing sophisticated circuits, I am not. It's the engineers at TI who are; and a few dollars⁷ allow me take advantage of their genius. I'd be nuts not to want to try it out!

How Class D Works

Class-D operation is simple in principle: a triangular waveform and the incoming audio signal pass through a

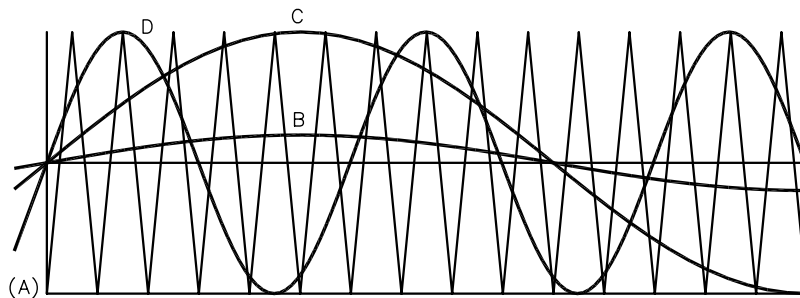


Fig 2—Output of the comparator for various signals. Curve A has a low-level audio input, curve B a higher-level audio input and curve C an input at a higher frequency than for curve B.

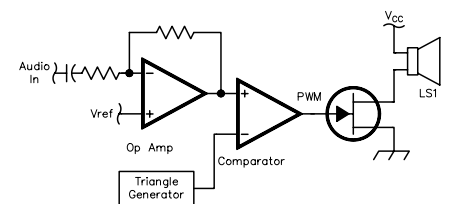


Fig 3—The basic elements needed for class-D operation.

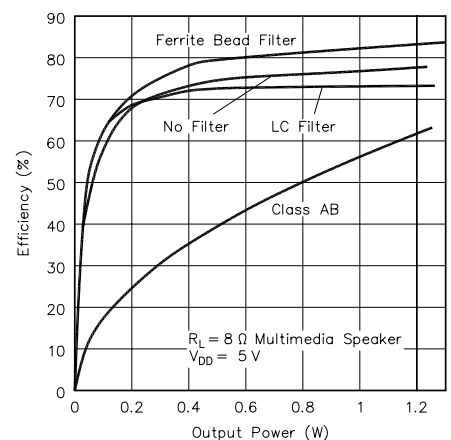


Fig 4—Efficiency versus output power for a TPA2000D2 compared to a typical class-AB amplifier (Courtesy of Texas Instruments).

comparator. The comparator output goes high when one input signal is greater than the other, and is 0 when it is lower. Fig 2 shows how the comparator output is comprised of a string of pulses whose width is dependent on the amplitude of the incoming signal.

Analyzing just how the volume and frequency information was encoded into the pulse stream was educational. Referring to Fig 2 again, for a low-volume signal of set frequency (see the sine wave “A” in Fig 2A, and the pulse waveform in Fig 2B) the pulse widths do not vary much when going from high to low volume. Sine wave “B” in Fig 2A shows a signal with the same frequency, but at a much higher magnitude. Here the pulse width (Fig 2B) varies a lot. Sine wave C has the same magnitude as sine wave B, but at twice the frequency. The pulse-width variations (Fig 2D) are also very large, but they happen twice as often.

The comparator output drives a voltage controlled device, a MOSFET, that controls the current through the speaker. (See Fig 3.) With the comparator output at 0 V, the MOSFET is off and no current flows. When the comparator output is high, the MOSFET is turned on. When the voltage is high for a long time, there is a long burst of current through the speaker giving a greater output power (I^2R). If the *on-and-off* is more rapid, the tone oscillations yield a higher pitch. For low distortion, it is important that the triangular waveform have a linear slope.

Amplifying the Signal

If the audio signal level is very low, how do we get a loud signal out? The signal that goes into the comparator must have a greater voltage swing to produce a larger change in the pulse widths—this is done using a linear preamplifier. If you’re wondering—as I did—if the linear amplifier degrades the efficiency of the amplifier overall, the answer is no. It has very little effect on the total efficiency because it is amplifying voltage, not power. The output load for the voltage-amplifier section is a comparator, which typically has an input resistance of at least 1 M Ω . If the amplifier boosts the input voltage to ± 2 V, the power out is only 2 μ W, (V_{RMS}^2/R). Even if the linear amplifier was only 10% efficient, its operating power of 0.02 mW would be insignificant compared to the 40 mW of the overall amplifier. It’s the stage controlling the current to the low-impedance load that must be efficient, and thanks to modern MOSFETs with “on” resis-

tances in the milliohm range and fast switching times, this part is efficient.

Real-World Efficiency

We previously noted that class AB has a maximum efficiency of around 50% and that class-D efficiencies could be 80 to 85%. Maximum efficiency numbers are a bit misleading for real-world use. Maximum efficiency is based on a constant large-magnitude input audio signal; but for real-world audio, voice or music applications the audio is often quite low and only peaks for a small part of the time. TI ran a “real world” test comparing class-AB amplifiers to class-D amplifiers and found that the efficiencies were 16% for Class AB and 45% for class D, with a resultant three-fold longer battery life using class D. Fig 4 shows how the efficiencies of a Class-D TPA2000D2 amplifier and a typical class-AB amplifier vary with at different output power levels. Class D offers great power savings at low signal levels.

A Homebrew Class-D Amplifier

It’s easy to homebrew a class-D amplifier. (See Fig 5.) While it isn’t very efficient, it is an interesting exercise letting us see how it works. To that end, I built several.

Originally I was going to use an LM566 waveform generator; but I learned this IC has been discontinued. I couldn’t find a simple inexpensive IC to make triangle waves. There were several circuits in the literature using an integrator and threshold detector, but the practical implementation of these circuits was more time consuming than I wanted—with pesky interactions, signal-size output limitations, poorly shaped waveforms, etc. Fortunately, I had a few ICL8038s lying around; and like the LM566 they could generate an instant triangular waveform. (The ICL8038 also appears to be becoming an “endangered” IC). IC products are ever changing, and I am surprised that triangle generators seem to be nonexistent. Perhaps this is so because all of the applications that need them now incorporate them in the same IC as the rest of the circuit, as done in the TPA2000D2. Besides the triangle waveform generator, I used a LM393 as a common comparator, along with a PNP transistor and inductor as shown in the schematic. I did not try to optimize this circuit and was pleased to see it worked.

The circuit needed several discrete components; and there would be a lot more needed if I tried to make this into

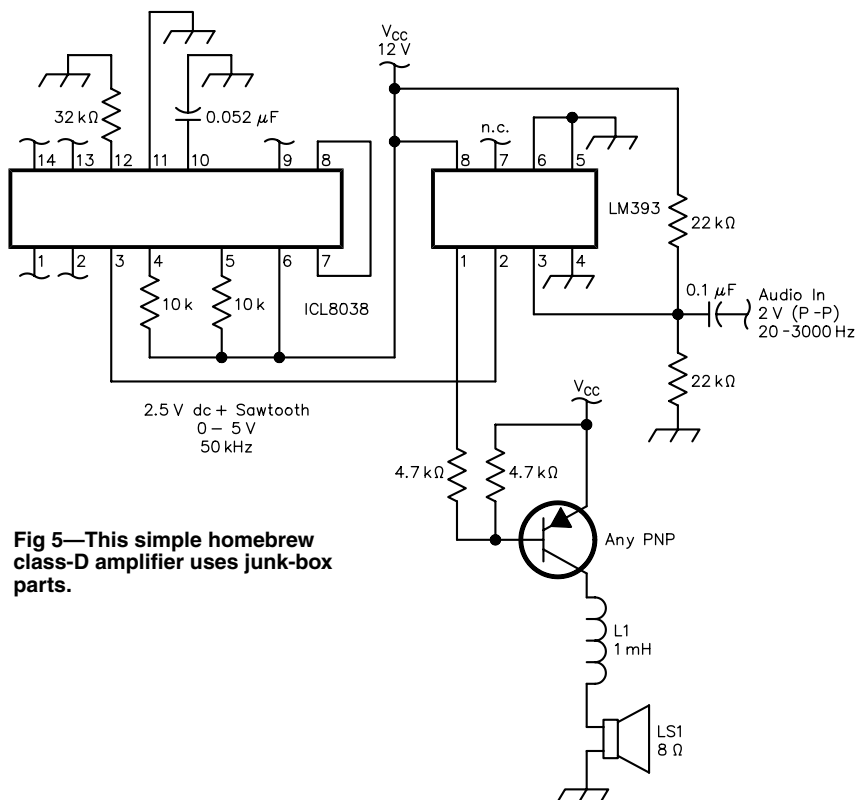


Fig 5—This simple homebrew class-D amplifier uses junk-box parts.

a production amplifier. By contrast, the TPA2000D2 has all the necessary supporting functions built in, such as the triangle waveform generator. (See Fig 6.) It also has many extra protection features built in, such as thermal, over-current and under-voltage protection.

Working With The TPA2000D2

Today there are several waves of change still out there at sea. The first headed our way is generated by the fact that integrated circuits are shrinking in size, which tends to about double the speed of computers every 18 months or so. Moore's Law, as this curve is called,

predicts that all kinds of digital devices will either perform the same job in smaller packages, or the same-sized devices will do twice as much. So in 20 years a Pentium chip will either fit in a die 1/10,000 its current size, or it will keep its size and have roughly 10,000 times its current processing power. A similar concept holds true for solid-state memory devices. RAM chips double in capacity every year and a half or so, and magnetic disk drives are on a steeper curve, doubling in performance every nine to 12 months. —Discovery Magazine⁸

You saw this same prediction years ago. It was correct then and it still holds

true today: electronics are inexorably getting smaller and faster.⁹ Smaller could be a drawback, if you haven't begun to adapt your skills to take advantage of the new surface-mount technologies. More and more amateurs are realizing that they need to gain SMT (surface mount) component skills. As seen in Fig 7, the TPA2000D2 is smaller than the popular 1/4-W LM386 IC, and it is not much larger than my 1-W SMALL project—my first SMT project. Its multitude of pins make the IC much larger than many of those I used in my SM¹⁰ series (like the little SOT23 IC on the lower left). The pins are very closely spaced, presenting a challenge. Rather

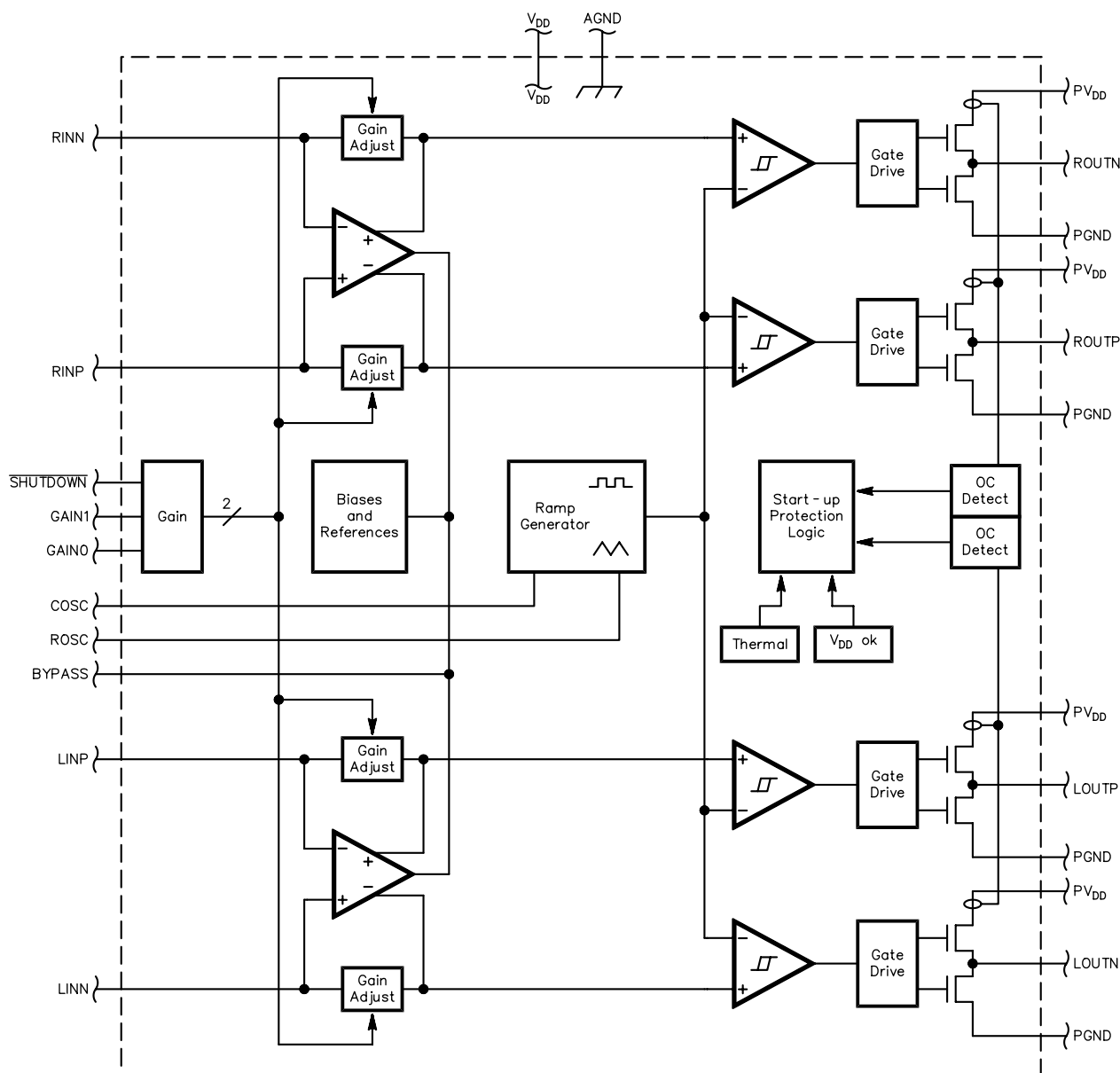


Fig 6—A functional block diagram of the TPA2000D2. Many functions are combined in one small IC package. (Courtesy of Texas Instruments)

than try to make a PC board using my Dremel-tool method, I asked FAR Circuits to make a few boards.¹¹ We are very fortunate to have FAR Circuits available to us. Fred—a ham himself—will make small quantities of PC boards for amateur projects. Most commercial outfits charge a hefty development fee for the first prototype and then expect sales of thousands of boards. Without FAR Circuits, the projects I have described in *QST*, 73 and *QEX* would not have had a PC board available, and I would not have had the opportunity to learn about this one.

Fig 8 shows the schematic of my stereo amplifier. For the ham version, I used the same circuit, but only one of the power amplifier sections. I did not run any power to the right side, and I “ac grounded” the inputs.¹² The input (or inputs if you are doing stereo) are differential to reduce common-mode noise. They can be driven single-sided as I did in my application by ac grounding the negative input. C7 and R2 set an internal oscillator. To accurately

replicate the audio signal with PWM, the sample rate (frequency of the triangle) is about 10 times that of the maximum audio-signal frequency, 250-kHz for high-fidelity work. A much lower frequency is acceptable for amateur voice work. C1 through C4 block the dc bias on the input pins. Gain pins 0 and 1 set one of four internal gains.

The remaining capacitors reduce power-supply noise. With the high-fidelity oscillator rate, the speaker signal has a 250-kHz component. Optional small-value capacitors and beads can be used on the output leads to reduce the high-frequency response for those applications where it is needed. That’s about it.

Maximum power output depends on speaker resistance; 3 Ω will permit 2 W continuous average power at less than 1% distortion. If an 8-Ω speaker is used at modest volume, you can expect 1 W at less than 0.08% distortion. No wonder it sounds so good! There is a shutdown pin on the device for standby power savings.

To increase output power, while reducing overall circuit size, the speaker is connected in a bridged mode.¹³ A bridged mode uses two amplifiers to drive the speaker with identical signals levels—*except* that the signals are 180° out of phase. This results in twice the ac voltage across the speaker as in

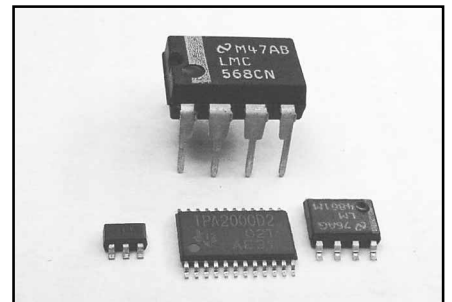


Fig 7—The TPA2000D2 compared to other ICs. Note the very close lead spacing—about 0.009 inches. While my hand-grinder method of board making can make cuts this fine using a 0.005-inch thick cutoff wheel, my hand is not steady enough to make 18 cuts with this degree of precision!

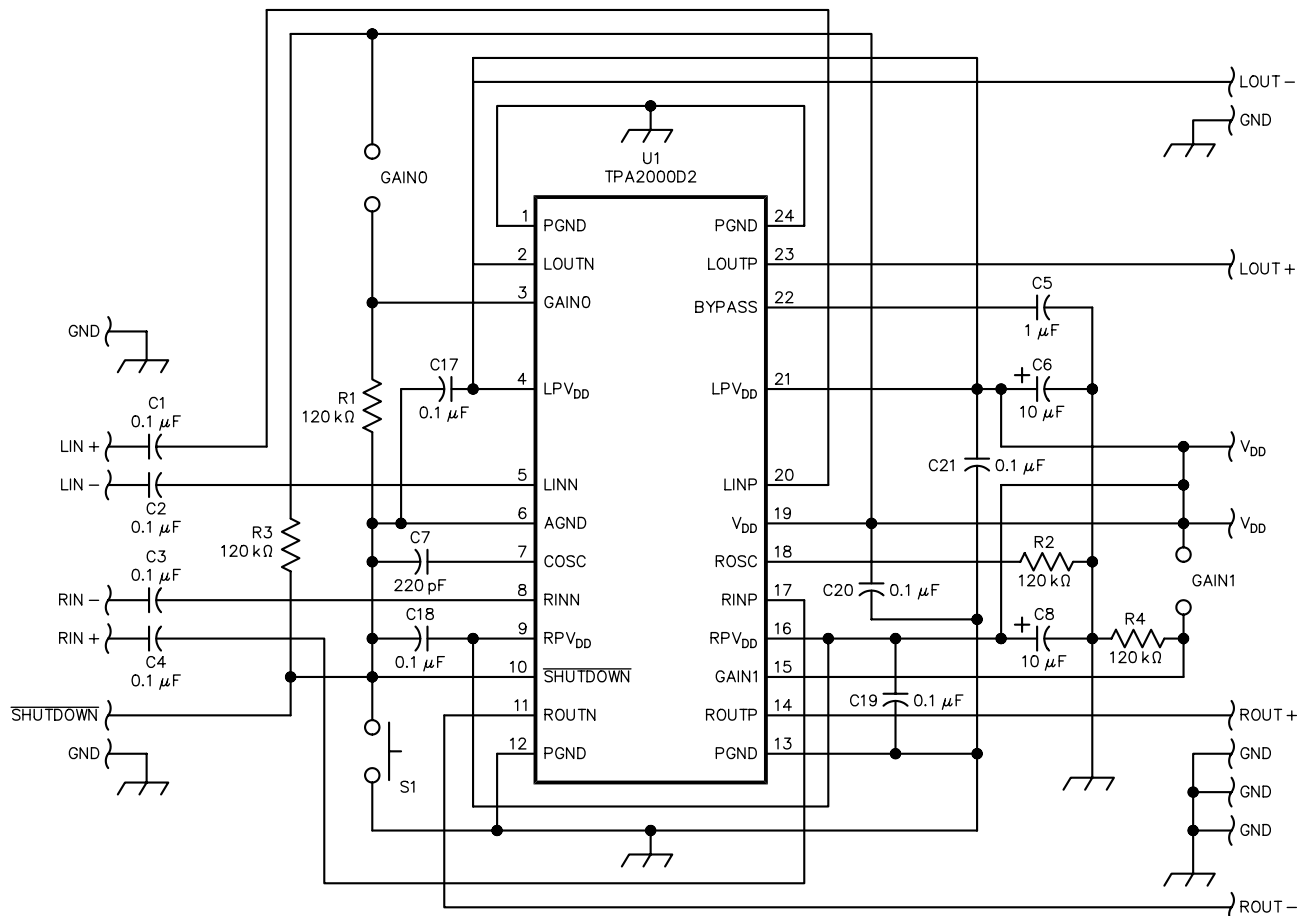


Fig 8—The circuit shown in the TPA2000D2 evaluation module datasheet that I referenced when building my amplifier.

delivered from a single-ended amplifier. The power is increased fourfold, and no large dc blocking capacitors are needed in the output as both sides are biased at the same $V_{cc}/2$ dc level.

With class D, the bridged mode causes some other problems, however. The out-of-phase pulses create a 10-V (P-P) 250-kHz differential voltage across the load. The inductive speaker load permits a triangular current to flow with a magnitude depending on the inductance and resistance of the circuit as Fig 9 shows. This causes noise, and it heavily loads the speaker. The high noise level varies as the pulses vary in width. In earlier class-D amplifier designs, a low-pass filter was used in the output line; but inductors needed for these filters are relatively large and costly.

What Makes The TPA2000D2 So Good?

According to TI the TPA2000D2's improvements over previous-generation devices include: lower supply current, lower noise floor, better efficiency, four different gain settings, smaller packaging, and it requires fewer external components. The IC has protection circuitry for thermal, over-current and under-voltage shutdown. However, the most significant advancement is a modulation scheme that eliminates the need for the output filter, saving approximately 30% in system cost and 75% in PC-board area.

Like earlier generations, the TPA2000D2 is configured as a Bridge-Tied Load (BTL) amplifier, but TI engineers have circumvented the standing-current problem by modifying the bridge arrangement. The output signals are phased so when there is no audio signal the pulses are in phase (not out of phase). As the audio signal gets larger, the two signals change phase—as one shifts positive, the other goes negative. Fig 10 illustrates the effects of the TI phasing scheme. The current flow resulting from the modulating pulses is much lower; and TI claims the small residual EMI noise can be handled by the speaker, or filtered with small beads.

Experimenting With The TPA2000D2

Once the PC board was designed (Fig 11), and produced by FAR Circuits, building the amplifier was straightforward surface-mount construction, as I have described in previous projects—except for the IC itself. While the TPA2000DC is physically a rather large

chip, it also has many leads that are closely spaced. This is the reason I didn't try making a board—but rather had FAR Circuits etch one.¹⁴ The IC has a metal power pad underneath it. To insulate the board traces from that pad, I used fingernail polish as a mask. To improve heat sinking I used a bit of heat-sink grease. This is not exactly the way TI recommends doing things, but it works for my needs.

The closely spaced leads on the IC make it very easy to get solder bridges. I avoided this by pre-tinning the pads and IC leads with 0.015-inch solder (the finest I could locate). Prior to tinning, I used a flux pen to enhance solder adherence. Solder bridges were easily corrected before connecting the IC, but if I needed to add more solder later to get a good contact it would invite bridges that would be hard to

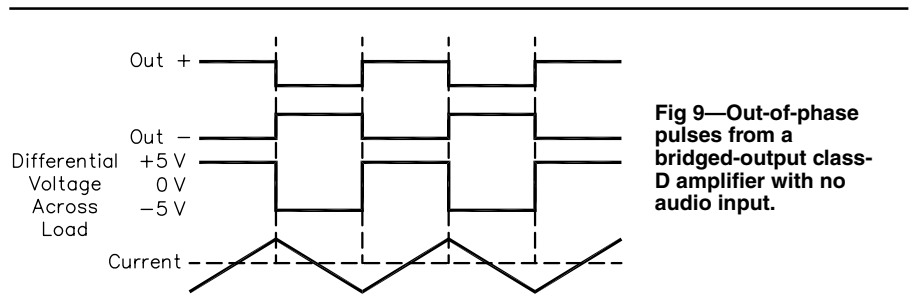


Fig 9—Out-of-phase pulses from a bridged-output class-D amplifier with no audio input.

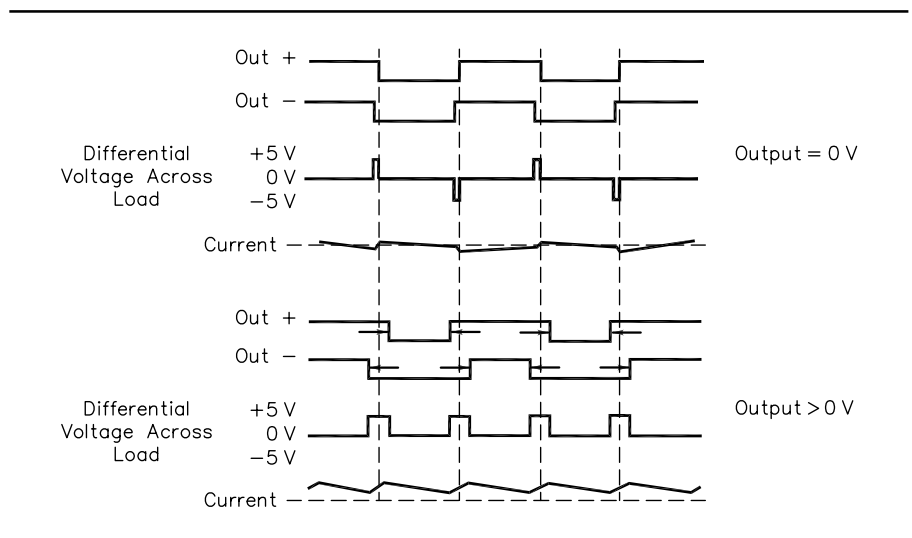


Fig 10—Output pulses from the TPA2000D2 with no input signal.

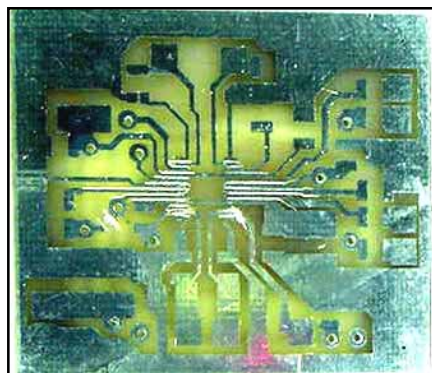


Fig 11—Top view of my FAR Circuits PC board before construction.

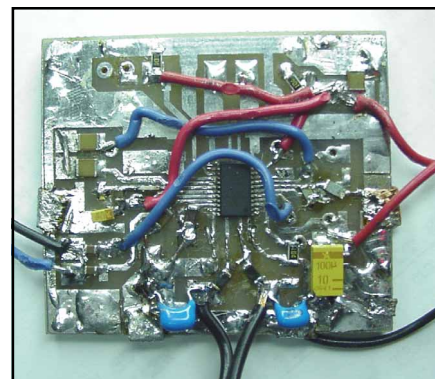


Fig 12—The modified monophonic version of the class-D amplifier for amateur use. It's mounted on the back of the speaker to minimize output lead length.

eliminate. Once everything was properly tinned, I placed the IC on its pads and heated the pins by putting the iron directly on the pin and pressing down for a second. I used only the solder already on the surfaces. The iron was set at a fairly low temperature (less than 700°F), and I was careful not to keep the contact too long with a little cooling off time between soldering pins. I did two diagonal pins to locate the IC; and then the others two at a time since the iron's tip was that wide. I checked for bridges between the pins and traces using both a strong magnifier and a continuity tester. The remaining parts were easily soldered.

The stereo amplifier has outstanding audio quality when driven by my portable CD player—as I noted earlier. When I turned on the ham rig, however, there was strong RFI about every 250 kHz! This was due at least in part to the current in the speaker wires—as the music volume peaked, so did the RFI.¹⁵

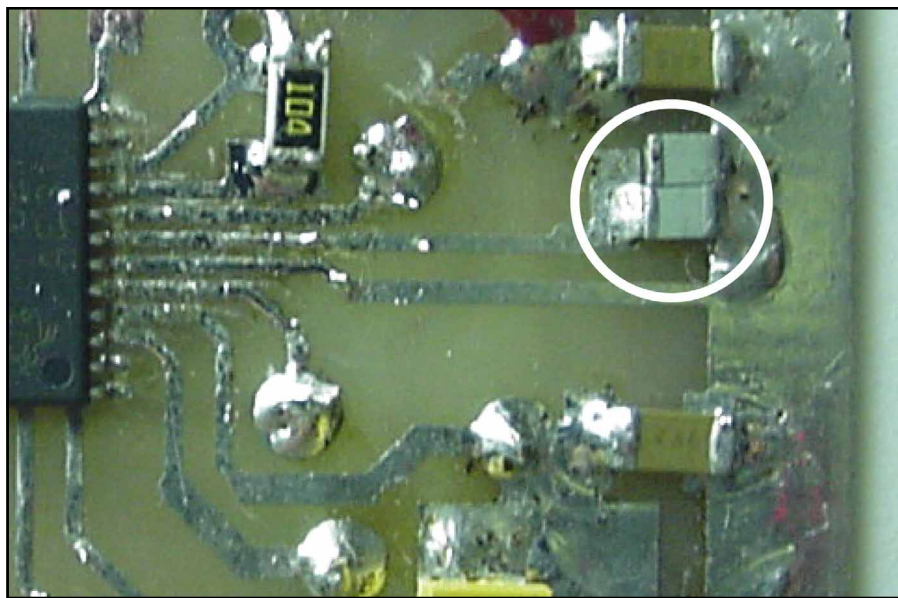
Next, I built a single-channel ham-radio version. I did not connect the second channel's power input, and I ac grounded the inputs, leaving the outputs open circuited. Quiescent current was the same as for the stereo version. I kept the speaker wires less than eight inches as recommended, but found strong RFI as soon as I connected the input lines to the HF rig's audio output.¹⁶ Even my *handheld* VHF radio showed a weaker received signal, indicating it too was being bothered by RFI. I tried all the standard RFI mitigating tricks: beads, inductors, capacitors to reduce the problem, but nothing seemed to eliminate it. Since I had a floating power source, I tried using a differential audio input, but the RFI problem remained. There was no noise unless the leads were connected to the radio. Even putting it in a metal box did not help. It was soon obvious that while my layout worked fine for non-ham use, I had a poor circuit layout for HF work.

I considered asking FAR to make a board exactly like the one TI uses for its evaluation kit, but that would be difficult to assemble by hand. FAR cannot make boards with plated *vias*,¹⁷ and several were under the IC and that negated using my via method. Also, the parts are so closely spaced that hand soldering would be very difficult or impossible. I was not about to spend several hundred dollars for a *via* board done at a professional PC board shop. In desperation, I tried modifying the layout of the existing board. This was small-scale work, but what the heck, I

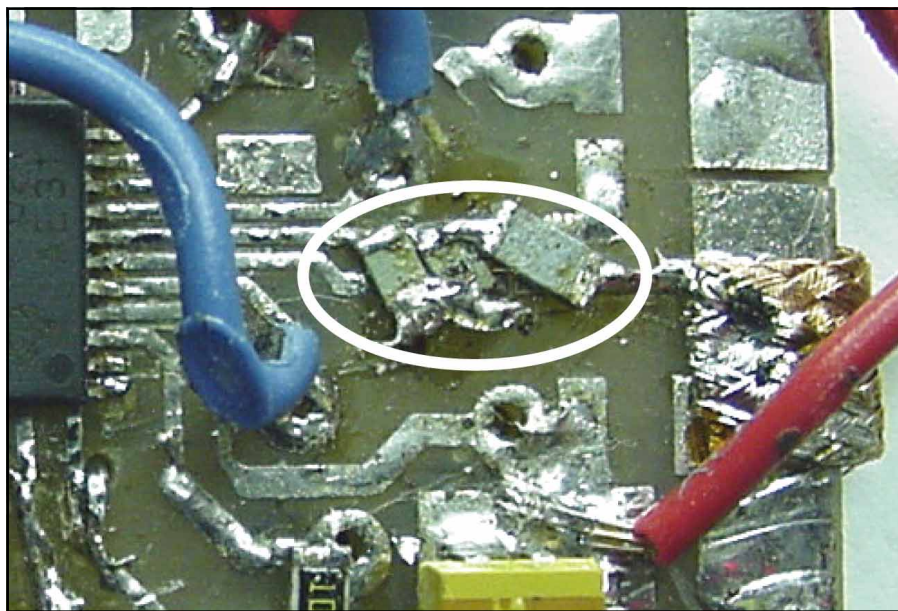
had nothing to lose. (See Fig 12.)

The datasheet information noted: “there are three main areas of concern in the layout: the ground plane, power plane, the inputs and the outputs. ... a solid ground plane works as well as other types...serves to assist the PowerPAD 2 in the dissipation of heat ...can act as a shield to help isolate the power pins from the output, reducing the impact of EMI on the traces and pins.” The power traces are kept short and the decoupling capacitors placed as close to the power pins as possible.

Terminate the capacitor ground as close to the ground for the particular power section as possible while paying attention to ground-return-current paths. This minimizes ground loops and provides very short ground-return paths and high-frequency loops. The Vdd pin supplies power for sensitive analog circuitry and is the most sensitive pin of the device. It must therefore be kept as noise-free as possible. Power traces should be placed directly over the ground plane to reduce EMI and minimize the ground return path.



(A)



(B)

Fig 13—(A) shows the oscillator capacitors (I used two). Notice the long lead length. In (B), the capacitors are moved up on the narrow trace and connected to ground through a *via* I added.

While the PC board was too small for me to make manually, I was surprised to discover that I was able to modify it when it became necessary. When designing the board I tried adhering to the guidelines mentioned above while maintaining a simple two-sided board without any jumper wires; but obviously I had to do better. My first change was to turn the entire backside into a ground plane. I used braided solder wick to connect traces together—thus shortening the paths to the ground plane.

I found that the oscillator-capacitor lead had a 2-V (P-P) 250-kHz triangular waveform—an obvious source for RFI. I moved the capacitor as close to the IC as I could,¹⁸ drilled a hole through to ground, and grounded it directly to the underside. Fig 13A shows the original capacitor placement and 13B the modification. I wasn't sure I could solder the capacitor to the trace since it was so narrow and close to adjacent runs, but I could! The two photos show the original and modified capacitor placement.

I also moved the oscillator resistor closer and grounded it through the board, although this lead had not shown any ac. To do this, I mounted the 1206-size surface-mount resistor on its side lest it short to the other traces. (See Fig 14A for the original location of resistor, and notice in Fig 14B how the resistor is now on its side.) While not recommended for new designs, I was delighted to see how much modifying could be done to improve the performance. I wouldn't have guessed it was possible with parts this small; my skills have come a long way! I ran separate wires from the battery to Vcc (pin 4), and to the analog Vcc (pin 19), to reduce noise generated by power surges in the traces. I moved the bypass capacitor (pin 22) and power-lead capacitors (pin 21) closer to the IC pins, and drilled the board permitting them to be grounded directly to the ground plane. I lowered the frequency of the oscillator to about 100 kHz by adding a bit more capacitance at the oscillator pin in an effort to reduce radiation. It could be lowered even more for amateur audio work. I moved the large 10- μ F capacitor closer to the power input (pin 4) for the output MOSFET, and drilled holes to allow both power grounds to connect directly to the ground plane.

These modifications required the use of jumpers, something I had tried to avoid in the original design—I was concerned they would look messy and invite noise. All these modifications

resulted in a major reduction of RFI. I shortened the speaker leads to about one inch and was rewarded with a further noise reduction. While the noise is still noticeable at the nodes, it is quite low. There is no noise in between these nodes, and the node location could be altered with small changes in the oscillator frequency.

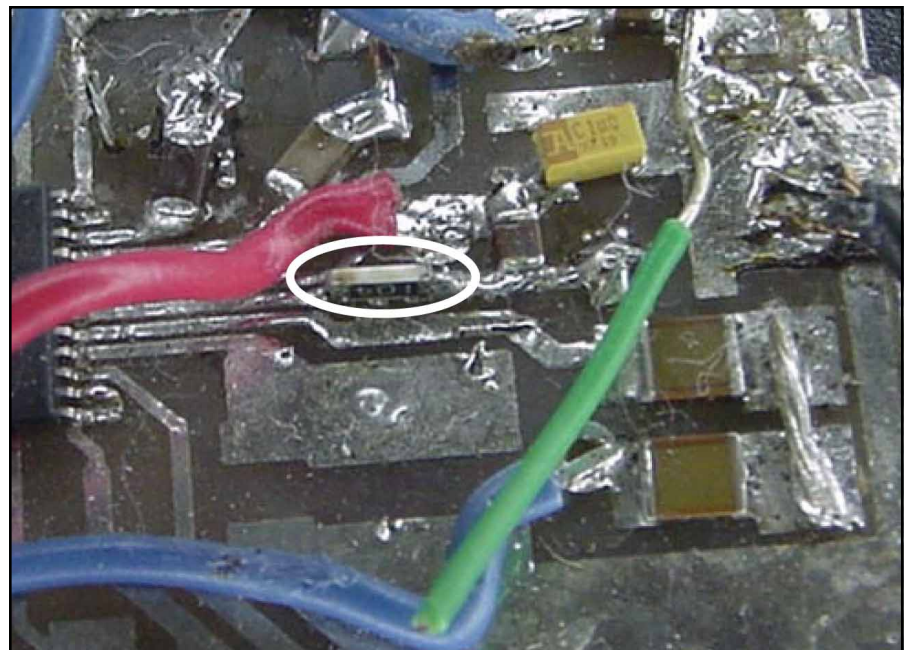
I experimented with output bead inductors and capacitors. A 68- Ω bead and 0.01- μ F capacitor increased the quiescent current to 26 mA, but the same bead with 0.001- μ F actually reduced the current to about 7.7 mA.

Neither appeared to make much difference in the RFI noise level. I left the latter in as continual soldering and desoldering in this area was causing the foil to detach. With such fine traces, this is just one more concern.

If I were to ask Fred for a new board, I would incorporate these changes and more. Clearly, I had everything spread out too far. Compactness is essential to reduce RF loops. The topside ground plane should be modified so it extends between inputs, outputs and power leads for additional isolation.



(A)



(B)

Fig 14—In the non-ham version (A) the 10 k Ω resistor is mounted conventionally. In the ham version (B), it's moved closer to the IC and mounted on its side (in the center, just below the wire). The large capacitor (marked "10 μ 16") isn't in the ham version because I am powering only one side of the IC.

Summary

What have I learned?

- Class D can make an excellent audio amplifier that—with modern ICs—is as easy to build as any other.
- By keeping parts closely spaced, routing grounds directly to a ground plane and using very short output leads, there is little RF noise and amateur applications are feasible.
- Amateurs can successfully work with small SMT parts.
- It's possible to modify a less-than-perfect layout and improve it—an important factor to learning by experimentation, one of our basic amateur tenets.

Rather than continue with this IC and a revised board, I am going to look for the “ideal” class-D amplifier IC. When it appears I will feel quite comfortable producing a “hands on” project for *QST*. Meanwhile, I have a *killer* stereo amplifier (Fig 15) and I can brag about to my friends about how I built it.

Notes

- ¹“Twenty Things that will be Obsolete in Twenty Years,” *Discovery Magazine*, October 2000, p 86.
- ²S. Ulbing, N4UAU, “My All-Purpose Voltage Booster,” *QST*, July 1997, pp 40-43. Before 1997, booster circuits were considered “one of the most difficult linear circuits to design”. Now they are often easy to design.
- ³S. Ulbing, N4UAU, “SMALL: A Surface-Mount Amplifier that's Little—and LOUD!,” *QST*, June 1996, pp 41-42.
- ⁴See “RF Power Amplifiers,” Chapter 13 of recent *ARRL Handbooks*.
- ⁵*The 1992 ARRL Handbook*, page 3-17.
- ⁶Tripath Technologies Inc, 3900 Freedom Cir, Santa Clara, CA 95054; tel 408.567.3000, fax 408.567.3003; e-mail techsupport@tripath.com; www.tripath.com. AN1 is available at www.tripath.com/downloads/an1.pdf.
- ⁷The TI TPA2000D2 is available at Digi-Key (#296-2467-5-ND) for \$3.38 + shipping in single-unit quantities. Digi-Key Corporation, 701 Brooks Ave S, Thief River Falls, MN 56701-0677; tel 800-344-4539 or 218-681-6674, fax 218-681-3380; www.digikey.com.
- ⁸“Twenty Things that will be Obsolete in Twenty Years,” *Discovery Magazine*, October 2000, page 85.
- ⁹If you think this TSSOP package is small look at the LM4872, a 1-W audio amplifier by National Semiconductor. It is in a “8-bump micro SMD package” measuring 1.31×1.97 mm with 8 “legs,” which are bumps on the bottom of the chip. Things are surely getting smaller.
- ¹⁰S. Ulbing, “Surface Mount Technology—You Can work with it!,” Part 1, *QST*, April 1999, pp 33-38.

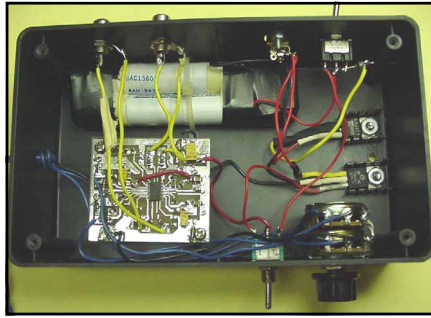


Fig 15—My killer stereo amplifier runs on internal batteries or from a wall transformer.

¹¹FAR Circuits, 18N640 Field Ct, Dundee, IL 60118, tel 847-836-9148 (voice or fax); e-mail farcir@ais.net; www.cl.ais.net/farcir/.

¹²The TPA2000D2 datasheet is available from the TI Web page at focus.ti.com/docs/prod/productfolder.jhtml?genericPartNumber=TPA2000D2.

¹³My SMALL project (Note 3) uses this technique in a linear amplifier.

¹⁴It is interesting to note that nearly all the lower power class-D amplifiers are in a similar package. National Semiconductor uses an even smaller one with bumps on the bottom instead of pins. I did not choose this package for the challenge, but rather that it is the only way to build a class-D amplifier of which I know.

¹⁵My ham shack is not very RFI proof, however. My radio hears my soldering iron go on and off and even my wife grinding coffee in the kitchen. I consider my rig to be a good piece of RFI test equipment.

¹⁶I tested both the high-impedance output from the IF stage on the rear of my IC-735 and the headphone jack. Results were similar.

¹⁷I've worked around the problem on this and other boards by having Fred provide holes where I can solder a Z-shaped jumper wire through the board to effect a simple low-impedance via, or path, between the top and bottom ground areas.

¹⁸If you want to see how good class D can be, the IC is available from Digi-Key and Fred has corrected the error on the PC board. Try it, you'll like it! □□

A Family Affair

The R.L. Drake Story

A Family Affair
The R.L. Drake story

By John Loughmiller, KB9AT

- Brand new!
- Printed October 2000
- 23 Chapters
- 300 Pages
- 150 Photos
- Glossy four color cover
- Over 150 pages of radio mods.
- \$29.95 (+\$4.95 ship)

John Loughmiller KB9AT reveals the behind-the-scenes history of the famous R.L. Drake Company, focusing on the glory days, when Drake was king in amateur radio. Every ham and SWL knew R.L. Drake from the outside, but now the inside story of this incredibly interesting company is told. This book also includes 150 pages of useful circuits and modifications for many Drake amateur radios. An entertaining read and a great technical reference for every Drake owner.

Universal Radio
6830 Americana Pkwy.
Reynoldsburg, OH 43068

◆ Orders: 800 431-3939
◆ Info: 614 866-4267
www.universal-radio.com

We Design And Manufacture To Meet Your Requirements

*Prototype or Production Quantities

800-522-2253

This Number May Not Save Your Life...

But it could make it a lot easier! Especially when it comes to ordering non-standard connectors.

RF/MICROWAVE CONNECTORS, CABLES AND ASSEMBLIES

- Specials our specialty. Virtually any SMA, N, TNC, HN, LC, RP, BNC, SMB, or SMC delivered in 2-4 weeks.
- Cross reference library to all major manufacturers.
- Experts in supplying “hard to get” RF connectors.
- Our adapters can satisfy virtually any combination of requirements between series.
- Extensive inventory of passive RF/Microwave components including attenuators, terminations and dividers.
- No minimum order.

NEMAL

Cable & Connectors
for the Electronics Industry

NEMAL ELECTRONICS INTERNATIONAL, INC.

12240 N.E. 14TH AVENUE

NORTH MIAMI, FL 33161

TEL: 305-899-0900 • FAX: 305-895-8178

E-MAIL: INFO@NEMAL.COM

BRASIL: (011) 5535-2368

URL: WWW.NEMAL.COM

RF

By Zack Lau, W1VT

An 852-MHz Local Oscillator Using Cell-Phone Parts

The advent of cellular phone technology has resulted in cheap helical filters around 850 MHz. Not only are they available cheaply if you scrap obsolete electronics, but they are small and light. I've found that the

225 Main St
Newington, CT 06111-1494
zlau@arrl.org

830-MHz 7HW Toko filters will tune up to 852 MHz, with just 2.3 dB of insertion loss. 852 MHz is quite useful for 10-GHz work, as it is an IF between 106.5 MHz and 2556 MHz. It can also be multiplied to 3408 MHz, which is easily tripled to 10224 MHz. This is the highly desirable low-side injection frequency for a 2-meter-to-10-GHz transverter. While I didn't try it, this design should also work on 828 MHz without retuning the filters. 828 MHz

can be multiplied to 3312 MHz, for a 2-meter-IF 3456-MHz transverter. 3312 MHz can be further multiplied to 9936 MHz, which is the low side injection frequency for a 432-MHz to 10-GHz transverter.

Thus, this filter is an ideal candidate for replacing the somewhat large PC-board filters used in a QST 10-GHz transverter design.¹ A complete

¹Notes appear on page 63.

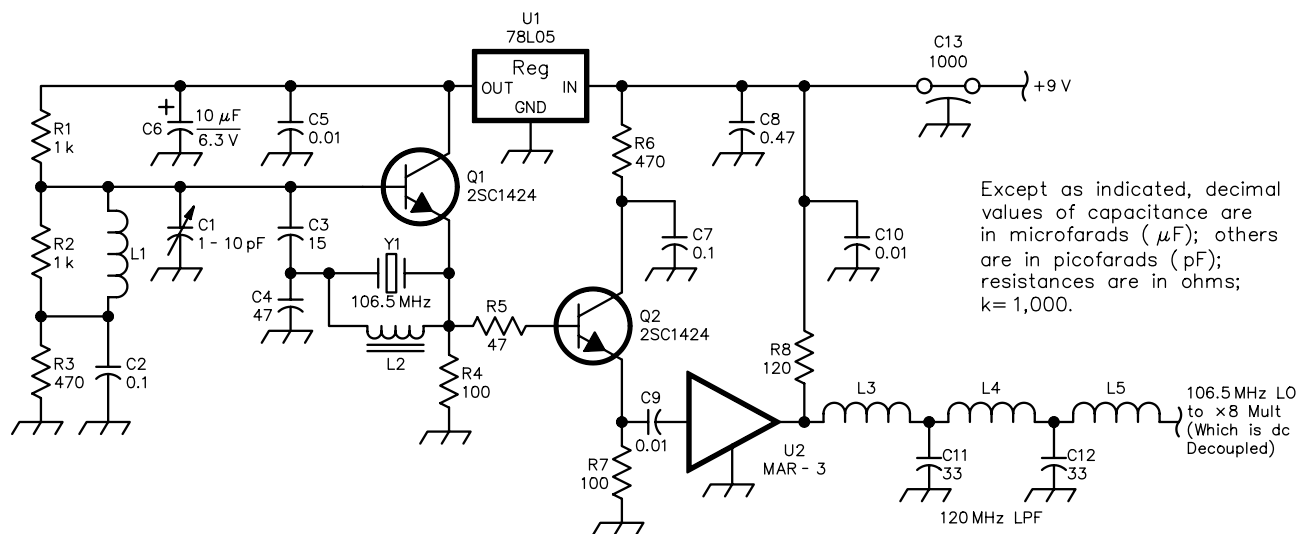


Fig 1—Schematic of 106.5-MHz local oscillator and amplifier.

L1—8 turns #24 AWG enameled wire close wound over a 0.113-inch OD form. Use the shaft of a #33 drill as temporary form.

L2—14 turns #28 AWG enameled wire on a T25-6 toroid core.

L3, L5—6 turns #28 AWG enameled wire over a 0.089-inch OD form. Use the shaft of a #43 drill as temporary form.

L4—10 turns #28 AWG enameled wire over a 0.089-inch OD form. Use the shaft of a #43 drill as temporary form.

Q1, Q2—2SC1424, 2N5179, BRF91 or equivalent NPN transistor.
U1—78L05 5-V regulator.

852 MHz LO, including the aluminum shields, weighs just 1.7 oz (47 grams). Its dimensions are 1.25×3.8×0.85 inches, including the screws and connectors. In contrast, the original 639-MHz LO is roughly triple that size and weight.

The 106.5-MHz oscillator shown in Figs 1 and 2 is unchanged from the original. I used 2SC1424s because I found a large supply—2N5179s or BR91s would work just as well. However, the optimum frequency of oscillation would be different, due to the internal capacitance of the transistors. Typically, the '5179s would oscillate slightly lower in frequency, and the BR91s would operate higher. I have found it useful to choose tuning capacitors that can be tuned when the shield is in place, like most piston trimmer capacitors. If you need an oscillator that can be netted precisely to a particular frequency, I suggest you adapt the VCXO design by John Stephensen, KD6OZH.² This low-noise design is voltage controlled, which makes it suitable for phase locking to an accurate reference.

I added a low-pass filter between the MAR-3 amplifier and the ×8 multiplier shown in Figs 3 and 4 to increase spectral purity. Without the filter, the 639-MHz ×6 multiplier product at the 852-MHz output was only 46 dB down—adding the filter reduced it to 57 dB down, an 11-dB improvement. We just want the ×8 product, which is at 852 MHz.

Ideally, you would be able to inspect the helical filter in the original circuit, to determine the proper input and output connections. Otherwise, it may take a bit of experimentation to determine the correct filter pinout. The pinout for the filters I used is shown in Fig 5. The one I measured had a bandwidth of 34 MHz, when tuned to 852 MHz. The -1 dB bandwidth was 27 MHz.

With 10 dBm of drive, the 852-MHz signal at the output of the first helical filter is just -22 dBm. Thus, with 2 dB of loss for another filter, 34 dB of gain is needed for a 10-dBm output. I used a pair of MAR-2s and a MAR-3 to obtain a +9-dBm output. The output could be increased by using high-quality chip capacitors instead of small NP0 ceramic capacitors. However, the little NP0 capacitors lend themselves to point-to-point wiring, avoiding the

need for etching a circuit board. In contrast, chip capacitors can be difficult to use without a circuit board, as they can easily break if something flexes.

I used the “Manhattan” style of construction for installing the chip bypass capacitors. I beveled the edges of little squares of unetched double sided circuit board, and then soldered the larger copper square to the ground plane, as shown in Fig 6. I then soldered the chip cap between the top foil and the ground plane. This provides structural support for the bypassed resistor—soldering the resistor directly to the capacitor does result in superior RF performance—until the chip capacitor breaks.

The sharp reader may spot the short section of UT-085 semi-rigid 50-Ω coax used to connect the low-pass filter to the multiplier input. Better

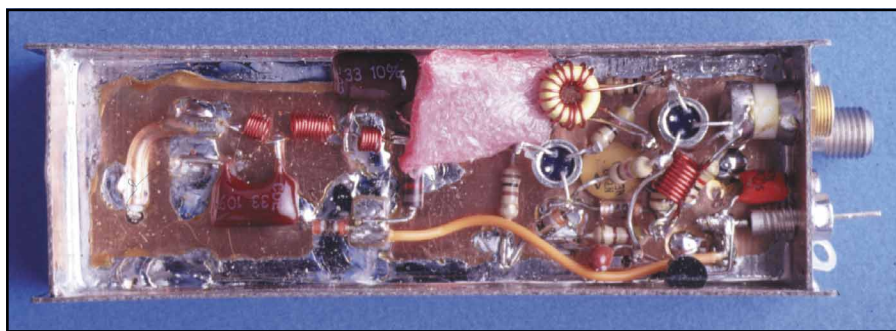


Fig 2—The local oscillator and amplifier described in Fig 1.

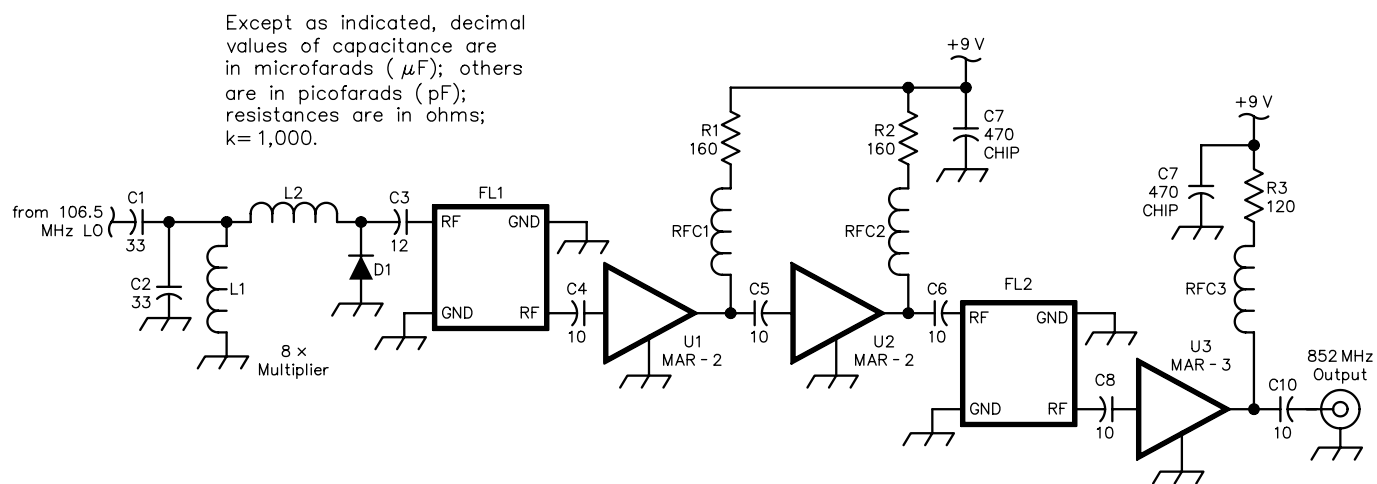


Fig 3—Schematic of 852-MHz ×8 multiplier and amplifier.

D1—HP5082-2835 Schottky diode.
FL1, FL2—Toko 7HW 830-MHz helical band-pass filter retuned to 852 MHz.
L1—5 turns #28 AWG enameled wire over a 0.113-inch OD form. Use a #33 drill as temporary form.

L2—8 turns #28 AWG enameled wire over a 0.113-inch OD form. Use a #33 drill as temporary form.

RFC1-3—5 turns #28 AWG enameled wire closewound over a 0.070-inch OD form. Use a #50 drill as a temporary form.

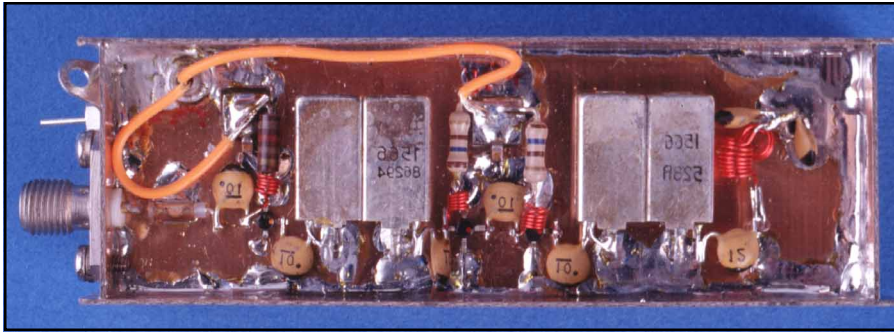


Fig 4—The 8× multiplier and amplifiers described in Fig 3.

planning would make this jumper unnecessary.

To reduce weight and cost, I used thin 25-mil-thick double-sided glass epoxy circuit board. This is often available cheaply at hamfests. The shields are made out of 20-mil-thick aluminum sheet stock.

Homebrewers with limited circuit-board-fabrication skills may wish to study the article “A Reliable Frequency Multiplier for 10 GHz,” by Dale Clement, AF1T, pages 361 to 366, in the *Proceedings of the 25th Eastern VHF/UHF Conference*. Dale describes a simple 568-to-10224-MHz multiplier using four pipe-cap filters. Dale used ERA MMICs as multipliers and gain blocks. Instead of etching a board, Dale cut and peeled away the unwanted copper foil, taking advantage of the poor adhesion to Teflon that occurs when circuit board is overheated.

This circuit should work just fine on 828 MHz with a 103.5-MHz crystal, for use in a 3312-MHz local oscillator. It may not even be necessary to retune the filters, if you get the ones designed for 830 MHz. There are also cell-phone filters designed for 870 MHz. A 3312-MHz LO can either be mixed with 144 MHz to get on 9 cm or multiplied by three to generate a 9936-MHz LO. The latter is useful for getting on 10 GHz with a 432-MHz IF radio.

Notes

- ¹Z. Lau, W1VT, “Home-Brewing a 10-GHz SSB/CW Transverter,” Part 1, May 1993, pp 21-28; Part 2, June, pp 29-31.
- ²J. Stephensen, KD6OZH, “A Stable, Low-Noise Crystal Oscillator for Microwave and Millimeter-Wave Transverters,” *QEX*, Nov/Dec 1999, pp 11-17.

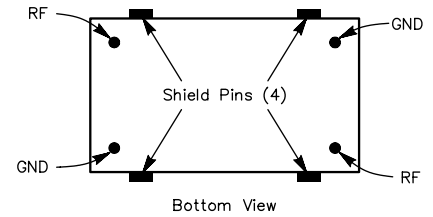


Fig 5—Pin diagram of a Toko 7HW helical band-pass filter.

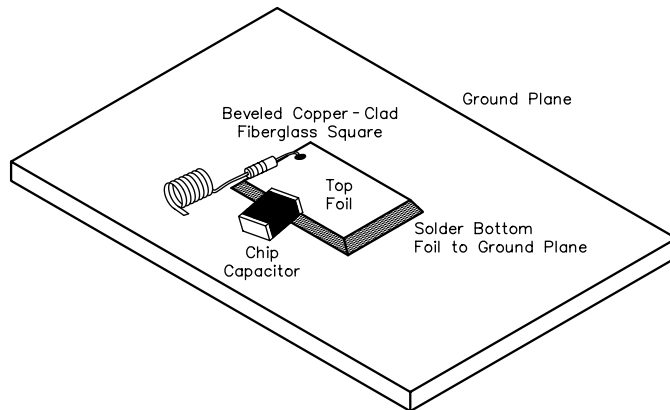


Fig 6—“Manhattan” style construction is used to mount a delicate chip capacitor over a ground plane.

Mike's Electronics

ICOM[®]

Amateur Radio

1001 North West 52nd St, Ft Lauderdale, FL 33309

Phone: 800-427-3066 • Fax: 954-491-7011

mspivak@bellsouth.net

Letters to the Editor

RF (Jul/Aug 2001)

Hello Doug:

I am writing to you concerning a minor technical error that appeared in the Jul/Aug 2001 issue of *QEX* (Fig 1, p 55) regarding the manner of stating return loss. Although you may consider the incorrect manner of stating return loss to be insignificant, I believe that if this error continues to be published in high-level technical publications such as *QEX* and *QST*, it will be assumed to be correct by your less-informed readers and therefore repeated in future articles. I believe it is imperative that we all be aware of the need to maintain the correctness of our technical language to prevent it from becoming degraded.

In Zack Lau's figure called "6-Element Yagi Return Loss/SWR," on the left-hand Y axis, the return-loss magnitudes are labeled: "0 dB, -10 dB, -20 dB and -30 dB." Please note that return loss is almost always positive (except in very unusual cases, one of which I will mention later), and therefore the negative signs should be omitted. If you want to keep the negative signs, you have the option of specifying the left-hand Y-axis parameter as S11, in which case the S parameter of input voltage reflection coefficient is specified; or you can use a non-standard term "return signal magnitude," which is in negative decibels.

The fact that return loss is normally positive is obvious from the standard equation for return loss (dB): $-10 \log(\rho^2)$, where ρ is the reflection coefficient's magnitude. For example, for a reflection coefficient of 0.10, the return loss is: $-10 \log(0.1^2) = -10 \log(0.01) = -10(-2) = 20$ dB. (For confirmation, please see Eq 14, p 5-6 in *The ARRL UHF/Microwave Experimenter's Manual*.)

Under special conditions, it is possible that a negative return loss can be measured; that is, a device can actually return more power than was fed into it. Because the returned power is greater than the input power, the loss is negative. Zack mentioned this unusual condition on p 27, at the top of the third column in the January 1995 *QEX*. Unfortunately, he incorrectly called the return loss "... a positive input return loss..." when actually it is a negative return loss!

We now can see how careless [inattention] to terminology can really turn things around! Negative becomes positive, positive becomes negative, black becomes white and so forth. I would appreciate it if the ARRL publications staff would pay particular attention to see that all future references to return loss are correctly stated.

On a less technical note, but still of interest to you as editor of *QEX*, I wish to voice my objection to the use of "gonna" instead of "going to" and similar sloppy terms in the *QEX* text. (See p 60, July/Aug 2001, third column, WA1VVH letter to the editor.) I don't care if "gonna" is now listed in one of the recently published dictionaries. The term may be common in speech, but in print, I feel it is unacceptable and I request you to refrain from publishing any further examples.—Ed Wetherhold, W3NQN, ARRL Technical Advisor, Passive LC Filters, 1426 Catlyn Place, Annapolis, MD 21401-4208

Zack responds:

Thanks for pointing out the error—I added the label "return loss" to the left-hand side of plot provided to me by Joe Riesert. I used negative numbers to match the numbers generated by the marker function of the analyzer.

I am not familiar with the instrument—perhaps you are more familiar with precise labeling of the different screens. The lab needs more experience with modern network analyzers,

but we have not had any luck in getting a suitable donation.—73, Zack Lau, W1VT, Contributing Editor
Doug adds:

You're right, Ed, that "gonna" is not good English grammar, but I hesitate to change a writer's voice and style too much in letters. In fact, another correspondent recently wrote me indicating that it is more fun to read colloquial language sometimes. Articles are an entirely different story.—73, Doug Smith, KF6DX, Editor

Next Issue in *QEX/Communications* Quarterly

Among other features in the next issue, Mark Mandelkern, K5AM, returns with his promised article about the HF "front ends" for his homebrew transceiver. That article augments a series about which we've gotten a lot of good feedback. Check it out.

The Nov/Dec 2001 issue marks the 20th anniversary of *QEX*. As we prepare to nestle into the holiday season, that will be a good excuse to reminisce a bit about the history of the magazine. We'll also take the opportunity to comment on some outstanding technical milestones from Amateur Radio's past and some of its gone-but-not-forgotten luminaries.

QEX

American Radio Relay League
225 Main Street
Newington, CT 06111-1494 USA

For one year (6 bi-monthly issues) of *QEX*:

- In the US
- ARRL Member \$22.00
 - Non-Member \$34.00
- In Canada, Mexico and US by First Class mail
- ARRL Member \$35.00
 - Non-Member \$47.00
- Elsewhere by Surface Mail (4-8 week delivery)
- ARRL Member \$27.00
 - Non-Member \$39.00
- Elsewhere by Airmail
- ARRL Member \$55.00
 - Non-Member \$67.00

QEX Subscription Order Card

QEX, the Forum for Communications Experimenters is available at the rates shown at left. Maximum term is 6 issues, and because of the uncertainty of postal rates, prices are subject to change without notice.

Subscribe toll-free with your credit card 1-888-277-5289

Renewal New Subscription

Name _____ Call _____

Address _____

City _____ State or Province _____ Postal Code _____

Payment Enclosed

Charge:



Account # _____ Good thru _____

Signature _____ Date _____

Remittance must be in US funds and checks must be drawn on a bank in the US. Prices subject to change without notice.

11/98



ARRL Marketplace!



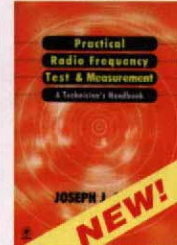
These publications have been added to the ARRL Library...
so you can add them to yours!



Microcontroller Projects with Basic Stamps
Microcontroller Projects with Basic Stamps
Complete guide to developing practical solutions with these tiny microprocessors. A wealth of example projects. Includes software.
ARRL Order No. 7865—\$44.95



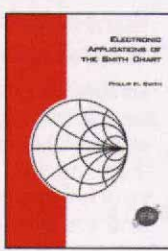
winSMITH 2.0
An easy-to-use, flexible computerized Smith Chart. Accelerate your RF and microwave designs! Unlock a greater understanding of transmission lines and simple matching problems. 3.5-inch installation diskette. Requires Microsoft Windows.
ARRL Order No. 7946—\$80



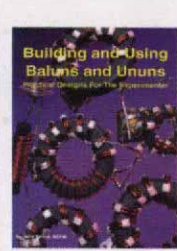
Practical Radio Frequency Test & Measurement
Learn the basics of performing tests and measurements used in radio-frequency systems installation, proof of performance, maintenance, and troubleshooting. Provides immediate applications, test set-ups, procedures, and interpretation of results.
ARRL Order No. 7954—\$34.95



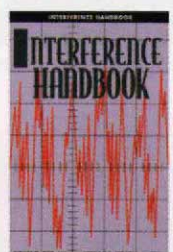
Transmission Line Transformers
This book stands alone in its coverage of the subject of broadband transmission line transformers. Many configurations of Ruthroff and Guanella types of transformers are described with complete performance measurements and construction details.
ARRL Order No. 7245—\$34



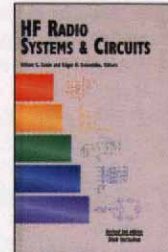
Electronic Applications of the Smith Chart
The legendary Smith Chart inventor's original, classic reference book describing how the chart is used for designing lumped element (inductors and capacitors) and transmission line circuits (coaxial, waveguide, stripline or microstrip lines). Includes tutorial material on transmission line theory and behavior, circuit representation on the chart, matching networks, network transformations and broadband matching.
ARRL Order No. 7261—\$59



Building and Using Baluns and Ununs
Practical Designs for the Experimenter! Transmission line transformer theory, design, and construction. Includes hundreds of examples for dipoles, Yagis, log periodics, beverages, multi-band antennas, antenna tuners, and more.
ARRL Order No. 7644—\$19.95



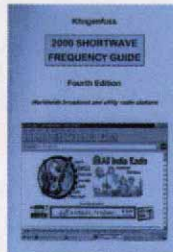
Interference Handbook
Locate and solve interference problems of every type. Suppression circuits for interfering devices are discussed in detail, and protection techniques for home entertainment equipment. THE book for power-line interference problems!
ARRL Order No. 6015—\$14



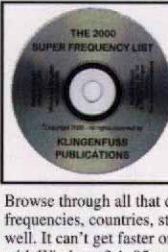
HF Radio Systems & Circuits
Includes Software!
Comprehensive coverage of system definition and performance requirements down to the individual circuit elements that make up radio transmitters and receivers. Thorough attention is given to key circuits like oscillators, synthesizers, filters and amplifiers, speech processing, AGC systems, high linearity amplifiers, and solid state power amplifiers.
ARRL Order No. 7253—\$75



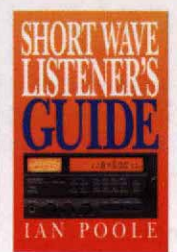
33 Simple Weekend Projects
A wide-ranging collection of do-it-yourself electronics projects. Useful accessories for VHF FMing, projects for satellite communications, CW, simple antennas, and a complete HF station you can build for around \$100!
ARRL Order No. 7628—\$15.95



2000 Shortwave Frequency Guide
Covers the latest 2000 schedules of all clandestine, domestic, and international broadcast stations worldwide! Features a gigantic broadcast frequency list with 10,703 entries, and a superb alphabetical list of stations. Also includes 11,247 entries for utility stations. User-friendly, clearly arranged, and up-to-date!
ARRL Order No. 7814—\$32.00



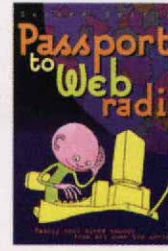
The 2000 Super Frequency List CD-ROM
More than 38,700 entries! Listings with the latest schedules of all clandestine, domestic and international broadcasting services on shortwave. Plus, frequencies for fascinating radio services such as International Red Cross, marathons, military, police, and United Nations.
Browse through all that data in milliseconds! Search for specific frequencies, countries, stations, languages, call signs, and times as well. It can't get faster or any easier than this! CD-ROM for PCs with Windows 3.1, 95 and 98.
ARRL Order No. 7822—\$32.00



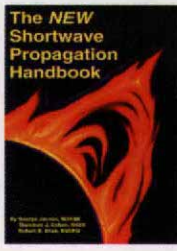
Short Wave Listener's Guide
Use this guide to understand exactly what shortwave listening is, how radio waves travel, and how to set up and run a shortwave listening station.
ARRL Order No. 7520—\$29.95



Passport to World Band Radio 2000
Experience the world through a new prism—world band radio. It's the home of new ideas, fresh perspectives and news that's totally different from one station to the next. What's on. What to buy. How to get started. Includes Passport's Blue Pages (2000); a channel-by-channel guide to world band schedules.
ARRL Order No. 7806—\$19.95

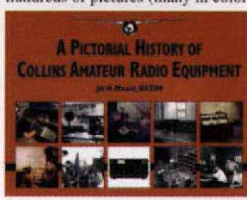


Passport to Web Radio
Web radio is where FM/AM stations from America and around the world now hang out. All you need is your PC and this book! Listings for 1,550 channels (Web address URLs), and everything's on!
ARRL Order No. 7059—\$19.95



The NEW Shortwave Propagation Handbook
Understand how HF signals propagate, and learn about sunspots and ionospheric predictions. Make productive use of the radio spectrum, regardless of the time of day, season, or sunspot cycle. Filled with illustrations, photos, charts and tables!
ARRL Order No. 7636—\$19.95

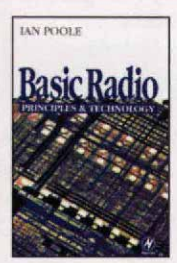
A Pictorial History of Collins Amateur Radio Equipment
The most complete history of Collins equipment is told with hundreds of pictures (many in color) and in the words of the men who made it happen.



Travel from the pre-war era through the 1980's, and enjoy an upclose profile of Arthur A. Collins.
ARRL Order No. 7830—\$39.95

Order Toll Free 1-888-277-5289

Shipping and Handling instructions: US orders add \$4 for one item, plus \$1 for each additional item (\$9 max.). US orders are shipped via UPS. International orders add \$1.50 to the US shipping rate (\$10.50 max.). Orders are shipped via surface mail. Other shipping options are available. Please call or write for information.
Sales Tax is required for shipments to CT 6% (including S/H), VA 4.5% (excluding S/H), CA (add applicable tax, excluding S/H) and Canada (excluding S/H).



Basic Radio: Principles and Technology
A wide ranging introduction to the principles of radio waves, transmission and reception. Suitable for students, technicians and hobbyists! Covers cellular phones, digital radio broadcasting, satellites, and more!
ARRL Order No. 7512—\$29.95

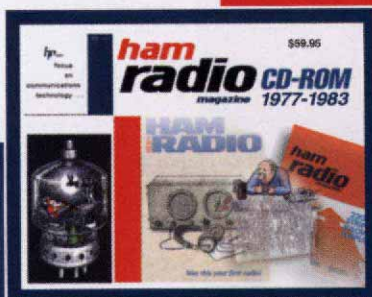
Name: **ham**
radio, born January, 1968.

Why **ham radio** (magazine)? *The electronics and communications industry is moving forward at a tremendous clip, and so is amateur radio. Single sideband has largely replaced a-m, transistors are taking the place of vacuum tubes, and integrated circuits are finding their way into the ham workshop. The problem today, as it has always been, is to keep the amateur well informed.*—Editor Jim Fisk, WIDTY (SK), from the preview issue of **ham radio** magazine, February, 1968 (last issue published in June, 1990).

hp focus
on
communications
technology...

Introducing Ham Radio CD-ROMs!

System Requirements: Pentium or equivalent IBM-compatible PC, and Microsoft Windows™ 95, 98, NT 4.0, Me, or 2000.



Now you can enjoy quick and easy access to back issues of this popular magazine! These CD-ROM sets include high quality black-and-white scanned pages, easily read on your computer screen or printed. All the articles, ads, columns and covers are included.

Readers will enjoy a wealth of material that spanned the gamut of Amateur Radio technical interests: **construction projects, theory, antennas, transmitters, receivers, amplifiers, HF through microwaves, test equipment, accessories, FM, SSB, CW, visual and digital modes.**

The complete set covers more than 30,000 pages!



Search--Select--Browse—it's all there!

- search for articles by title and author
- select specific year and issue
- browse individual articles and columns

Only \$59.95 per set!* Each set includes four CDs!

- Ham Radio CD-ROM 1968-1976 ARRL Order No. 8381
- Ham Radio CD-ROM 1977-1983 ARRL Order No. 8403
- Ham Radio CD-ROM 1984-1990 ARRL Order No. 8411

SAVE \$80! when you order the complete set:*

All 3 Ham Radio CD-ROM Sets (1968-1990)
ARRL Order No. HRCD **\$149.85**

*Shipping/handling fee: US orders add \$5 for one set, plus \$1 for each additional set (\$10 max, via UPS). International orders add \$2.00 to these rates (\$12.00 max, via surface delivery). Sales tax is required for orders shipped to CA, CT, VA, and Canada.



Ham Radio CD-ROM, © 2001,
American Radio Relay League, Inc.
Ham Radio Magazine © 1968-1990,
CQ Communications, Inc.

ARRL The national association for
AMATEUR RADIO

225 Main Street, Newington, CT 06111-1494
tel: 860-594-0355 fax: 860-594-0303

In the US call our toll-free number **1-888-277-5289** 8 AM-8 PM Eastern time Mon.-Fri.
Quick order **www.arrrl.org/shop**